



Evaluating rangeland condition using fine-scale remote sensing from Unoccupied Aerial Vehicles

A dissertation submitted in partial fulfilment of the requirements for the award of the degree of Master of Science Degree in Animal Science (Animal Management Systems)

By

ALAN DUMEZWENI NARE

Student Number: 202200875

November 2024

Supervisors

Dr. Lawrence Akanyang (BUAN)

Professor Jeremy Perkins (University of Botswana)

Dr. Andrew Cunliffe (University of Exeter, UK)



University
of Exeter



DECLARATION

I, **Alan Dumezweni Nare**, hereby declare that this MSc dissertation entitled "**Evaluating rangeland condition using fine-scale remote sensing from unoccupied aerial vehicles**" is entirely my work, except where otherwise acknowledged. This work has not been submitted in whole or in part for any other degree or qualification at this or any other university. All sources used or referred to have been duly acknowledged, and any citations are accurately indicated.

Signed: 

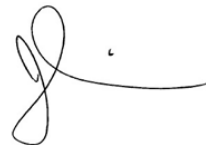
Date: 08/01/2025

Alan Dumezweni Nare (Candidate)

Signed: 

Date: 08/01/2025

Dr. Lawrence Akanyang (Supervisor)

Signed: 

Date: 8/1/2025

Professor Jeremy Perkins (Co-supervisor)

Signed: 

Date: 8th of January 2025

Dr. Andrew Cunliffe (Co-supervisor)

ABSTRACT

Savanna ecosystems require precise monitoring tools for sustainable management. Traditional field methods are resource intensive and spatially limited, while satellites lack fine-scale resolution, and commercial high-resolution options are costly. Unoccupied Aerial Vehicles (UAVs) have become an established tool for fine-scale rangeland monitoring, offering a critical bridge between spatially limited field surveys and coarse-resolution satellite data. However, there is underutilised potential for applying these approaches in African landscapes to yield useful management insights. This study evaluated UAV Structure from Motion photogrammetry (SfM) -derived canopy height and multispectral reflectance for estimating herbaceous aboveground biomass (AGB), a key indicator of rangeland condition and forage availability across grazing gradients in the Southwestern Kalahari, Botswana. Data from 90 harvest plots and three 50 m × 50 m sites were analysed using robust linear regression to assess (1) the relationship between UAV SfM-derived canopy height and spectral reflectance for estimating AGB, (2) the effectiveness of UAV observations in predicting herbaceous biomass of foraging importance, and (3) the transferability of these models by testing them across gradients of grazing intensity. Results showed canopy height strongly predicted AGB ($R^2 = 0.72$), while spectral reflectance as measured by NDVI showed no significant relationship, challenging vegetation greenness as a proxy for forage. The canopy height-AGB relationship remained consistent across forage importance categories (low, average, high) and grazing intensities, supporting ecosystem level allometric applications. This study contributes to the limited knowledge of UAV applications in African rangelands, demonstrating their utility in enhancing ecosystem monitoring and management. This research underscores the potential of UAVs in providing high-resolution data for rangeland monitoring, offering valuable tools to refine insight from wide-scale satellite observations and provide better insight for land managers and policymakers.

DEDICATION

To the resilient people who rely on Kalahari savanna ecosystems-may this research contribute to sustainable rangeland management and a better understanding of our natural world.

ACKNOWLEDGEMENTS

I gratefully acknowledge the support received from the Oppenheimer Programme in African Landscape Systems (OPALS), jointly funded by the University of Exeter, Sarah Turvill, and Oppenheimer Generations Research and Conservation, as well as the Botswana University of Agriculture and Natural Resources. Additionally, I extend my appreciation to Agisoft for providing a free licence of the Metashape software to the Botswana University of Agriculture and Natural Resources.

I would like to express my sincere gratitude to my supervisors, Dr. Lawrence Akanyang, Professor Jeremy Perkins, and Dr. Andrew Cunliffe, for their invaluable guidance, unwavering support, and insightful feedback throughout every stage of this research. Their expertise, encouragement, and constructive criticism have been instrumental in shaping the direction and refining the quality of this thesis.

Special thanks to Glenn Slade for his dedicated support in drone training and technical assistance. His expertise played a pivotal role in the execution of the fieldwork and data collection processes. Furthermore, I acknowledge the members of the Terrestrial Ecosystem Science and Services (TESS lab) for their contributions to refining the design and value of this project. I also extend my appreciation to the invaluable support of my field assistants, Kelebogile Basima and Ezekiel Tuahuku.

Lastly, I am deeply indebted to my wife, Joestina, and my daughter, Kaboentle, for their unwavering love and boundless inspiration throughout this academic journey.

To all individuals and organisations mentioned above, as well as those who have supported me in various capacities throughout this journey, I extend my heartfelt thanks. Your contributions have been instrumental in the successful completion of this thesis.

Contents

ABSTRACT	iii
DEDICATION	iv
ACKNOWLEDGEMENTS	v
Contents.....	vi
List of figures	ix
List of tables	xi
List of Appendices.....	xii
List of abbreviations	xiii
1 Introduction	1
1.1 Background.....	1
1.2 Problem statement	5
1.3 Research aim	6
1.4 Justification	7
2 Literature Review.....	8
2.1 Introduction	8
2.2 Current status of rangelands in Botswana	9
2.3 Challenges of assessing aboveground biomass (AGB) in the Kalahari Savanna.....	10
2.3.1 Spatial heterogeneity	10
2.3.2 Unique ecological conditions	12
2.3.3 Impact of climate variability and herbivory	12
2.4 Methods of assessing AGB.....	14
2.4.1 Traditional rangeland monitoring techniques.....	14
2.4.2 Rangeland monitoring with remote sensing	15
2.5 Brief history of UAVs.....	19

2.6 UAV technology in ecological research.....	20
2.7 UAVs in measuring AGB.....	23
2.7.1 Field data collection	24
2.7.2 UAV data processing	32
2.7.3 Predictive model generation.....	35
2.8 Conclusions.....	43
2.9 Research gaps and future directions	44
3 Methodology.....	45
3.1 Study site description.....	45
3.1.1 Location.....	45
3.1.2 Dune system	48
3.1.3 Climate and pans	48
3.1.4 Soils and associated vegetation	49
3.3 Area of interest (AOI) selection and plot layout.....	51
3.3.1 Geolocating AOIs and Ground Control Points (GCPs)	51
3.3.2 Detailed AOI descriptions	52
3.4 Aerial surveys	55
3.4.1 UAV RGB data collection for SfM canopy height modelling.....	55
3.4.2 UAV multispectral data collection for spectral reflectance.....	56
3.5 Field sampling	58
3.6 Biomass harvest.....	59
3.6.1 Oven drying of samples.....	59
3.6.2 Plant palatability classification	60
3.7 Image-based modelling.....	62
3.7.1 Photogrammetric data processing point cloud generation	62

3.7.2 Canopy Height Modelling	63
3.8 Processing vegetation indices	66
3.9 Statistical analysis.....	68
4 Results	69
4.1 How well can aboveground biomass in Kalahari savanna ecosystems be predicted by fine-scale UAV observations of canopy height and spectral reflectance?.....	69
4.2 How well can herbaceous biomass of foraging importance be predicted by fine-scale UAV observations of canopy height and spectral reflectance?	72
4.3 Do these relationships between biomass components and remotely sensed attributes differ across different levels of grazing intensity?	74
5 Discussion	77
5.1 How well can aboveground biomass in Kalahari savanna ecosystems be predicted by fine-scale UAV observations of canopy height and spectral reflectance?.....	77
5.2 How well can herbaceous biomass of foraging importance be predicted by fine-scale UAV observations of canopy height and spectral reflectance?	79
5.3 Do these relationships between biomass components and remotely sensed attributes differ across different levels of grazing intensity?	81
6 Conclusion.....	83
7 Open Research.....	85
8 References.....	86
9 Appendices.....	118

List of figures

Figure 1. Vegetation's spectral reflectance curve. The major characteristics of absorption and reflectance are displayed (Miller et al., 1990).	17
Figure 2. There is an increasing interest in using UAVs to study rangelands.	21
Figure 3. Geographic distribution of UAV-based AGB estimation studies (2012-2022).	24
Figure 4. Brightly coloured canvas used as GCPs with black backgrounds to enhance visibility and precision.	25
Figure 5. Accurate and evenly distributed GCPs significantly improve UAV data quality.	27
Figure 6. Fifty meters is the most frequently used UAV flight altitude among the 64 reviewed studies (Bazzo et al., 2023).	30
Figure 7.	47
Figure 8. Map of the Kalahari plateau and Mean Annual Precipitation (MAP) in Botswana.	49
Figure 9. Geolocation of GCPs using the DJI D-RTK2 base and Phantom 4 multispectral rover system.	52
Figure 10. Rangeland condition decreases near the borehole along grazing intensity gradients.	54
Figure 11. Equipment used for RGB SfM survey. a) Digital anemometer for measuring wind speed. b) DJI Phantom 4 Pro drone (Zutshwa, 25/03/2024).	56
Figure 12. Equipment used for multispectral survey. a) DJI Phantom 4 Multispectral drone. b) DJI D-RTK 2 high precision GNSS mobile station (Zutshwa, 26/03/2024).	58
Figure 13. 0.342m ² circular quadrat and centre pin flag with plot ID. The herbaceous species shown is <i>Schmidtia kalahariensis</i> (Zutshwa, 26/03/24).	59

Figure 14. Accurate canopy height modelling and smoothing techniques in R.....	65
Figure 15. Visualisations of reconstructed point clouds and plant scale canopy heights of individual plants.....	66
Figure 16. The general workflow of the UAV observations of canopy height and spectral reflectance used to characterise AGB (right side). The field observations (right side) were used for calibrating allometric relationships between height or spectral reflectance.....	67
Figure 17. Canopy height strongly predicted aboveground biomass, while NDVI reveals more variable species-specific relationships.....	71
Figure 18. Canopy height is a strong predictor of aboveground biomass across all grazing value categories, while NDVI shows inconsistent predictive power.....	73
Figure 19. The canopy height model is reproducible and predicts AGB across all grazing intensities.....	76

List of tables

Table 1. UAV derived structural information used to model vegetation biomass.....	37
Table 2. RGB survey flight parameters	55
Table 3. Multispectral survey flight parameters.....	57
Table 4. Classification of herbaceous species by grazing value	61
Table 5. Model summaries for aboveground biomass as predicted from Mean Canopy Height.	70
Table 6. Model summaries for aboveground biomass as predicted from NDVI.....	70
Table 7. Model performance metrics for predicting Aboveground Biomass (AGB) Using UAV- Derived Canopy Height and NDVI across different grazing value categories	73
Table 8. Summary of model performance metrics for predicting AGB using Canopy Height Model across varying levels of grazing intensity	75

List of Appendices

Appendix A. Number of samples per species and grazing value	118
Appendix B. Outlier and leverage diagnosis for Canopy Height.	119
Appendix C. Outlier and leverage diagnosis for NDVI.	120
Appendix D. Density plot for distribution of Canopy Height, NDVI, and AGB.	121
Appendix E. Computational hardware specifications.....	121

List of abbreviations

AGB	Aboveground Biomass
DSM	Digital Surface Model
DTM	Digital Terrain Model
MAE	Mean Absolute Error
NDVI	Normalised Difference Vegetation Index
NIR	Near-Infrared
RMSE	Root Mean Square Error
RPM	Rising Plate Metre
SfM	Structure from Motion (SfM) photogrammetry
UAV	Unoccupied Aerial Vehicle
DEM	Digital Elevation Model
GNSS	Global Navigation Satellite System
RTK	Real-time kinematic positioning
GCP	Ground Control Point
AOI	Area of Interest
CHM	Canopy Height Model
CI	Confidence Interval
DEM	Digital Elevation Model
3D	Three-Dimensional

1 Introduction

1.1 Background

The Kalahari plateau is a distinctive and ecologically important region in Southern Africa, occupying a significant part of Botswana (Leistner, 1967; Perkins, 2018; Roodt, 2015). Up until the 1980s, the Kalahari was primarily a wildlife-dominated ecosystem (Mbaiwa & Thakadu, 2022). However, technological advances in borehole drilling led the Botswana government to implement a livestock expansion policy, prioritizing cattle production through proliferating water points (Moleele & Perkins, 1998a). Consequently, the dominant Kalahari thornveld now serves as a forage source for livestock and wildlife feeding on the Kalahari savanna vegetation (Dikgang & Muchapondwa, 2017). Herbaceous plants constitute the primary dietary choice for grazing animals (Al-bukhari et al., 2018). These plants grow during the rainy season (usually November to April) and are consumed by grazing animals in both rainy and dry seasons (Roodt, 2015). Herbaceous plants also offer benefits like water infiltration, dune stabilisation, biodiversity support, nutrient cycling, and carbon sequestration (Ahirwal et al., 2021; Oduor et al., 2018).

However, the transition to sedentary livestock production, through the establishment of stationary cattle posts facilitated by boreholes, has intensified the risk of grazing-induced degradation due to the increased concentration of livestock and prolonged grazing pressure on specific areas (Basupi et al., 2019; Perkins, 2018). This negatively impacts the livelihoods of those who directly rely on the ecosystem service of foraging that rangeland vegetation offers. Measurable indicators are thus important in inferring rangeland condition and improving rangeland management. Herbaceous above ground biomass (AGB) is a useful and common indicator of rangeland condition (Retallack et al., 2023).

The quantification of AGB provides a useful proxy for assessing rangeland condition and thus the amount of forage available for grazing animals (Hoppe et al., 2016; Jamsranjav

et al., 2018; Jhariya & Singh, 2021; Vahidi et al., 2023). Changes in AGB can be a useful indicator of disturbances, including overgrazing, and the resulting impacts on biodiversity and productivity (Piipponen et al., 2022). These changes may manifest as a reduction in vegetation cover, an increase in bare ground, alterations in species composition, or changes in nutrient cycling, among other effects (Dougill et al., 2016; Jhariya & Singh, 2021).

There are two primary approaches to evaluate the condition of rangelands, traditional plot level field measurements and remote sensing (Bazzo et al., 2023; Prabhakara et al., 2015). Plot level field measurements of AGB are the widely used method for accurately monitoring changes in rangeland condition over time (Kendie et al., 2021; Myers-Smith et al., 2020a; Tokozwayo et al., 2021). However, this approach is limited in spatial scope and coverage due to its time and resource-intensive nature (Bjorkman et al., 2018). Since the advent of satellite-based imaging, satellite remote sensing has proven to be a valuable tool in overcoming various limitations of plot-level field measurements (Meshesha et al., 2020). Remote sensing from satellites can provide regional or global scale monitoring of vegetation communities but is typically conducted at moderate to coarse spatial resolution ranging from 15 m to 2 km (Retallack et al., 2023), which poses challenges in mapping across diverse landscapes and making informed decisions (Sankey et al., 2019). Fine-resolution satellite imagery remains costly and is limited in temporal resolution (Aplin et al., 2021; Fang et al., 2020). Furthermore, remote sensing from satellites often aggregates various herbaceous species when estimating AGB, which can obscure important details regarding rangeland condition (Fern et al., 2018a; Meshesha et al., 2020).

Unoccupied aerial vehicles (UAVs) have emerged as a valuable tool for remote sensing, providing fine resolution imagery at landscape scales that bridges the gap between spatially sparse field measurements and coarse resolution satellite remote sensing (Amputu et al., 2023; Cunliffe et al., 2016; Eskandari et al., 2020; Gillan et al., 2020; Retallack et al., 2023). One method of detecting AGB involves using vegetation indices (VIs) to estimate AGB (Amputu et al., 2023; Cunliffe et al., 2020; Doughty & Cavanaugh,

2019; Fern et al., 2018a). This method is however limited in its ability to detect the biomass of dry vegetation because VIs are sensitive to chlorophyll (Doughty & Cavanaugh, 2019). Furthermore, estimating biomass from VIs can be challenging due to the asymptotic relationship between biomass and surface reflectance. As biomass increases, the amount of radiation absorbed by the vegetation approaches saturation, and changes in biomass may not result in proportional changes in reflectance (Colomina & Molina, 2014; Cunliffe et al., 2020; Myers-Smith et al., 2020b). This makes it difficult to accurately estimate biomass using spectral reflectance, especially at higher biomass levels (> 1500 kg/ha) (Amputu et al., 2023; Prabhakara et al., 2015; Théau et al., 2021). In addition, variable ground reflectance can also contribute to uncertainty in biomass estimates from spectral reflectance (Cunliffe et al., 2022; Myers-Smith et al., 2020).

Another method involves using 3D point clouds to characterise the structural characteristics of vegetation (Cunliffe et al., 2016, 2020, 2022). UAVs can measure structural traits such as canopy height which can be used as an excellent predictor of aboveground biomass (Cunliffe et al., 2022; Poley & McDermid, 2020). Studies have utilized 3D models generated from UAV-acquired imagery, processed using structure-from-motion (SfM) photogrammetry, to reconstruct vegetation. These models demonstrate strong correlations between predicted biomass values and field-measured biomass (Cunliffe et al., 2020, 2022; Shahbazi et al., 2015; Westoby et al., 2012). The number of publications on estimating AGB using UAVs has grown over time and is still on the rise (Figure 3), indicating scientific interest from the research community (Cunliffe et al., 2022; McIntire et al., 2022; Myers-Smith et al., 2020b; Slade et al., 2024). The growing body of literature on UAV-based AGB estimation (Cunliffe et al., 2022; McIntire et al., 2022; Slade et al., 2024) confirms the technology's maturity for general applications. As such, UAVs have become an established tool for fine-scale rangeland monitoring, offering a critical bridge between spatially limited field surveys and coarse-resolution satellite data (Cunliffe et al., 2022; Retallack et al., 2023).

While UAV remote sensing has matured as a tool for biomass estimation globally (Cunliffe et al., 2022; Slade et al., 2024), its application in African savannas must resolve a critical

ecological-management disconnect: current methods cannot reliably differentiate between total herbaceous biomass and forage-relevant biomass. This limitation is acutely evident in borehole-adjacent degradation zones, where rapid colonisation by prostrate-growing, non-palatable species such as *Tribulus terrestris* contributes substantially to AGB while offering negligible grazing value (Kashe et al., 2020; Perkins, 2018). Conventional UAV approaches, whether spectral (VI-based) or structural (canopy height) were developed for ecosystems where biomass correlates consistently with forage quality, an assumption invalidated in Kalahari rangelands (Amputu et al., 2023).

The present study therefore aims to assess how UAV fine-scale remote sensing could contribute to monitoring and mapping herbaceous biomass in Kalahari savanna ecosystems. Accurate assessment of AGB is an asset for land managers and policy makers, providing valuable information necessary for the sustainable utilisation of rangelands. Another possible contribution of this project is enhancing the capabilities of researchers and practitioners in using fine-scale remote sensing to understand rangelands and to help develop new approaches and insights that are appropriate for the unique challenges and contexts of African rangelands.

1.2 Problem statement

The Kalahari savanna, crucial for both biodiversity and the livelihoods of local communities, is increasingly threatened by degradation due to intensive livestock grazing and unsustainable land use. The quantification of AGB provides a useful proxy for assessing rangeland condition and thus the amount of forage available for grazing animals. Traditional plot level rangeland monitoring techniques, like plot-level biomass field measurements, are limited by their spatial coverage and high resource demands, while satellite-based methods often fail to provide the necessary resolution to detect fine-scale variations in rangeland condition. Although commercial high-resolution satellites exist, their operational costs typically preclude routine monitoring applications in resource-limited settings.

UAVs have demonstrated significant potential to bridge the limited spatial scope and coverage of traditional plot level techniques and the coarse resolution of satellite remote sensing. While UAV remote sensing has proven effective for general rangeland assessment, its application in African savannas must address a critical ecological distinction: the capacity to differentiate between total herbaceous biomass and biomass of actual foraging value. This challenge is particularly pronounced in grazing zones near water points, where vegetation communities become dominated by prostrate growing, lush and green forbs such as *Tribulus terrestris* that are not of foraging importance. Conventional UAV-derived metrics often fail to capture this functional difference, creating significant limitations for pastoral systems where accurate assessment of palatable biomass determines sustainable stocking rates and grazing management decisions.

1.3 Research aim

The aim of this study was to assess how UAV fine-scale remote sensing could contribute to monitoring and mapping AGB in Kalahari savanna ecosystems. AGB in the context of this study refers to the total amount of herbaceous vegetation (grasses and forbs) available to grazing animals, excluding woody vegetation. The specific research questions were:

1. How well can aboveground biomass in Kalahari savanna ecosystems be predicted by fine-scale UAV observations of canopy height and spectral reflectance?
2. How well can herbaceous biomass of foraging importance be predicted by fine-scale UAV observations of canopy height and spectral reflectance?
3. Do these relationships between biomass components and remotely sensed attributes differ across different levels of grazing intensity?

1.4 Justification

The tools developed in this study could assist with precise AGB prediction in rangelands. The limited application of fine-scale remote sensing in African rangelands underscores the need for innovative techniques to enhance monitoring and management of these unique and important ecosystems. By developing and applying advanced fine scale remote sensing techniques, this research could improve our understanding of rangeland conditions for people, livestock, and wildlife. This work could also provide valuable insight that can be refined to help improve the quality of information provided to pastoralists, land managers, and policymakers, supporting evidence-based frameworks for rangeland utilisation and management. Additionally, it will strengthen the capacity of researchers and practitioners to utilise fine-scale remote sensing effectively, offering new insights and approaches tailored to the unique challenges of African rangelands.

2 Literature Review

2.1 Introduction

Rangelands play a crucial ecological and economic role, contributing significantly to the food security of millions of people (Niamir-Fuller & Huber-Sannwald, 2020). African rangelands are particularly vital in meeting the ecosystem requirements of more than 268 million pastoralists and agro-pastoralists who rely on them (Liniger & Studer, 2019). When managed sustainably, these areas have the potential to actively contribute to carbon sequestration, enhance air and water quality, contribute to nutrient cycling, dune stabilisation, biodiversity support, food production, and to supply forage for grazing animals (Ahirwal et al., 2021; Lewis, 1936; Oduor et al., 2018). However, the arid Kalahari savanna rangelands are prone to desertification due to substantial climate variability and herbivory, resulting in inconsistent herbage availability for livestock both spatially and temporally (Lomax et al., 2024; Schmiedel et al., 2021).

As such, suitable, accurate, repeatable, and easy to apply techniques to estimate herbaceous biomass are required for timely decision making and the sustainable use of rangelands (Al-bukhari et al., 2018; Amputu et al., 2023; Revermann et al., 2018). Conventional plot level field measurements have provided detailed information on the compositional, structural, and functional aspects of vegetation at a local scale but are limited in spatial scope and coverage (Al-bukhari et al., 2018; Bazzo et al., 2023; Bjorkman et al., 2018). Satellite remote sensing allows for regional or global-scale monitoring of vegetation communities at a moderate to coarse spatial resolution (Retallack et al., 2023). There is a need to bridge the limited spatial scope of field measurements, and the coarse resolution of satellites to provide land managers actionable and reliable information.

This chapter critically analyses the potential of using UAV-based remote sensing in rangeland monitoring and management. First, it provides an assessment of the status of rangelands in Botswana. Following this, the specific challenges of assessing aboveground biomass (AGB) in the Kalahari savanna, are presented. The third part of

the review discusses the current status of plot-level field measurements and satellite remote sensing in rangeland monitoring, emphasising the need for integrating UAV remote sensing. The fourth and fifth sections detail the characteristics, procedures, current status, and areas for improvement in UAV-based rangeland monitoring. The final section identifies opportunities for integrating UAVs into monitoring forage and animal production.

2.2 Current status of rangelands in Botswana

Botswana's rangelands are characterised by a semi-arid to arid climate, with fluctuating rainfall patterns affecting the growth and distribution of vegetation (Maruatona & Moses, 2022; Schmiedel et al., 2021; Vossen, 1990). The Kalahari Plateau, covering a large part of the country (Figure 1), has sandy soils and sparse vegetation primarily consisting of grasses, shrubs, and occasional woody species (Dougill et al., 2016; Lancaster, 1978; Lewis, 1936; Perkins, 2019).

There is increasing concern about rangeland degradation, owing to anthropogenic and natural factors (Dougill et al., 2016; Kgosisikoma, 2012). Research in Botswana has revealed an increase in bush encroachment, bare ground (Kgosisikoma, 2012), heightened soil erosion (Webb et al., 2020), and a reduction in perennial grass species (Dougill et al., 2016), aligning with other studies in the Kalahari Plateau (Geißler et al., 2024; Westhuizen et al., 2022; Zimmer et al., 2024). Herbaceous species loss and the increase in bush encroachment, particularly by *Vachellia hebecladan*, *V. karroo*, *V. nilotica*, *V. tortilis*, *S. mellifera* and *Dichrostachys cinerea*, and *Rhigozum trichotomum* have also been identified as an emerging problem in the late nineteenth and early twentieth century (Dougill et al., 2016; Lewis, 1936; O'Connor et al., 2014; Perkins, 2018; Thomas & Wiggs, 2022; Webb et al., 2020). There is strong evidence that an increase in atmospheric CO₂ has an impact on increased woody growth in the setting of Southern Africa (Bond, 2008; Midgley & Bond, 2015). These changes are predicted to reduce biodiversity over the Kalahari, and also raise the risk of more frequent and severe fires because of the hotter and drier weather (Midgley & Bond, 2015).

There is also a consensus that land degradation is primarily caused by pressures from land use and livestock grazing, as evidenced by studies on the effects of land use change and grazing livestock as drivers of ecosystem change (Dougill et al., 2016; Perkins, 2018; Porporato et al., 2003; Thomas & Wiggs, 2022). Notably, the abundance of perennial species declines as borehole density and animal density rise (Akanyang, 2019; Dougill et al., 2016; Meyer et al., 2019; Moleele & Perkins, 1998b). Sacrifice zones, characterised by severe rangeland degradation and loss of biodiversity due to concentrated livestock activity, show significant ecological impact. However, the influence of piospheres can extend beyond these zones, affecting broader ecosystem functions and co-existence with wildlife by impeding their mobility (Perkins, 2018). To attempt to address these challenges, the Botswana Government has recently adopted a 'Herding for Health' approach in some areas, based on Holistic Rangeland Management (HRM) principles (Heermans et al., 2021). Additionally, the proliferation of invasive species such as *Prosopis* and poisonous plants further complicates rangeland management. Therefore, to ensure sustainable utilisation of rangelands, it is critical to monitor the condition of herbaceous species to enable timely decision-making to adapt stocking densities.

2.3 Challenges of assessing aboveground biomass (AGB) in the Kalahari Savanna

2.3.1 Spatial heterogeneity

Recently, the value of heterogeneity as a constituent of ecological systems has grown (Fuhlendorf et al., 2017). Insights into the factors controlling rangeland heterogeneity can be drawn from findings across the Kalahari. Drylands exhibit significant intrinsic and disturbance-driven heterogeneity in the composition and productivity of their plant communities at both the landscape and regional levels (Dougill et al., 2016; Meyer et al., 2019). Soil physical and chemical properties contribute to intrinsic variability, creating diverse microhabitats that support different plant species (Dougill & Thomas, 2004). Topographical features such as elevation, slope, and aspect affect microclimates within rangelands, leading to variations in plant communities (Breshears, 2006). Additionally,

genetic diversity within plant species results in different growth forms and stress tolerances, enhancing ecosystem resilience (Hughes et al., 2008; Vellend, 2006).

Herbivory impacts plant community composition and productivity through selective grazing and overgrazing, which can alter species composition (Adler et al., 2001; Todd et al., 1998). Fire frequency and intensity also shapes vegetation types, with fire-adapted species benefiting from frequent fires (Archibald et al., 2009; Bond, 2008). Climate variability, including rainfall and temperature fluctuations, affects plant cover and biomass, interacting with other disturbances to create dynamic ecosystems (Craine et al., 2012; Knapp et al., 2008). Moreover, anthropogenic activities, such as land use changes and agricultural practices, introduce additional heterogeneity by altering soil properties and plant communities (Dougill & Thomas, 2004).

Several benefits of landscape heterogeneity have been shown in studies. For example, increasing spatial heterogeneity in rangeland biomass could reduce the temporal variance in forage production (McGranahan, 2008; Winter et al., 2012). This is a unique use of landscape heterogeneity, and in terms of ecological theory, it would add to our knowledge of the connections between biodiversity and ecosystem stability and variability. Ecosystem productivity and stability have been linked to a number of biodiversity metrics, including functional diversity, and species richness (Mori et al., 2013; Naeem & Li, 1997; Tilman et al., 2006).

Because of the heterogeneity of rangelands driven by intrinsic and disturbance driven-factors, field measurements across large areas are costly (Al-bukhari et al., 2018; Bareth & Schellberg, 2018). As a result, monitoring in other areas has focused on areas with observed or expected impacts (Karl et al., 2017). The principal limitation of this targeted approach is that it can introduce bias in data collection, as it may overlook areas that are currently unaffected but are critical for understanding broader ecological patterns and processes (Bennett, 2013). The lack of comprehensive baseline data from less impacted areas hampers accurate assessment of changes and the development of effective management strategies (Lindenmayer & Likens, 2018). Furthermore, it can cause missed

opportunities for early intervention by ignoring early warning signs of degradation in less monitored regions (Hobbs & Norton, 1996). This approach also limits the understanding of the natural variability and resilience of these ecosystems, which is essential for making generalisable conclusions about the health of rangelands (Wiens & Milne, 1989). Resource allocation might become inefficient, with concentrated efforts potentially neglecting emerging issues elsewhere (Turner, 2005). As a result, management decisions based on incomplete data may be inaccurate, underscoring the need for a more balanced and comprehensive monitoring strategy (Caughlan, 2001).

2.3.2 Unique ecological conditions

The unique ecological conditions of the Kalahari savanna further complicate AGB assessment. The region is characterised by its sandy soils, low and highly variable rainfall, and extreme temperatures. These conditions result in a dynamic and often stressed ecosystem, where vegetation growth can be rapid following rain but may quickly decline during dry periods. The adaptive strategies of the flora, such as deep-rooted plants accessing groundwater, fire adaptation, and ephemeral species that rapidly complete their life cycles, add layers of complexity to biomass measurement. The interplay between these factors means that biomass assessments must account for temporal variations and the phenological characteristics of the vegetation, which are not easily captured through traditional methods.

2.3.3 Impact of climate variability and herbivory

The two primary factors limiting vegetation growth in Botswana are the country's low sparse seasonal annual rainfall, and the low moisture-holding capacity of sandy soils (Millington & Townshend, 2009). The country's vegetation types range from sparsely distributed, highly productive riparian woodlands to bare salt pans (Lancaster, 1978; Millington & Townshend, 2009). Periodic droughts and irregular rainfall patterns, often intensified by El Niño-Southern Oscillation (ENSO)-induced events, lead to significant inter-annual differences in vegetation growth, while increasing heatwave frequencies, driven by persistent high-pressure systems such as the Botswana High, further reduce

available biomass during drought seasons (Mbokodo et al., 2023; Porporato et al., 2003). These fluctuations are compounded by the effects of herbivory, primarily from livestock, which is a prevalent land use in the region. Intensive grazing pressure can lead to degradation of vegetation, reducing biomass and altering plant community composition (Dougill & Thomas, 2004; Perkins, 2018). Overgrazing, in particular, can result in the dominance of less palatable species and the loss of key forage plants, thereby affecting overall biomass productivity. Assessing AGB in such a dynamic environment requires methods that can accurately reflect these variations and provide reliable data for sustainable rangeland management.

In summary, the Kalahari savanna presents a challenging environment for AGB assessment due to its spatial heterogeneity, unique ecological conditions, and the compounded effects of climate variability and herbivory. These factors necessitate the development and application of reliable, repeatable, and cost-effective monitoring techniques, which can offer more precise and comprehensive data to inform rangeland management practices.

2.4 Methods of assessing AGB

AGB assessment and estimation methods are categorised into traditional field methods and remote sensing techniques (Revermann et al., 2018). Traditional field methods include both destructive and non-destructive sampling. Destructive sampling considered the most accurate at a local level (Bjorkman et al., 2018; Kendie et al., 2021; Myers-Smith et al., 2020a; Tokozwayo et al., 2021), involves clipping and harvesting quadrats but is labour-intensive and limited in spatial scope and coverage. Non-destructive field methods involve calibration with harvested samples and include visual estimations, manual and rising plate metres, and capacitance probes (Karl et al., 2017).

Remote sensing techniques, developed to address the labour intensity and limited spatial scope of traditional methods, include the use of hand-held spectroradiometers and various remote sensing technologies (Retallack et al., 2023). These methods offer a non-destructive approach to AGB assessment, allowing for larger area coverage and repeated measurements over time. Both traditional plot level methods and remote sensing methods will be discussed.

2.4.1 Traditional rangeland monitoring techniques

Traditional assessment of AGB at local scales is typically conducted through destructive sampling, specifically by clipping all AGB within defined quadrats (Haydock & Shaw, 1975). This method involves clipping the biomass directly to the ground, harvesting the cut sample, sorting it, and drying it in an oven at a specific temperature. The dry matter (DM) yield, which refers to the dry weight of both green and dead material after drying, is then calculated. Although clipping AGB within quadrats is considered accurate, provided enough quadrats are sampled to capture spatial heterogeneity (Lu, 2006), the process is labour-intensive and time-consuming, involving locating, cutting, sorting, drying, and weighing the samples (Marsett et al., 2006). The accuracy of estimation decreases as spatial heterogeneity increases (Catchpole & Wheeler, 1992; Jansen et al., 2022; Psomas et al., 2011).

In heterogeneous rangeland ecosystems, many destructive samples are required, even when using double-sampling techniques (Laca, 2009). While this method provides reasonably accurate AGB estimates at a local scale, it is impractical and challenging to extrapolate this information to a landscape level (Psomas et al., 2011). As a result, it is frequently employed in specialised research projects and in developing biomass equations for large scale biomass estimation (Harmse et al., 2019). In Kalahari savanna ecosystems, different researchers are using other traditional plot level non-destructive methods such as the disc pasture metre with accurate estimates (Harmse et al., 2019). However, despite the promising results, these methods remain limited in spatial scope and coverage.

2.4.2 Rangeland monitoring with remote sensing

Remote sensing involves the acquisition and interpretation of data about the environment and Earth's surface from a distance. This is achieved by detecting radiation that is naturally emitted or reflected by the Earth's surface or atmosphere (passive remote sensing), or by analysing backscattered signals from sensor-emitted pulses, as in the case of RADAR (active remote sensing) (ESRI, 2024). This definition includes various energy sources and mechanisms for measuring radiation or signals. Passive remote sensing captures electromagnetic radiation from the sun that is reflected or transmitted across the electromagnetic spectrum (EMS). In contrast, active remote sensing involves a sensor detecting a pulse of synthetic (non-solar) energy that is emitted from a device and then reflected back to it (Ph. D. Thenkabail, 2015). In both types, sensors can be mounted on the ground, UAV, aircraft or satellites. The predominant type of energy used in remote sensing is electromagnetic energy, which includes visible light, infrared, radio waves, heat, ultraviolet light, SONAR, and x-rays.

Before the advent of digital remote sensing, photointerpretation was the primary method for analysing aerial photographs, relying on visual assessment of tone, texture, and context to classify vegetation and land cover (Lillesand et al., 2015). With the shift to digital image processing, techniques such as spectral unmixing, classification algorithms, and vegetation indices enabled more quantitative and reproducible analyses

(Schroeder et al., 2015). While photointerpretation remains valuable for historical comparisons and local-scale validation, digital methods now dominate due to their scalability and integration with multispectral and hyperspectral data (Campbell & Wynne, 2011).

The images produced by sensors vary based on their spatial, spectral, radiometric, and temporal resolutions. Spectral information is crucial for mapping and modelling the biophysical properties of vegetation. To accurately estimate herbaceous AGB, leaf area index (LAI), or cover, remote sensing must differentiate vegetation from soil features (Todd et al., 1998). Vegetation and soils must exhibit distinct spectral signatures. The typical spectral reflectance curve of green vegetation shows that leaf pigments (chlorophyll) absorb the visible portion of the EMS strongly (Figure 1). Green vegetation significantly absorbs electromagnetic radiation (EMR) in the red portion around 0.68 μm but reflects EMR strongly in the near-infrared portion between 0.76 and 0.90 μm . Factors like moisture and protein content, among others, influence reflectance from the NIR to the middle-IR portions of the EMS (Liang, 2003). This high NIR reflection makes images acquired at this wavelength attractive for vegetation studies. The characteristic features of green vegetation diminish during leaf senescence due to the loss of pigments, cell structure, and moisture content (Todd et al., 1998).

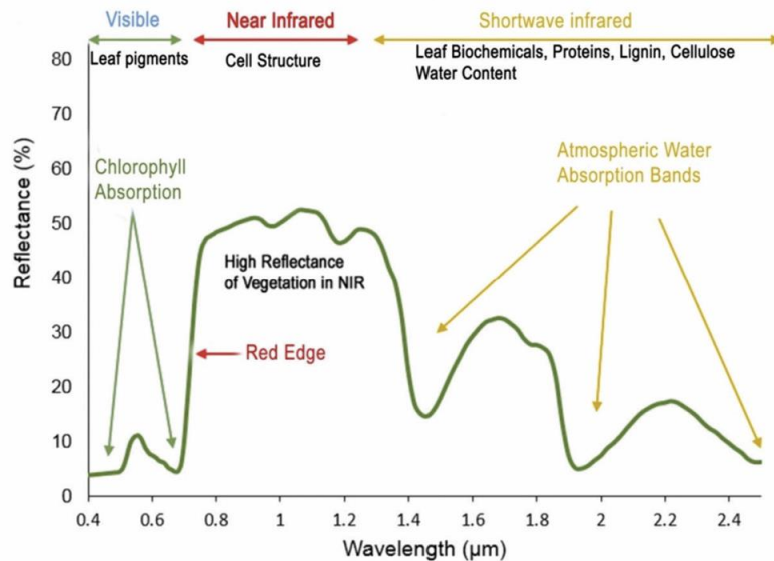


Figure 1. Vegetation's spectral reflectance curve. The major characteristics of absorption and reflectance are displayed (Miller et al., 1990).

Satellite-based remote sensing has been instrumental in monitoring large areas, such as rangelands, providing objective, automated, and repeatable long-term data on vegetation condition and land cover changes (Bastin et al., 2024; Collado, 2002). The assessment of rangeland condition has been successfully conducted using both hyperspectral and multispectral remote sensing, though their applications differ due to sensor capabilities and platform availability. Hyperspectral data, with its narrow, contiguous spectral bands (such as 200+ bands), enables detailed biochemical and biophysical characterization of vegetation, making it ideal for detecting changes in rangeland health (P. S. Thenkabail et al., 2019). However, most hyperspectral systems are airborne (such as AVIRIS, HyMap), limiting spatial coverage and temporal frequency. In contrast, multispectral sensors (such as Landsat, Sentinel-2), though coarser in spectral resolution (that is, 4–15 broad bands), provide consistent, large-scale, and repeatable satellite-based monitoring, which is critical for long-term rangeland management (Chaves et al., 2020).

This technology can track vegetation greenness and categorise broad surface types, offering valuable insights for management policies and decision-making on national and global scales (Tehrany et al., 2017; Xue & Su, 2017); for example, Namibia's rangeland early warning and monitoring system (<http://www.namibiarangelands.com/>).

The assessment of rangeland condition has found success through the utilisation of hyperspectral and multispectral data obtained from satellite sources (Kumar & Mutanga, 2017; Lehnert et al., 2014; Retallack et al., 2023). This is typically accomplished using empirical statistical methods, often employing vegetation structural characteristics (Joetzjer et al., 2017; Santi et al., 2014; X. Zhang et al., 2021) and vegetation indices (Fern et al., 2018a; Retallack et al., 2023; Tian et al., 2021). The procedure entails establishing the correlation between on-site measured indicators of rangeland condition, such as AGB, and vegetation structural traits and vegetation indices like the Normalised Difference Vegetation Index (NDVI), Generalised Difference Vegetation Index (GDVI), Transformed Difference Vegetation Index (TDVI), and Enhanced Vegetation Index (EVI), which are commonly recommended for dryland systems (Fern et al., 2018a; Kumar & Mutanga, 2017; Tian et al., 2021).

However, semi-arid savanna rangelands pose unique challenges for satellite-based remote sensing due to cloud cover during the short growing season, high soil reflectance, low aboveground biomass, and a complex mosaic of bare ground, herbaceous, and woody plants (Collado, 2002). These factors often lead to inaccurate estimates of ecosystem parameters at the local scale (D. Lu, 2006). Moreover, the coarse resolution of freely available or affordable satellite data is generally insufficient for detailed rangeland management (Knox et al., 2013; Sankey et al., 2019). Fine-resolution satellite imagery, which can distinguish between different plant species, remains costly and is limited in temporal resolution (Aplin et al., 2021; Fang et al., 2020). Many studies use vegetation greenness as measured by the Normalised Difference Vegetation Index (NDVI) or Enhanced Vegetation Index (EVI) as indicators of 'ecosystem health' and available grass biomass. However, these indices can be fundamentally flawed when the biomass primarily consists of unpalatable vegetation (Fern et al., 2018a). As such, NDVI and EVI provide a crude measure of available forage, often failing to accurately represent the quality and usability of the biomass for grazing. To address these limitations, new approaches must be developed to improve the accuracy and applicability of remote sensing for rangeland management, enabling adaptive strategies for these dynamic

landscapes. UAVs have emerged as a promising source of information to help address these challenges.

2.5 Brief history of UAVs

The evolution of UAVs can be traced back to early innovations such as hot-air balloons, which marked the initial forays into UAV technology before the 1800s (Gülci et al., 2022). Throughout the 20th century, advancements in UAV technology and their associated equipment whether for military or civilian use have seen the integration of various payloads, including humans, sensors, and weapons (Palik & Nagy, 2019). The terminology surrounding UAVs has evolved, encompassing terms such as "remote-controlled aerial vehicles (Klodt et al., 2015), "remotely piloted systems (Frew & Brown, 2008)," "unmanned air platforms," and more specific names like "unmanned combat aerial vehicles" and "drones," among others. These terms reflect the ongoing development and diverse applications of UAVs over time (Gupta et al., 2013; Newcome, 2004).

Today, UAVs have diversified into numerous types for civilian applications, leveraging advanced technologies such as inertial measurement units (IMUs), Global Navigation Satellite System (GNSS) receivers, various sensors (including cameras, radar, and laser detection systems), digital memory for data recording, and telemetry systems for transmitting data to ground control stations (González-Jorge et al., 2017). The proliferation of UAVs with varying features has made them popular for both fully automatic and semi-automatic uses.

Modern UAVs, capable of both vertical and horizontal take-offs, are frequently employed in scientific research and social sciences, utilising commercial or open-source software and self-programmed applications (González-Jorge et al., 2017). These versatile UAVs, some as compact as a mobile phone, can execute photogrammetric flight plans with the onboard microprocessors (Gupta et al., 2013). Moreover, even amateur users can now operate UAVs equipped with advanced systems to facilitate safe autonomous flights with obstacle avoidance and assisted landing systems.

2.6 UAV technology in ecological research

In recent years, there has been a growing interest in the application of UAV remote sensing for in ecological research (Anderson & Gaston, 2013; Cunliffe et al., 2022; Fern et al., 2018a; Lussem et al., 2019; Slade et al., 2024; X. Zhang et al., 2021). UAVs offer several advantages over traditional plot level field measurements and satellite-based remote sensing, including user defined temporal resolution, and centimetre to decimetre level spatial resolution (Gallacher, 2019), and the ability to operate under different illumination conditions (Arroyo-Mora et al., 2021). These capabilities make UAVs particularly suited for the complex and heterogeneous landscapes typical of dryland rangelands.

To explore current peer-reviewed publications, Google Scholar, SCOPUS, PubMed, and Web of Science Core Collection were searched for current peer-reviewed publications using Boolean Operators (AND, OR) and a combination of keywords including: AGB, UAV, Fine-scale remote sensing, Structure from Motion photogrammetry, multispectral, hyperspectral, ecological monitoring, LIDAR, spectral reflectance, Canopy Height Model, drone, and High resolution. I used "snowballing" to gather additional studies, by searching for references within the bibliographies of published work. Relevant studies, articles, and reports focusing on advances in methods for assessing rangeland condition with UAVs were identified and organised into themes and topics.

To further explore and visualise the scientific interest in UAV technology, the '**EuropePMC**' R package (Jahn, 2016) was utilised. This package provides easy access to a comprehensive database of life sciences literature. By querying the database with specific keywords related to UAV applications in ecological research, visualisations (Figure 3) of publication trends over time were generated., highlighting the increasing number of studies focusing on UAV technology in ecological contexts, demonstrating a clear upward trend in both the volume and diversity of research in this field.

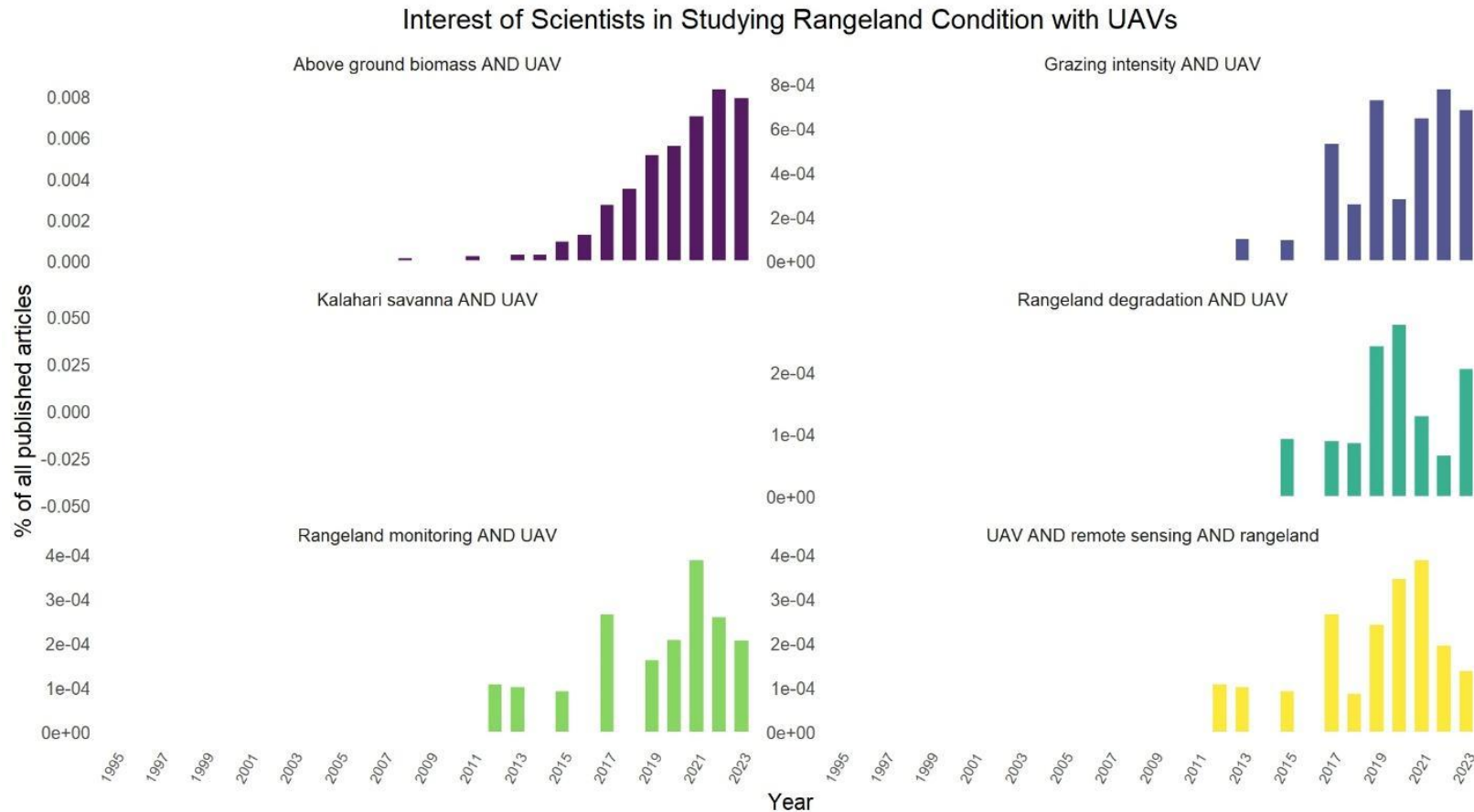


Figure 2. **There is an increasing interest in using UAVs to study rangelands.**

This figure shows the percentage of all published articles from 1995 to 2023 that include the specified keywords. Data was retrieved using the `europepmc` R package (Jahn, 2016) to query the Europe PubMed Central database. The plot indicates an increasing interest in the application of UAV technology in rangeland monitoring, with notable growth in publications focusing on UAV remote sensing and rangeland degradation.

UAVs have proven to be useful tools for a wide range of ecological applications, including monitoring vegetation structure and composition, assessing plant health, and measuring biomass and productivity (Crutsinger et al., 2016). UAVs equipped with multispectral and hyperspectral sensors can capture detailed spectral information, enabling the differentiation of vegetation types and the detection of stress indicators such as chlorophyll content and water stress.

In addition to AGB, UAVs have been employed in wildlife monitoring (Hartmann et al., 2021; Mangewa et al., 2019), habitat mapping, and the assessment of ecological disturbances such as fire and invasive species (Baskaran et al., 2017). The ability to rapidly deploy UAVs and cover large areas with fine-resolution imagery makes them invaluable for ecological surveys and long-term monitoring programs (Gallacher, 2019).

Overall, the integration of UAV technology into ecological research represents a significant advancement, offering new perspectives and capabilities for monitoring and managing rangeland ecosystems. By providing fine-resolution, timely, and accurate data, UAVs are transforming the way ecologists study and understand complex ecological processes.

2.7 UAVs in measuring AGB

Recently, there has been a growing interest in using UAV remote sensing to estimate AGB in rangelands. Structural and spectral features of rangelands have been employed for estimating grassland height and AGB (Amputu et al., 2023; Cunliffe et al., 2020, 2022; Doughty & Cavanaugh, 2019; Lussem et al., 2019; Slade et al., 2024). However, research is not well distributed globally, with African rangelands underrepresented (Figure 3). Generally, studies have followed a similar workflow to AGB in grasslands using UAV data. Although not all studies follow every step, the standard process was widely adopted in the literature reviewed (Amputu et al., 2023; Bareth & Schellberg, 2018; Cunliffe et al., 2020, 2022; Lussem et al., 2018; McIntire et al., 2022; Slade et al., 2023). Typically, the workflow included the following steps:

1. **Field data collection:** This step involves setting up ground control points (GCP), capturing UAV imagery, and collecting ground-based field data.
2. **UAV data processing:** This involves pre-processing steps such as creating photogrammetric 3D point clouds and orthomosaics, georeferencing these point clouds and orthomosaics, and generating canopy height models (CHM) using digital terrain models (DTM) and digital surface models (DSM). It also includes the derivation of spectral indices from multispectral UAV data.
3. **Data analysis:** This involves creating predictive models for AGB and/or vegetation indices.

The aim of the following sections is to provide a detailed description of this comprehensive workflow for AGB estimation in rangelands using UAVs, with a particular focus on the three main elements: field data collection, image pre-processing, and data analysis.

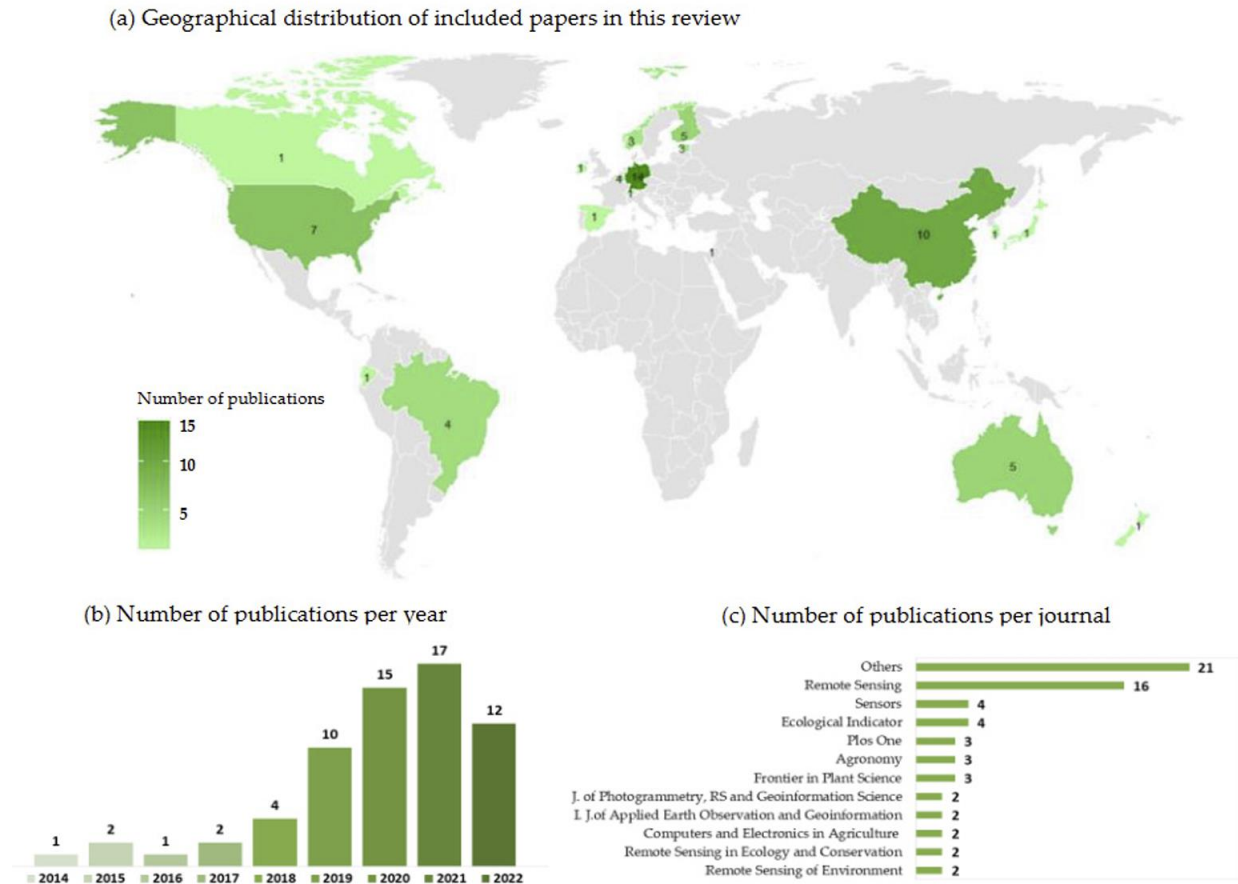


Figure 3. Geographic distribution of UAV-based AGB estimation studies (2012-2022). African rangelands are underrepresented in studies utilising UAV-based techniques to estimate aboveground biomass (AGB). This figure illustrates the geographic distribution of such studies included in a review, spanning the years 2012 to 2022 (Bazzo et al., 2023). The studies were identified using specific search terms and criteria.

2.7.1 Field data collection

The first step in the process for estimating AGB with UAVs is gathering field data. This step entails setting up ground control points (GCPs), collecting UAV images, and gathering ground-based field data. The precision of GCPs, which are used to add spatial constraint to the UAV data, is a critical component in the accuracy of models created from UAVs (Villanueva & Blanco, 2019). Furthermore, gathering information from ground-based measurements, such as biomass samples and vegetation height provides the data required for establishing the allometric relationship between AGB and drone measurements (Amputu et al., 2023; Cunliffe et al., 2020, 2022).

2.7.1.1 Setting up ground control points (GCPs)

To effectively constrain UAV models to ground values, one of the critical aspects that can significantly improve the quality of data products is the use of accurate and evenly distributed Ground Control Points (GCPs) (Cunliffe et al., 2019; Villanueva & Blanco, 2019; Yu et al., 2020). GCPs are distinct, visible markers (Figure 4) that are positioned at specific locations (Bazzo et al., 2023). These markers must be secured to prevent movement and geolocated using survey-grade GNSS equipment capable of sub-centimetre accuracy. Their placement, distribution, quantity, and density within the area of interest (AOI) play an important role in achieving both local and global accuracy across datasets collected over various periods (Gindraux et al., 2017). For applications requiring accurate measurements, such as vegetation monitoring, local precision is essential.



Figure 4. **Brightly coloured canvas GCPs with black backgrounds enhance visibility and precision.** The GCPs, measuring 50 cm x 50 cm, were constructed using brightly coloured canvas material with a black-painted background for enhanced visibility. The centre of each GCP was precisely measured using a DJI Phantom 4 multispectral drone, maintaining a 1 m altitude from the ground.

Finding the best method for GCP establishment is thus crucial to ensure accurate and consistent data while minimising operational time and costs. Several studies have explored different strategies for GCP placement to enhance the accuracy of UAV-derived Digital Surface Models (DSMs) (Awasthi et al., 2020; Gašparović et al., 2017; Gomes Pessoa et al., 2021). For example, a higher density of GCPs significantly improves the vertical and horizontal accuracy of DSMs (Villanueva & Blanco, 2019). Similarly, Yu et al., (2020) emphasised the importance of even distribution of GCPs, suggesting that an optimal configuration can reduce errors and improve the accuracy of spatial data. These findings highlight the trade-off between the number of GCPs used and the accuracy achieved, pointing towards the need for a balanced approach to GCP deployment.

Gindraux et al., (2017) provide a comprehensive analysis of how GCP density and distribution affect DSM accuracy. The study, conducted on glaciers in the Swiss Alps, found that DSM accuracy improves asymptotically with an increasing number of GCPs until an optimal density is reached. Beyond this point, additional GCPs do not significantly enhance accuracy. The research also noted that local accuracy decreases with increasing distance from the nearest GCP, approximately by 0.09 m per 100 m distance. These findings underscore the importance of strategic GCP placement, particularly in challenging environments such as the Kalahari savanna, where maintaining high accuracy is essential for monitoring changes in vegetation and dunes.

Establishing GCPs involves technical, logistical, and financial considerations, so optimising their deployment is key to balancing accuracy and efficiency. A carefully planned GCP setup can achieve high accuracy without excessive use of resources. For example, (Cunliffe & Anderson, 2019) recommend a systematic approach to GCP placement that involves evenly spacing the GCPs throughout the survey site, ensuring

coverage of both the edges and the centre of the site with multiple markers (Figure 5).

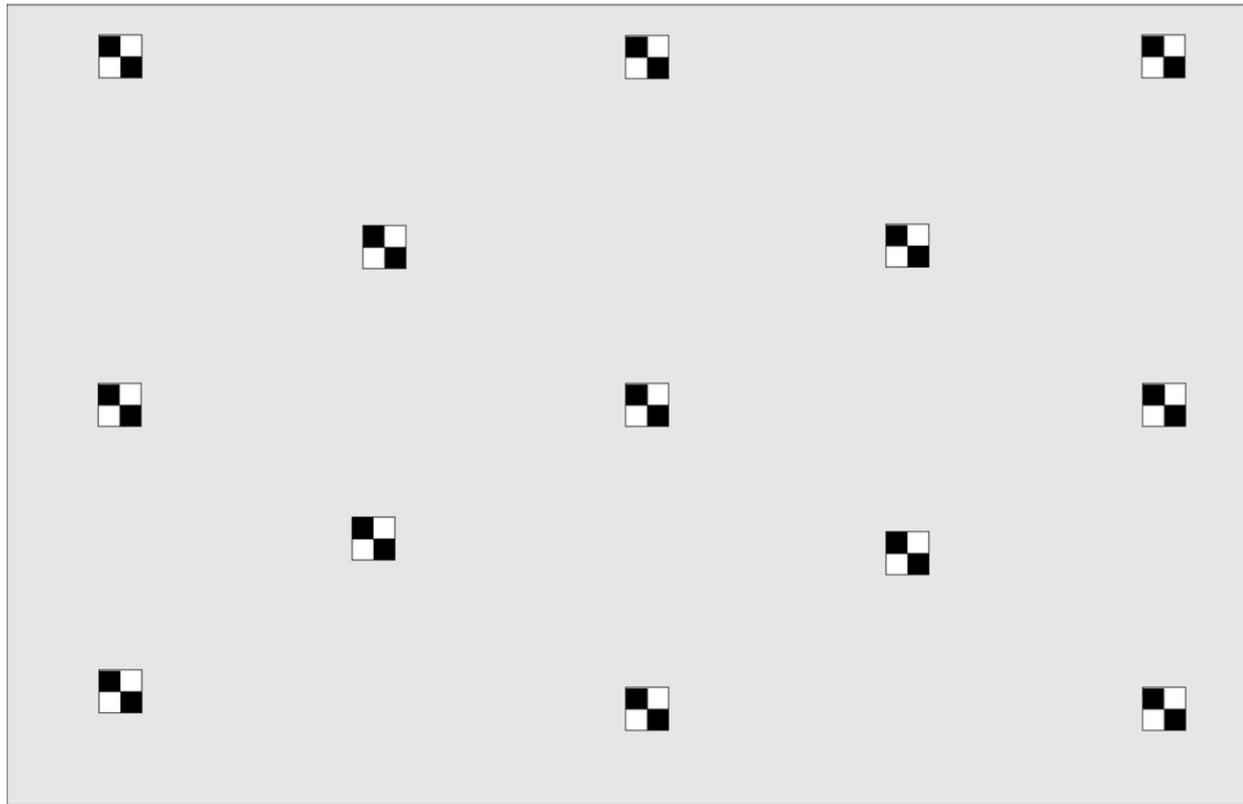


*Figure 5. **Accurate and evenly distributed GCPs significantly improve UAV data quality.*** This figure highlights that to effectively constrain UAV models to ground values, one of the critical aspects that can significantly improve the quality of data products is the use of accurate and evenly distributed Ground Control Points (GCPs) (Cunliffe & Anderson, 2019).

2.7.1.2 UAV surveys

UAVs have the capability to fly closer to the ground compared to satellites or full-scale manned aircrafts, broadening the range of available sensors and enhancing spectral imaging capabilities (Bazzo et al., 2023; Eskandari et al., 2020). They can capture spectral data using simple RGB cameras or more specialised cameras such as multispectral, thermal, or hyperspectral cameras (Bazzo et al., 2023; Mangewa et al., 2019; Vahidi et al., 2023). RGB sensors are the most frequently used, followed by multispectral, hyperspectral, and Light Detection and Ranging (LiDAR) sensors (Bazzo et al., 2023). In terms of resolution, sensors can be categorised as fine resolution (0 to 10 cm), medium resolution (10 to 20 cm), and low resolution (more than 20 cm) (Eskandari

et al., 2020). The majority of research utilises fine-resolution data (0 to 10 cm), employing this level of spatial detail, primarily using visible and multispectral images (Amputu et al., 2023; Cunliffe et al., 2020, 2022; Gašparović et al., 2017; McIntire et al., 2022). RGB are widely used because of their affordability and fine image resolution, which make them suitable for a wide range of applications.

The increasing availability of UAVs equipped with commercial RGB cameras has facilitated research using these cost-effective sensors for rangeland monitoring (Bareth & Schellberg, 2018; Cunliffe et al., 2022; Gašparović et al., 2017; Lussem et al., 2018). While RGB sensors have lower spectral resolution compared to multispectral, hyperspectral, or thermal sensors, they offer higher spatial resolution and can be used to calculate vegetation indices (Lussem et al., 2018; Marcial-Pablo et al., 2019) and estimate plant height (Cunliffe et al., 2022) from the same set of images. This makes RGB sensors an economical choice, particularly beneficial for farm-level applications. Over the past decade, near-infrared (NIR) multispectral and hyperspectral sensors have also become more accessible for UAVs (Assmann et al., 2019; Manfreda et al., 2018). Multispectral cameras, such as the MicaSense RedEdge 3, provide more spectral bands (e.g., red edge: 760 nm; NIR: 810 nm), offering fine-resolution spectral information for vegetation applications (Amputu et al., 2023).

Despite their limitations, LiDAR sensors outperform image-based techniques in terms of ground point capture and physical biomass parameter estimation, making them promising for AGB estimation in grasslands (Gašparović et al., 2017). However, commercial LiDAR sensors for UAVs remain significantly more expensive than spectral sensors, necessitating careful consideration of the most cost-effective sensor for each specific aim (Eskandari et al., 2020). UAV LiDAR collects data using a nadir view, which can be hindered by dense rangeland vegetation (Bazzo et al., 2023). LiDAR sensors tend to miss canopy data at the tops in grassland ecosystems, leading to underestimation of canopy height and fractional cover. Despite these challenges, LiDAR continues to show potential for accurate AGB estimation when calibrated with field data (Zhang et al., 2021).

Many interdependent factors during UAV flights have a substantial effect on the quality of UAV-based outputs and, as a result, the precision of AGB estimates (Mesas-Carrascosa et al., 2015). Flight altitude is one of the most important parameters as it influences the ground sampling distance (GSD) (Nagendran et al., 2018). The GSD, which determines the imagery's spatial resolution, is the distance between the centres of two adjacent pixels (DJI Enterprise, 2024). Higher altitudes result in a UAV's GSD to increase, which means that each pixel covers a greater ground area and reduces spatial resolution (Sanz-Ablanedo et al., 2018). This is advantageous for scanning wide areas as it allows more coverage. In heterogeneous environments, reduced spatial detail obscures fine-scale vegetation patterns, leading to higher uncertainty in pixel-level AGB estimates due to mixed-signal effects. Conversely, a lower GSD ensures higher spatial resolution, where each pixel represents a smaller, more homogeneous ground area, thereby capturing critical vegetation detail and minimizing spectral mixing errors (DJI Enterprise, 2024)

Studies have demonstrated that for UAV photogrammetry of vegetation structure, optimal results are achieved when flying at altitudes scaled to canopy height (typically 17-22 m above vegetation), yielding a ground sampling distance of approximately 0.005 m (Cunliffe et al., 2019). This approach has proven particularly valuable for aboveground biomass estimation across diverse ecosystems (Amputu et al., 2024; Cunliffe et al., 2022). UAV flight altitudes range from <10 m to 140 m, with 50 m representing the median value (23% of cases). Lower altitudes (<50 m) are generally more frequent than higher ones (Figure 6: Bazzo et al., 2023). They also advised experimenting with different altitudes to better understand the relationship between pixel resolution and field data for AGB estimation. While a 25 m flight height delivered the best grassland AGB estimation model, UAV data collected at 100 m provides key benefits for farm-scale applications, including wider coverage, faster acquisition, and smaller file sizes that streamline data processing (Karunaratne et al., 2020). Therefore, to develop best practice guidelines for using UAVs in on-farm applications and to keep pace with technological advancements, it is essential to understand the effects of different flying altitudes on the quality of grassland AGB predictions. Researchers should also determine the necessary GSD for identifying features relevant to AGB estimation, considering the specifications of the

sensor used. To balance spatial resolution, acceptable error, and point cloud density with optimal coverage, we recommend flying where a GSD of 0.005 m is achievable.

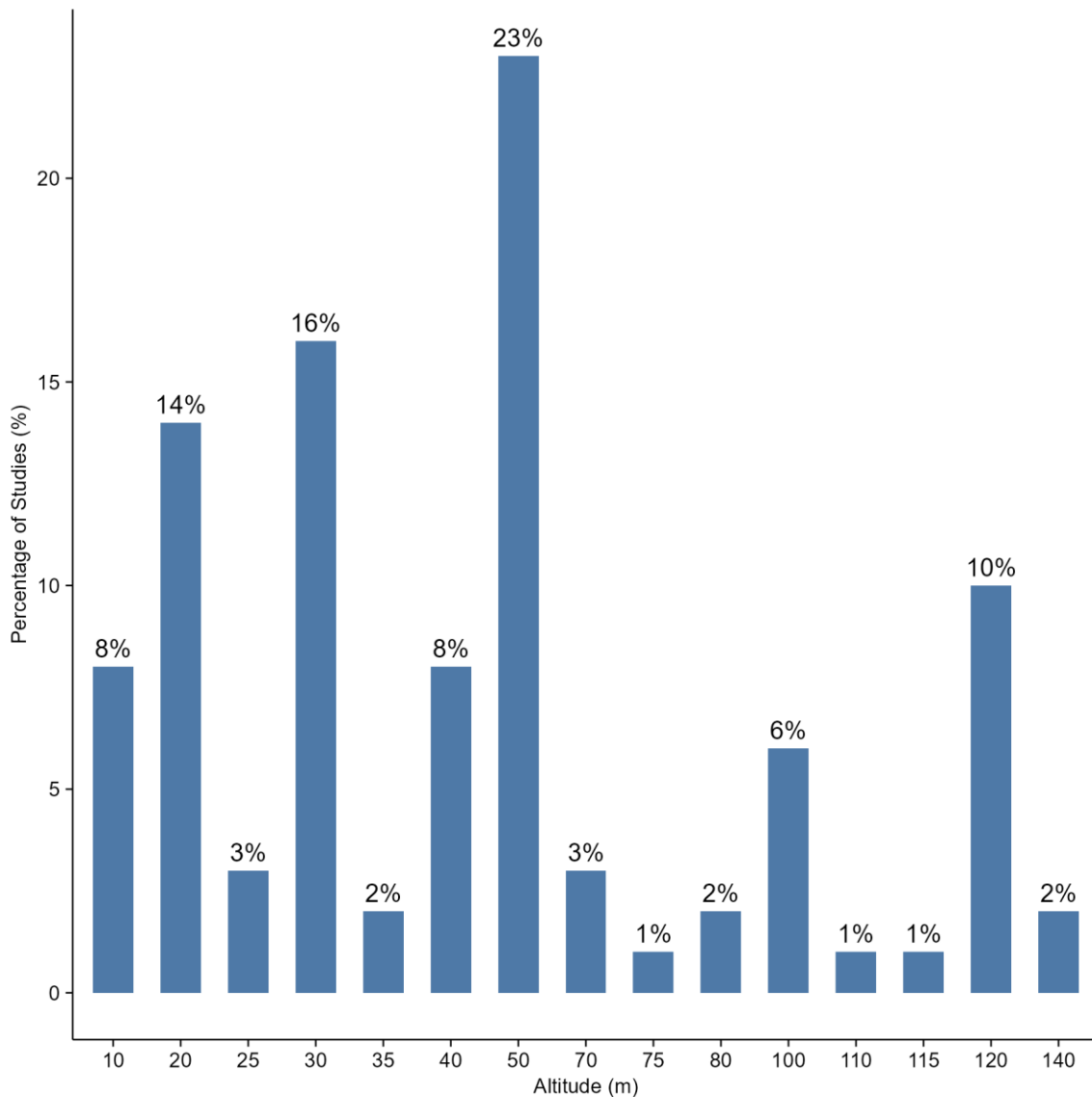


Figure 6. Fifty meters is the most frequently used UAV flight altitude among the 64 reviewed studies (Bazzo et al., 2023). Less commonly reported altitudes occurred in fewer than 10% of studies (Bazzo et al., 2023).

The flight sequence of a UAV also influences data quality. Determining the forward and side image overlap is crucial in mission planning, particularly for SfM photogrammetric

reconstructions, which rely on features visible in multiple photos to create digital models, orthomosaics, and 3D models (Bazzo et al., 2023; Cunliffe & Anderson, 2019). The level of image overlap can affect the quality of the final SfM product, with higher overlap resulting in more accurate models. However, higher overlap requires capturing more photos, which increases data volumes and computing time (Tmušić et al., 2020). There is general consensus on the overlap thresholds for rangeland applications (Amputu et al., 2023; Cunliffe et al., 2020, 2022; McIntire et al., 2022). Most studies have used significant front and side overlaps, typically 80% forward overlap (resulting in approximately 5-6 photos per part of the scene) and 70% side overlap (resulting in around 4-5 photos per side). Research consistently shows that a forward overlap of 80% and a side overlap of 60–75% produce high-quality orthomosaics. Cunliffe et al., (2022) reported that optimal overlaps for Structure from Motion (SfM) photogrammetry over grassy ecosystems are 75% forward and 75% side. This results in a minimum of approximately 33 images per unobscured location (Cunliffe & Anderson, 2019).

When measuring vegetation canopy height using SfM, it is crucial to consider the use of convergent flights flown at off-nadir angles. Employing off-nadir imagery and conducting flights at slightly higher altitudes are postulated to significantly enhance measurement accuracy (Cunliffe et al., 2016). Research indicates that capturing off-nadir images with angles between 20° and 35° during two convergent flights provides the optimal combination for achieving the highest accuracy and precision (Agüera-Vega et al., 2022; Cunliffe et al., 2022).

2.7.1.3 Ground based field data

Effective biomass estimation models derived from UAV data rely heavily on accurate and comprehensive ground-based field data collection. This is necessary so as to establish, train, and assess biomass estimation models obtained from UAV data (McIntire et al., 2022). Typically, this process involves gathering quantitative data directly from the vegetation, which is then used as a reference for measurements derived from UAVs. Conventional ground-based techniques can be either destructive or non-destructive (Bazzo et al., 2023). Destructive techniques, like harvesting and weighing biomass

(Amputu et al., 2023; McIntire et al., 2022), yield precise measurements but are labour and time intensive. Among the non-destructive techniques with the most documented applications is the use of the point intercept method (Cunliffe et al., 2020) and the rising plate metres (RPM) (Borra-Serrano et al., 2019; Lussem et al., 2018; Zambatis et al., 2006). RPMs are commonly used because they are effective at producing accurate estimations of biomass. They measure compressed sward height, which integrates height and density across a given area. RPM techniques, however, are less successful in areas with non-uniform growth or rough terrain and might be impacted by operator variability (Amjad, 2014). Destructive approaches are still the preferred approach for establishing and training UAV-derived AGB models in spite of their drawbacks.

In regions with heterogeneous vegetation and high dynamics, frequent sampling over extended periods and with large sample sizes is required to provide robust biomass estimates (Franceschini et al., 2022). Increasing dataset size is critical for improving AGB estimation models in grasslands, as larger and more representative field samples enhance model accuracy. Limitations such as small sample sizes and the complexity of field trial methodologies can hinder model performance. A review of UAV-based AGB estimation techniques found field sample sizes ranging from 13 to 1403, with an average of 90 (Bazzo et al., 2023; Capolupo et al., 2015; Lin et al., 2021; Morais et al., 2021). Thus, addressing the limitations of sample size and methodological complexity is vital for enhancing the robustness of AGB estimation models derived from UAV data in diverse and dynamic rangeland ecosystems.

2.7.2 UAV data processing

The UAV image preprocessing step is essential to ensure the data's suitability for further analysis. Images captured during a UAV flight are often converted into 3D data using SfM software. This 3D data enables the classification of various objects within the captured imagery. Several companies offer software solutions for processing UAV photographs, providing functionalities such as generating 3D spatial data for Geographic Information Systems (GIS) platforms, creating DTMs and DSMs, producing georeferenced orthomosaics, and performing area and volume measurements.

While there is a growing body of research on extracting canopy height from 3D point clouds generated by RGB photogrammetry, it remains less extensive compared to the more established body of work using LiDAR. However, as computer and photogrammetry technologies have advanced, the wider use of SfM has emerged as a significant trend. Different SfM software packages employ various algorithms and processing options, which can influence the final outputs. Among the commonly used software, Agisoft Metashape (Agisoft, 2024) and Pix4Dmapper (Pix4D, S.A., Lausanne, Switzerland) are frequently mentioned in literature for processing UAV imagery (Amputu et al., 2023; Balestra et al., 2024; Cunliffe et al., 2022; Gülci et al., 2022). Additionally, other software like QGIS, ArcMap, and TerraScan are also utilised in different studies (Duarte et al., 2018; Parent et al., 2022).

Despite the widespread use of these software solutions, few studies have compared their preprocessing capabilities directly. Experiments comparing Agisoft Metashape and Pix4Dmapper found that while Metashape produced clearer images, it had poorer displacement extraction, whereas Pix4Dmapper, despite z-value fluctuations, excelled in displacement extraction. A comparative study over a 235.2-hectare forested area showed that Agisoft Metashape generated more detailed results from UAV-SfM (Fraser & Congalton, 2018; Kitagawa et al., 2018).

The first essential step in UAV data processing is the generation of a sparse point cloud. This step entails identifying and matching feature points across multiple images to reconstruct an initial 3D structure of the surveyed area (James et al., 2013; Westoby et al., 2012). The sparse cloud acts as the base framework for further densification and 3D modelling. During this process, the software detects distinct features in the images and triangulates their positions in three-dimensional space (Turner, 2005). The precision and quality of the sparse cloud are critical, as they significantly influence the accuracy of the dense point cloud and other derived products such as DTMs, DSMs, and Orthomosaics (Fonstad et al., 2013). This foundational stage is crucial to ensure that subsequent data processing steps produce precise and reliable spatial information.

Accurate georeferencing relies heavily on reliable ground reference data. By pinpointing GCPs with known coordinates visible in the imagery, a transformation can link the point cloud coordinate system to a real-world coordinate system, thus georeferencing the point cloud derived from SfM data (Bazzo et al., 2023). Numerous studies have underscored the importance of GCPs for the geometric correction of UAV images (Awasthi et al., 2020; Gallacher, 2019; Villanueva & Blanco, 2019).

After geometric correction, the georeferenced sparse cloud is converted into a dense point cloud (Agisoft, 2024). The software aligns the images to compute depth information for all points. This dense point cloud can then be exported as a Digital Elevation Model (DEM), which is crucial for constructing a Canopy Height Model (CHM) of the vegetation. Typically, two types of DEMs are created, i.e., DTM, representing the ground, and (2) DSM, which includes the canopy.

DEMs are raster representations of elevation data, encompassing both DTMs and DSMs (Höfle & Rutzinger, 2011). While DTMs depict the bare-earth surface, DSMs include all above-ground features such as vegetation canopy. In UAV-based surveys, DTMs are typically derived through ground-point classification of dense point clouds, while DSMs represent the highest surface returns (A. M. Cunliffe et al., 2022; Slade et al., 2024).

There are two main methods for extracting CHM information from UAV data. The first involves generating both DSM and DTM in raster format, with CHM being the difference between DSM and DTM (Cunliffe et al., 2022; Grüner et al., 2019; Slade et al., 2024). Slade et al. (2024) calculated CHM for each point in the point cloud by using the difference between the interpolated DTM raster of the harvest plots. This method is straightforward and quick due to raster analysis, but it may cause unwanted data smoothing, particularly in heterogeneous ecosystems, leading to a loss of CHM variability (Viljanen et al., 2018). The second method uses the raw SfM point cloud dataset instead of an interpolated DSM raster (Tian et al., 2021). Evaluations have shown that both methods produce similar

DTMs and correlations to AGB in grasslands (Viljanen et al., 2018). However, Tian et al., (2021) argues that using raw SfM point cloud data is rapid and preserves the fine-scale variability of the canopy structure, making it a superior choice for vegetation analysis.

Creating a high-quality DTM with precise and accurate terrain representation is essential for deriving reliable estimates of vegetation structure from UAV imagery, which in turn is critical for dependable AGB estimation (Tian et al., 2021). High vegetation density can impede the production of accurate DTMs due to insufficient ground points, while moderate density facilitates easier extraction of ground points (Zhang et al., 2021). When ground points can be identified to them from points above ground from a point cloud, manual GPS point collection for creating the DTM is an alternative but is too time-consuming for large sampling areas (El-Ashmawy, 2014).

Exporting a multispectral orthomosaic allows for the calculation of various vegetation indices, including the Normalised Difference Vegetation Index (NDVI) and several indices specifically adapted for dryland ecosystems. Notably, the Generalised Difference Vegetation Index (GDVI), the Optimised Soil Adjusted Vegetation Index (OSAVI), with an optimum constant of 0.16 as determined by Fern et al., (2018b), and the Transformed Difference Vegetation Index (TDVI) have all been tested for their effectiveness in predicting plant biomass (Baghi & Oldeland, 2019; Fern et al., 2018b). These indices can be used for assessing vegetation health, biomass, and productivity, and are frequently used as proxies for estimating AGB. Studies indicate that using vegetation indices in ecological assessments improves the understanding of spatial patterns and temporal changes in vegetation, making them invaluable tools in remote sensing applications focused on AGB estimation (Anuar et al., 2023; Fern et al., 2018b).

2.7.3 Predictive model generation

The effectiveness of UAV-derived models in accurately predicting AGB is influenced by various factors related to the methodologies employed in the analysis. Studies using UAVs to estimate AGB were reviewed and the data analysis techniques and key findings are summarised (Table 1). A significant number of these studies utilised statistical

regression methods, including ordinary linear regression (OLR), random forest (RF), polynomial regression (PR), stepwise linear regression (SWL), multiple linear regression (MLR), and partial least squares regression (PLSR).

Cunliffe et al., (2020) reported coefficients of determination of $R^2 = 0.90$ for canopy height and R^2 ranging from 0.14 to 0.23 for NDVI using OLS regression. Viljanen et al. (2018) achieved a high coefficient of determination ($r^2 = 0.98$) using MLR at a mixed grass experimental site with RGB and hyperspectral sensors. In a study by Maesano et al., (2022), utilising integrated UAV RGB images, LiDAR data, and ground truth data, two modelling techniques, SWL and RF were assessed for predicting above ground biomass in a wooded watershed in Southern Italy. When compared to the SWL model, the RF model showed better accuracy; its coefficient of determination, R^2 increased from 0.81 to 0.86. Furthermore, the RF model decreased the mean absolute error (MAE) from 34.2 to 22.1 Mg ha⁻¹ and the root mean square error (RMSE) from 45.5 to 31.7 Mg ha⁻¹.

Villoslada et al., (2020) also noted high R^2 values using RF and MLR (0.981). RF has shown competitive accuracy in biomass estimation compared to other methods in agricultural contexts. Additionally, Morais et al., (2021) provided a review highlighting the application of machine learning for estimating biomass in grasslands, with RF being the most utilised method, followed by PLSR. However, the outcomes of these studies vary significantly, making comparisons challenging, due largely to differences in the study areas and the sensor technology used (RGB, multispectral, etc).

To fully understand the predictive capabilities of UAV-derived data for estimating AGB, it is essential to explore two critical factors: structural information and spectral reflectance.

2.7.3.1 Structural information as a proxy for AGB

Structural features derived from UAV data, such as canopy height, volume, and density, have proven useful as proxies for estimating vegetation AGB (Table 1). These metrics provide valuable insights into biomass, with varying degrees of accuracy depending on the species studied, the structural features used, and the modelling approach.

Table 1. UAV derived structural information used to model vegetation biomass.

Type	Variable used	Reference
Height	Mean height	(Cunliffe et al., 2016, 2020, 2022; Jing et al., 2017; Lu et al., 2019; Maimaitijiang et al., 2019; McIntire et al., 2022; Slade et al., 2024; Wijesingha et al., 2019)
	Maximum height	(Jayathunga et al., 2019; Jiang et al., 2019; Maimaitijiang et al., 2019; Niu et al., 2019)
	Minimum height	(Domingo et al., 2019; Jayathunga et al., 2019; Maimaitijiang et al., 2019; Wijesingha et al., 2019; Zahawi et al., 2015)
	Median height	(Lu et al., 2019; Michez et al., 2018; Roth & Streit, 2018; Wijesingha et al., 2019; Zahawi et al., 2015)
	Mode of height	(Domingo et al., 2019)
	Count of height	(Wijesingha et al., 2019)
	Standard deviation of height	(Jayathunga et al., 2019; Jiang et al., 2019; Jing et al., 2017; Lu et al., 2019; Maimaitijiang et al., 2019; Wijesingha et al., 2019; Zhang et al., 2021)
	Coefficient of variation of height	(Jayathunga et al., 2019; Jing et al., 2017; Lu et al., 2019; Maimaitijiang et al., 2019)

	Variance of height	(Domingo et al., 2019)
	Skewness of height	(Domingo et al., 2019; Kachamba et al., 2016; Moeckel et al., 2017)
	Kurtosis of height	(Domingo et al., 2019; Kachamba et al., 2016; Moeckel et al., 2017)
	Entropy of height	(Jiang et al., 2019)
	Relief of height	(Jiang et al., 2019; Moeckel et al., 2017)
	Height percentile	(Domingo et al., 2019; Jiang et al., 2019; Kachamba et al., 2016; Moeckel et al., 2017; Niu et al., 2019; Ota et al., 2019; Roth & Streit, 2018; Wijesingha et al., 2019)
	Canopy point density	(Domingo et al., 2019; Jayathunga et al., 2019; Kachamba et al., 2016)
	Proportion of points > mean height relative to total number of points	(Domingo et al., 2019; Jayathunga et al., 2019)
	Proportion of points > mode height relative to total number of points	(Domingo et al., 2019)
Canopy density and	Crown/vegetation area (canopy cover)	(Guerra-Hernández et al., 2017; Maimaitijiang et al., 2019; Roth & Streit, 2018)
	Canopy relief ratio	(Domingo et al., 2019)

	Crown isle- proportion of site (Zahawi et al., 2015) where canopy has height greater than 2/3 of the 99 th percentile of all heights
	Canopy openness— (Zahawi et al., 2015) proportion of site area <2m in height
	Canopy roughness— (Zahawi et al., 2015) average of SD of each pixel from mean CHM
Volume	Canopy/crown volume (Alonzo et al., 2018; Ballesteros et al., 2018; Guimarães et al., 2020; Maimaitijiang et al., 2019)
	VI-weighted canopy volume
Change based	Amount of change in DSM (Ota et al., 2019) before and after plant removal
Other	Height*Spectral (various (Bendig et al., 2014; Peña et al., 2018; spectral indices) Yue et al., 2017)
	Grassl (RGBVI+CHM (Possoch et al., 2016)
	TIN-based structure, area, (Jiang et al., 2019) slope

Height metrics: Canopy height is one of the most commonly used structural metrics, with studies reporting strong relationships between height measurements and AGB across different ecosystems. For example, maximum and median height are particularly effective for woody plants, including trees, where height strongly correlates with biomass (Guerra-Hernández et al., 2017; Lin et al., 2018). Conversely, non-woody plants, such as grasses, show strong associations with mean canopy height (Bendig et al., 2015; Cunliffe et al., 2022). However, height measurements alone may sometimes overestimate AGB, particularly in dense or heterogeneous canopies, where capturing the full vertical extent can be challenging (Bendig et al., 2015; Grüner et al., 2019).

Volume and density metrics: Canopy volume and density are additional structural features that can enhance AGB estimation, particularly when used in conjunction with height data. Volume, for example, has been shown to perform well in predicting biomass, particularly in crop systems such as onion fields (Ballesteros et al., 2018). However, sparse and heterogeneous canopies remain difficult to model accurately, which can reduce the precision of biomass estimates in some ecosystems (Grüner et al., 2019). These challenges highlight the importance of selecting appropriate structural metrics based on canopy structure and vegetation type.

Integrating structural features: Combining multiple structural metrics such as height, volume, and canopy density often leads to improved accuracy in AGB models. Studies have shown that integrating several height measures or combining height with spectral information can result in more reliable predictions. For example, random forest models that include both structural and spectral features have demonstrated high accuracy in estimating AGB for both tropical trees and crops like maize (Cen et al., 2019; Jayathunga et al., 2019).

Challenges and limitations: Despite the potential of structural features, several factors can affect model accuracy. These include the quality of the geometric control used in SfM reconstructions (James et al., 2013), as well as environmental factors like shadows, sun angle, and wind-induced movement (Cunliffe et al., 2022). Additionally, variations in biomass accumulation patterns such as differences between tall-growing versus

sprawling species can complicate the use of structural features for AGB estimation (Grüner et al., 2019; Roth & Streit, 2018).

In summary, structural metrics derived from UAV data, particularly canopy height, volume, and density, are valuable tools for estimating AGB in various ecosystems. While these metrics can provide moderate to excellent accuracy, their effectiveness depends on the specific vegetation type, the combination of metrics used, and the methodological approach. The integration of structural features with spectral data can further enhance model performance, though challenges related to canopy structure and environmental factors must be carefully considered.

2.7.3.2 Spectral reflectance as a proxy for AGB

The use of vegetation indices derived from UAV data has become crucial in monitoring and estimating AGB in rangelands. Indices such as the NDVI, Normalised Difference Weighted Index (NDWI), Weighted Difference Vegetation Index (WDVI), and Optimised Soil Adjusted Vegetation Index (OSAVI) are widely used due to their ability to utilise the near-infrared (NIR) and red wavebands (R) (Amputu et al., 2023; Bazzo et al., 2023; Fern et al., 2018b). Among these, NDVI has been the most commonly applied index for AGB estimation (Cunliffe et al., 2020; Fern et al., 2018b; Lee et al., 2016). Although NDVI is sensitive to chlorophyll-containing leaves, particularly during the vegetative growth phase, it has limitations as its response saturates at a leaf area index (LAI) of 2 to 3, leading to inaccuracies in fully vegetated areas (Davi et al., 2006). Furthermore, estimating biomass from vegetation indices can be challenging due to the asymptotic relationship between biomass and surface reflectance. As biomass increases, the amount of radiation absorbed by the vegetation approaches saturation, and changes in biomass may not result in proportional changes in reflectance (Colomina & Molina, 2014; Cunliffe et al., 2020; Myers-Smith et al., 2020b). This makes it difficult to accurately estimate biomass using spectral reflectance, especially at higher biomass levels (> 1500 kg/ha) (Amputu et al., 2023; Prabhakara et al., 2015; Théau et al., 2021).

Previous research has shown strong relationships between vegetation indices and AGB in grassland ecosystems. For instance, studies in Botswana rangelands have reported

high coefficients of determination for ground cover and AGB estimation (Wylie et al., 2002). However, the effectiveness of these indices can vary due to factors such as spatially-variable soil backgrounds and the presence of senescent vegetation (Todd et al., 1998). In semi-arid environments like the Kalahari, soil-vegetation spectral mixing can distort AGB estimation, necessitating the use of soil-adjusted indices such as OSAVI and the Soil Adjusted Total Vegetation Index (SATVI) (Amputu et al., 2023).

Fajji et al., (2017) conducted their study in semi-arid Kalahari savanna environments and found that vegetation indices, particularly NDVI and SAVI, were less effective in predicting AGB in areas with high grazing intensity compared to those with low grazing intensity. This reduced effectiveness was attributed to the presence of senescent or dry vegetation and a higher proportion of bare soil in heavily grazed sites. In these areas, the accumulation of standing dead material and litter increases, resulting in more exposed ground. As such, since non-photosynthetic vegetation reflects more visible light, indices relying on the contrast between visible and near-infrared reflectance are likely to struggle to accurately estimate AGB. Moreover, the increased reflectance from dry vegetation further restricts the response of spectral indices to biomass variations, particularly as the contrast between green biomass and dry soil diminishes when vegetation dries out. Cunliffe et al., (2020) found that NDVI had a positive relationship with AGB but explained only a small proportion of the variance (R^2 between 0.14 and 0.23). The presence of moss cover significantly influenced the NDVI-phytomass relationship, suggesting limitations in using NDVI to estimate biomass in complex Arctic ecosystems.

In the Kalahari savanna context, similar challenges may be observed as a result of the heterogeneous vegetation. Stress-related indices, which respond to both near and middle infrared wavelengths, have shown promise in other regions in the Kalahari plateau by accurately predicting vegetation cover (Amputu et al., 2023, 2024b). This underscores the need for novel and context specific approaches to improve AGB estimation accuracy in semi-arid rangelands.

In summary, the relationship between vegetation indices and AGB is highly species and location specific. Commonly used indices must be rigorously tested to evaluate their effectiveness in different environments, including the Kalahari savanna. Previous studies have highlighted the need for high-accuracy AGB estimation methods, particularly in semi-arid regions where traditional indices may fall short due to complex spectral responses from heterogeneous vegetation and soil backgrounds.

2.8 Conclusions

The performance and generalisability of vegetation AGB estimation findings can be strongly impacted by several parameters at different stages of the biomass modelling process, from data collection to analysis. The type and stage of vegetation development have an impact on plant canopy density and structure, which in turn have an impact on UAV AGB modelling. When designing methodologies for AGB estimation, each of these variables should be carefully taken into consideration since they have an influence on how useful spectral and structural metrics are for precisely estimating and predicting plant biomass. The following key findings were drawn from the literature review.

- There has been a growing interest in the application of UAV remote sensing for in ecological research
- There is a lack of studies applying UAVs to estimate AGB in the specific ecological context of African rangelands highlights.
- The heterogeneity, growth stage, and kind of grassland can all have a significant impact on the AGB estimate model.
- Lower altitude flights increase spatial resolution (and reduce GSD), consequently improving AGB estimates. It is recommended to fly at altitudes that will allow the attainment of desired GSD.
- Better data quality can be obtained by combining self-calibration during photogrammetric processing with large picture forward and side overlaps of around 75-80%.
- The accuracy of georeferencing models is increased when a greater number of ground control points are distributed uniformly across the investigation.

- There were observed good to excellent associations ($R^2 = 0.54\text{--}0.99$) between structural measures and AGB. The mean canopy height was better suitable for herbaceous vegetation.
- Structural metrics are less effective for herbaceous plants that accumulate biomass by growing low and spreading outwards, as opposed to those that grow tall and narrow.
- With an R^2 ranging from 0.36 to 0.94, multispectral data may estimate vegetation biomass with moderate to exceptional accuracy. When examined, NIR-based indices showed a good correlation with vegetation biomass, with NDVI regularly ranking among the most important model variables.
- The presence of senescent or dry vegetation and a higher proportion of bare soil may reduce the robustness of vegetation indices prediction models.

2.9 Research gaps and future directions

In conclusion, the integration of UAVs in rangeland assessment offers significant potential for improving our understanding of herbaceous biomass dynamics and its role as an indicator of rangeland condition. This literature review shows that across a wide range of plant functional types in heterogeneous environments, precise estimations of AGB may be obtained using UAV-derived data. However, research is not well distributed globally, with African rangelands underrepresented and heterogeneity in rangelands and plant growth stages could greatly influence the estimation of AGB. Therefore, more research is needed in significant regions such as Kalahari savanna ecosystems. Most plant functional types can have a reliable AGB prediction using spectral and/or structural UAV data.

3 Methodology

3.1 Study site description

3.1.1 Location

The study was conducted in Zutshwa village (Figure 7) in Botswana (24.1186°S, 21.2464°E), located in Kgalagadi District 2 (KD2), which is a Wildlife Management Area (WMA) covering 6425 km² in the southwest of Botswana (Keeping et al., 2018). In Botswana, a Wildlife Management Area (WMA) is a designated region primarily aimed at conserving wildlife and their habitats. These areas are intended to be managed to maintain sustainable wildlife populations while allowing for regulated human activities that do not disrupt the ecological balance. WMAs serve as critical buffer zones around national parks and game reserves, providing essential corridors for wildlife movement and reducing human-wildlife conflict (Heermans et al., 2021; Keeping et al., 2018). WMAs also play a significant role in community-based natural resource management (CBNRM) initiatives, where. Through CBNRM, local communities are actively involved in the management of these areas, benefiting economically from eco-tourism, sustainable hunting, and other wildlife-related activities. This collaborative approach integrates conservation objectives with the socio-economic development of local communities, fostering a harmonious coexistence between humans and wildlife (Mbaiwa, 2005).

Zutshwa, the sole community within KD2, has a population of approximately 500 residents consisting mainly of Basarwa and Bakgalagadi people (Kalahari Research & Conservation, 2018). This setting offered a natural spectrum of grazing intensities, ranging from heavily grazed areas closer to settlements around Zutshwa, to less impacted areas further away from the settlements, still within the WMA. This allowed us to collect a dataset encompassing a range of vegetation states reflecting different levels of grazing impact and different herbaceous species allowing us to develop robust biomass models that can be applied in other settings.

Livestock mainly graze closer to settlements, close to boreholes and occasionally further away from boreholes (Akanyang, 2019). This influences the vegetation dynamics in the

area, and the distribution of large herbivores such as the Blue wildebeest (*Connochaes taurinus* Burchell), Common Eland (*Tragelaphus oryx* Pallas), and Gemsbok (*Oryx gazella* Linnaeus) which are then restricted to graze in WMAs due to competition from livestock (Akanyang, 2019).

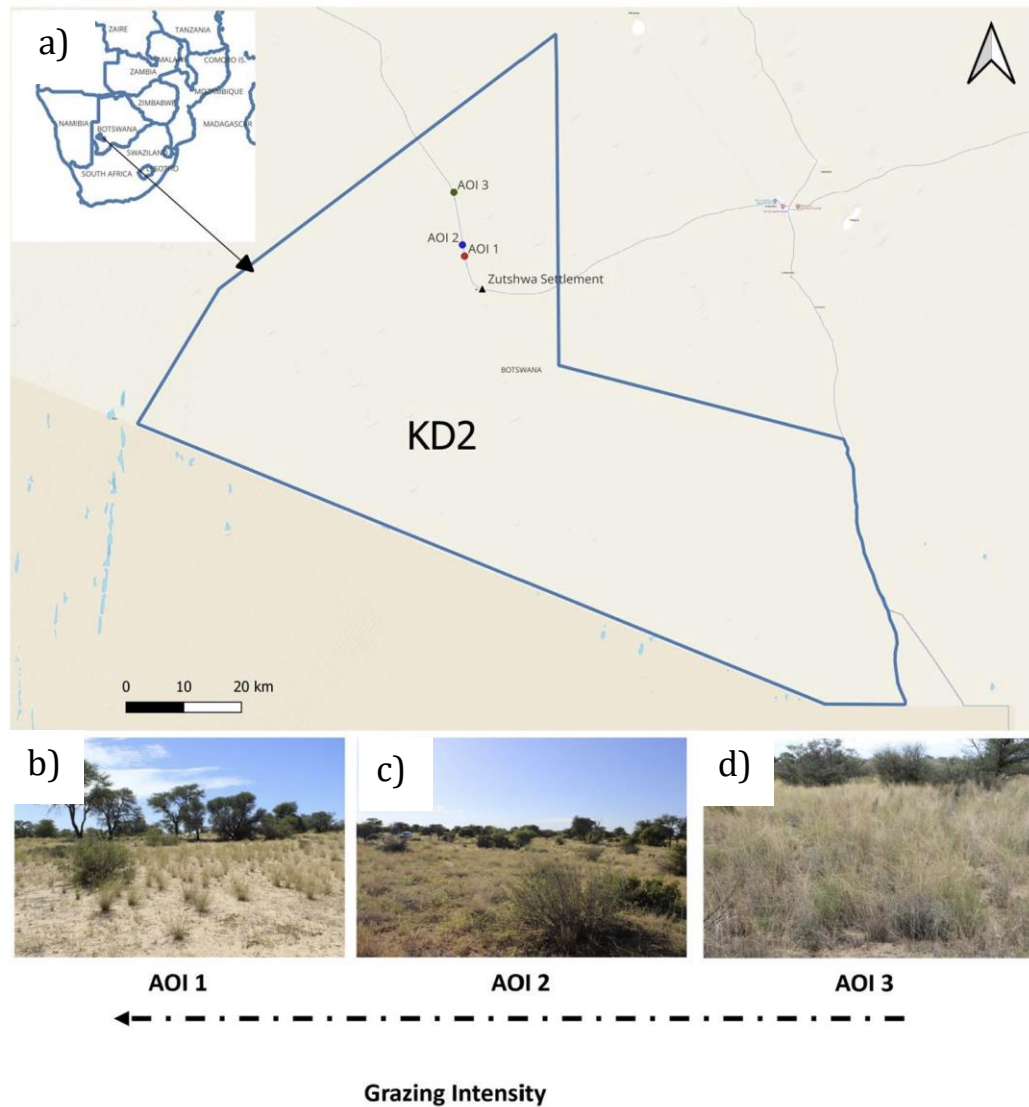


Figure 7. Geographic distribution of study sites and grazing intensity in the Kalahari Plateau, Southwest Botswana. The figure illustrates the location of the study area and the varying grazing intensities across different areas of interest (AOIs) in Zutshwa. a) Location of the study site in relation to Africa and Botswana. b) Photo of AOI 1, an area with high grazing intensity. c) Picture of AOI 2, an area with moderate grazing intensity. d) Picture of AOI 3, an area with low grazing intensity (Photos taken on 25/03/24)

3.1.2 Dune system

South of the Kalahari plateau, there are two noticeably different types of sandy terrain: to the east and northeast, the surface is relatively flat and undulating, whereas in the west and southwest, the sands form dunes (Leistner, 1967). The study focuses on this second type, the dune-covered, southernmost part of the expansive Kalahari system. The dunes predominantly form lengthy and nearly parallel ridges; however, intermittently, they merge or separate, creating a pattern reminiscent of ripple marks (Leistner, 1967; Lewis, 1936). The typical elevation of the dune crest is 8.23 m, although the tallest dune can exceed a height of 30 m (Lewis, 1936). Kalahari sand dunes can manifest in two distinct states: stabilised dunes, achieved through factors such as vegetation cover or calcrete formation, and mobile dunes, wherein the dunes are prone to movement. It is noteworthy that the study area under consideration features dynamic, mobile sand dunes (Leistner, 1967).

3.1.3 Climate and pans

The region's climate is arid, characterised by hot summers and mild winters, with a mean annual rainfall of 240 mm (Figure 8). Precipitation primarily occurs between November and April (Maruatona & Moses, 2022). Surface water is thus a limiting factor in the Kalahari. In the southern Kalahari, one can observe the presence of pans, which retain water during the rainy season (Lancaster, 1978). These pans are typically characterised as shallow, flat-bottomed depressions that intermittently hold water (Leistner, 1967). They are commonly situated in conjunction with level terrain that exhibits minimal to no significant surface slope. The majority of settlements are situated near these pans, enabling the manual digging of wells by hand to access groundwater beneath the pans, which are also frequented by both livestock and wildlife for drinking water (Government of Botswana, 2000).

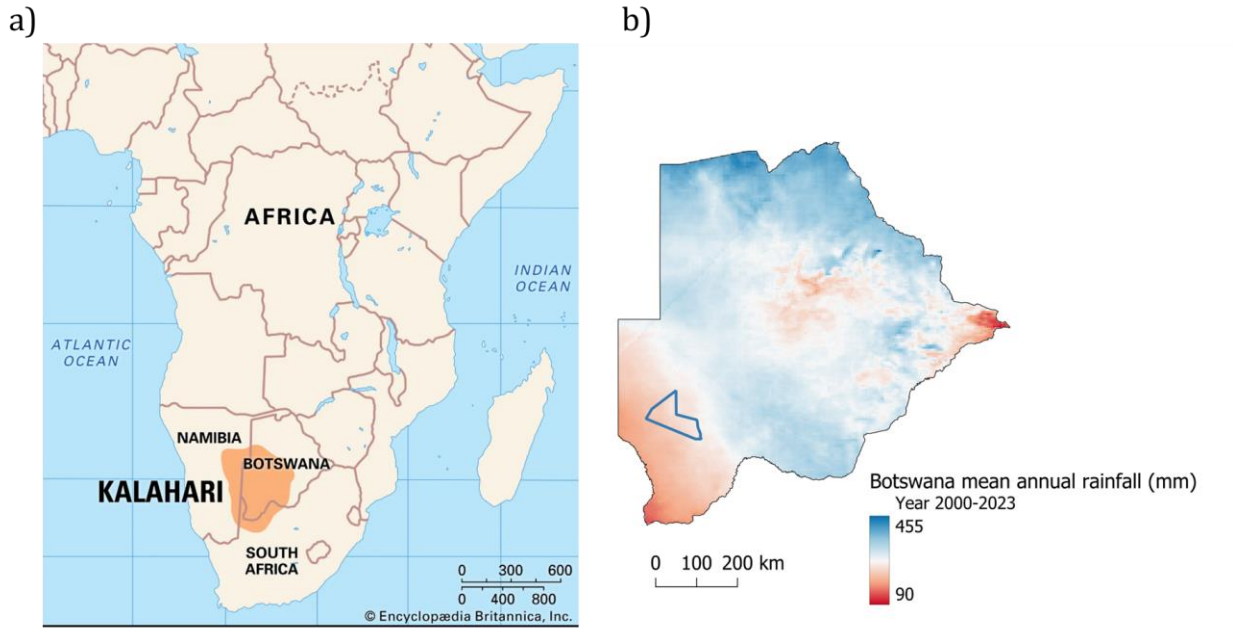


Figure 8. Map of the Kalahari plateau and Mean Annual Precipitation (MAP) in Botswana. a) shows a map of the Kalahari plateau, illustrating the geographical extent of the region (Leistner, 1967). b) MAP across Botswana derived from CHIRPS data, with the study area, Zutshwa, highlighted by a blue boundary.

3.1.4 Soils and associated vegetation

Sandy soils dominate the landscape in the Southern Kalahari, covering over 90% of the surface area, with sand content ranging from 86 % to 99 % (Lewis, 1936). The sand primarily comprises over 90% quartz, with minor traces of zircon, garnet, feldspar, and typically some ilmenite and tourmaline (Lewis, 1936; Wang et al., 2007). Based on characteristics such as colour, chemical composition, and associated vegetation, the Southern Kalahari's sandy soils are categorised into three types: 'white,' 'pink,' and 'red.'

This nomenclature, convenient and previously used by local scholars (Leistner, 1967), distinguishes red sand as the most prevalent soil type, with both white and pink sands considered its variations. Vegetation typically found in red sand areas includes woody plants like *Albizia anthelmintica*, and grasses such as *Aristida stipitata*, and *Eragrostis pallens*. Pink sand areas are often associated with woody plant species like *Rhigozum trichotomum* and grass species such as *Schmidtia kalahariensis*, although these species

are not exclusive to such regions (Leistner, 1967). In various locations, the woody vegetation is a diverse blend of different species and varying sizes. Nevertheless, specific woody species, including *Vachellia erioloba* E. Meyer, *Senegalia mellifera* Vahl, *Terminalia sericea* Burch ex DC., *Vachellia luederitzii* Engler, and *Boscia albitrunca* (Burch.), tend to form distinct groupings (Skarpe, 1986). Additionally, you can find shrubs measuring less than 2 m in height, such as *Grewia flava* DC., *Lycium namaquense* Dammer, and *Rhus tenuinervis* Engler, within this vegetation as well (Skarpe, 1986).

The study region encompasses two main land uses, communal grazing and semi-protected areas. In semi-protected areas, there is a diverse range of wildlife, including a variety of mobile wild ungulates such as Blue wildebeest (*Connochaetes taurinus* Burchell), Red hartebeest (*Alcelaphus bucelaphus* Hilaire), Eland (*Tragelaphus oryx* Pallas), Gemsbok (*Oryx gazella* Linnaeus), Steenbok (*Raphicerus campestris* Thunberg), and Springbok (*Antidorcas marsupialis* Zimmermann) and large carnivores such as lions (*Panthera leo* Linnaeus), cheetahs (*Acinonyx jubatus* Schreber), Brown hyena (*Parahyaena brunnea* Thunberg), and Spotted hyena (*Crocuta crocuta* Erxleben), (Roodt, 2015). In contrast, the communal grazing land use system is characterised by livestock overgrazing, leading to the progressive degradation of the land (Dougill et al., 2016; Perkins, 2018)). The stages of degradation observed in excessively grazed vegetation exhibit variability. Nevertheless, several researchers (Dougill et al., 2016; Leistner, 1967; Perkins, 2018) have noted that in areas subjected to overgrazing, there has been a transition from the original presence of decreaser species such as *Antheophora pubescens* and *Stipagrostis ciliata* to the dominance of annual grasses like *Schmidtia kalahariensis*, along with non-palatable forbs characterised by a prostrate growth form, such as *Tribulus terrestris* (commonly known as Devil's thorn) and *Alternanthera pungens* (referred to as Paper thorn), and other forbs like *Indigofera flavicans*, *Indigofera alternans*, and *Sida cordifolia*. This shift contributes to the overall vegetation biomass but does not significantly enhance forage value.

3.3 Area of interest (AOI) selection and plot layout

During the peak season from March 24 to 30, 2024, three 50 m x 50 m Areas of Interest (AOIs) were established along a transect extending from Zutshwa towards Ngwatle, a settlement in KD1 (Figure 7). This transect sampled three locations along a gradient of grazing intensity, determined by distance from the nearest borehole (Perkins, 2018; Pickup & Chewings, 1994). This sampling criteria ensured a representative sample of the landscape, enabling the evaluation of the transferability of the AGB estimation models.

Late March was strategically selected based on field observations confirming it coincided with peak herbaceous biomass. Additionally, this period provided optimal cloud-free conditions for UAV data collection, thereby addressing both the phenological and logistical requirements of the study. This sampling criteria ensured a representative sample of the landscape, enabling the evaluation of the transferability of the AGB estimation models.

3.3.1 Geolocating AOIs and Ground Control Points (GCPs)

To support accurate georeferencing of imagery, each AOI was marked with 13 evenly distributed ground control points (GCPs), measuring 50 cm x 50 cm (Cunliffe & Anderson, 2019; Villanueva & Blanco, 2019; Yu et al., 2020). These GCPs were placed such that they were visible in the air and were composed of black and beige high contrast canvas to enhance detection of the centre point across all sampled spectral bands. The GCPs were geolocated by using the paired base (DJI D-RTK2) and rover DJI Phantom 4 Multispectral (P4MS) system with absolute accuracy of ca. ± 2 m and relative accuracy of ca. ± 0.02 m), with holding the multispectral drone 1 m above each GCP to obtain centimetre level relative positions (Figure 8).



Figure 9. Geolocation of GCPs using the DJI D-RTK2 base and Phantom 4 multispectral rover system. This figure illustrates the process of geolocating GCPs with the DJI D-RTK2 base station paired with the DJI Phantom 4 Multispectral (P4MS) drone. A 1-meter-long rod was used as a height offset for the drone to have a consistent height measurement (Photo taken on 26/03/24).

3.3.2 Detailed AOI descriptions

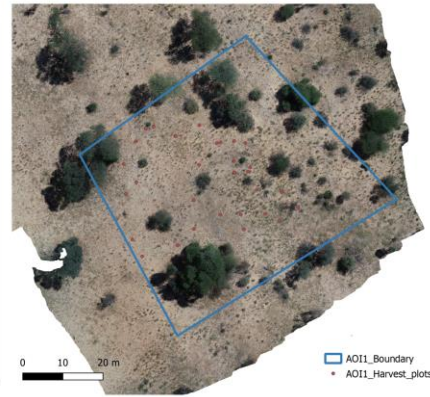
AOI 1 was situated 6.8 km from the borehole at Zutshwa settlement, where grazing intensity was notably high. The landscape appeared somewhat bare due to high grazing pressure, with varying vegetation conditions across the site. The herbaceous layer was dominated by a diverse mix of forbs and grass species, including *Schmidtia kalahariensis*, *Stipagrostis uniplumis*, and *Tribulus terrestris*. Most grass tufts showed signs of grazing, indicating high grazing pressure. The annual *Schmidtia kalahariensis* appeared greener than *Stipagrostis uniplumis*. This could have been because of its low palatability, making it less targeted by grazers. Tree cover in AOI 1 was relatively low, with sparse presence of species such as *Grewia flava*, *Boscia albitrunca*, and *Vachellia erioloba*. The rangeland condition in AOI 1 reflected high grazing pressure, with visible bare patches and signs of heavy grazing on the grass tufts. The presence of an **Increase II** grass (*Schmidtia*

kalahariensis) in a rangeland ecosystem typically indicates that the area has been subjected to heavy grazing pressure over time (Figure 10). **Increaser II** grasses tend to increase in abundance as grazing pressure intensifies because they are less palatable to livestock or are more resilient to grazing than other species (Van Oudtshoorn, 2012). The presence of the forb *Tribulus terrestris* was also an indication of disturbance. It is a pioneer species that quickly colonises open, bare patches of soil where there is high grazing intensity (Kashe et al., 2020).

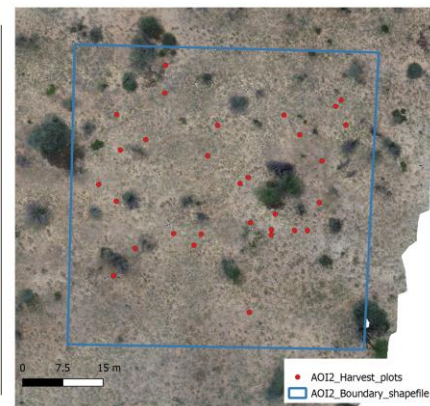
AOI 2 was located 8.9 km from the borehole at Zutshwa settlement, slightly further from the village compared to AOI 1. The area exhibited distinct vegetation characteristics with a mix of grass and shrub species. Grazing pressure in this area was moderate, as evidenced by the uniform height of the grasses and the absence of moribund material. The primary grasses were *Stipagrostis uniplumis* and *Schmidtia kalahariensis*, with a persistent presence of *Aristida congesta*, *Melinis repens*, and the forb *Tribulus terrestris*. The moderate grazing intensity allowed for a relatively healthy and stable herbaceous layer, with no signs of severe degradation. Tree and shrub species in AOI 2 included the dominant shrub species *Grewia flava*, which is prevalent throughout the area. Other woody species observed include *Vachellia erioloba*, *Senegalia mellifera*, *Boscia albitrunca*, and *Ziziphus mucronata*.

AOI 3 was located approximately 18.9 km from the borehole at Zutshwa settlement, further away from the village than both AOI 1 and AOI 2. The area featured taller grasses with good grazing value, and a notably healthier grass cover compared to areas closer to the settlement. The presence of moribund grasses also suggested that this area experienced less grazing pressure. The dominant grass species in AOI 3 were *Stipagrostis ciliata* and *Schmidtia pappophoroides*, both of which are considered high in grazing value (Van Oudtshoorn, 2012). Tree species in AOI 3 included *Terminalia sericea*, *Grewia flava*, *Boscia albitrunca*, and *Senegalia mellifera* as the dominant species.

a)



b)



c)

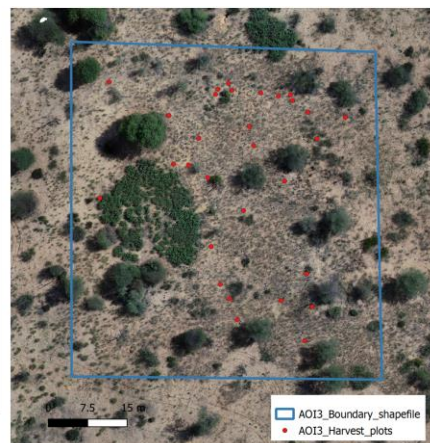


Figure 10. Rangeland condition decreases near the borehole along grazing intensity gradients. This figure compares the AOI photos and orthomosaics, illustrating the decline in rangeland condition with proximity to the borehole. a) AOI 1, located near the borehole, is dominated by herbaceous species of low foraging value and exhibits poor rangeland condition with sparse vegetation cover. b) AOI 2, located further from the borehole, is dominated by species of average foraging value, showing moderate rangeland condition and more vegetation cover. c) AOI 3, the furthest from the borehole, is characterized by herbaceous species of high foraging value and displays the best rangeland condition with abundant vegetation cover.

3.4 Aerial surveys

3.4.1 UAV RGB data collection for SfM canopy height modelling

A DJI Phantom 4 Pro drone equipped with a high resolution 20MP RGB camera (camera model FC6310) was used to acquire RGB images (Figure 11). The flight plan for capturing images was created using DJI GS Pro software (v2.0.17) and executed with autopilot functionality. All RGB images were captured within one day before each biomass harvest to maximise temporal correspondence. Flight campaigns were between 0900-1700 in cloud-free sunny conditions to minimise shadowing and optimise the quality of data collected for Structure from Motion (SfM) modelling (Assmann et al., 2019). These drone surveys proceeded if the average wind speed was below approximately 4 m/s (Cunliffe et al., 2022; Slade et al., 2023, 2024). It has been shown that wind speed influences the reconstructed canopy heights, with higher wind speeds leading to a reduction in mean canopy height (Slade et al., 2024).

Table 2. RGB survey flight parameters

Menu	Parameter	Setting
Basic	Drone:	Phantom 4 pro (RGB)
	Shooting angle:	Parallel to Main Path
	Capture model:	Capture at Equal Distance Intervals
	Flight course mode:	Scan Mode
	Altitude:	As appropriate to give 5 mm spatial grain (in our case 20 m), 22 m for convergent image flights
Advanced	Front Overlap ratio:	75%
	Side Overlap Ratio:	75%
	Course Angle:	
	Margin:	10-15 m

Two convergent flight campaigns were conducted for each AOI to increase image overlap and enhance the accuracy of resulting 3D models (Bazzo et al., 2023; Cunliffe et al., 2022; Cunliffe & Anderson, 2019). This approach resulted in a minimum of approximately 33 images per unobscured location (Cunliffe & Anderson, 2019). The nadir flight altitude was set to achieve a spatial resolution of approximately 5 mm at the top of the canopy (0° , with 75% x 75% side and forward overlap). Convergent image flights were conducted with the camera angled off-nadir (20° , with 75% x 75% side and forward overlap) at a slightly higher altitude (approximately 2 m) than the nadir survey (Cunliffe & Anderson, 2019).

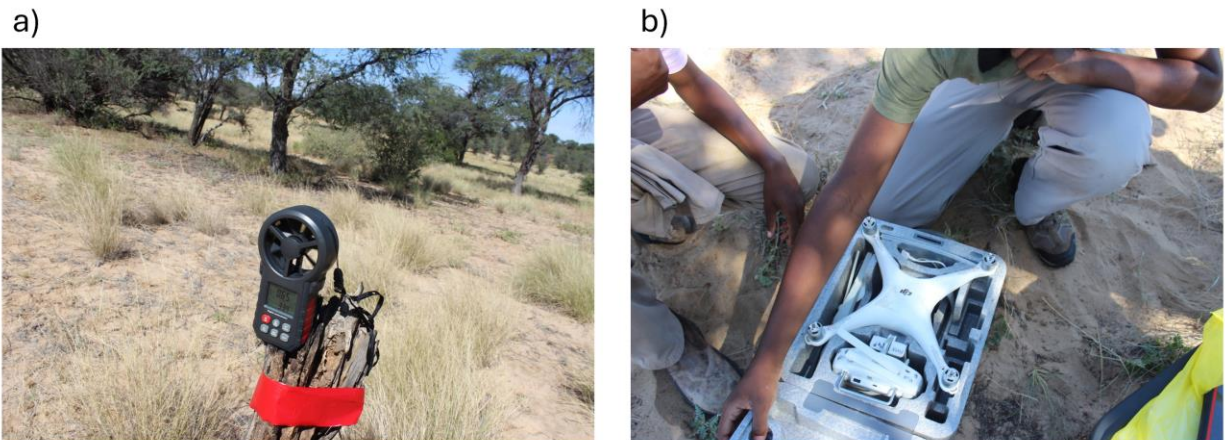


Figure 11. Equipment used for RGB SfM survey. a) Digital anemometer for measuring wind speed. b) DJI Phantom 4 Pro drone (Zutshwa, 25/03/2024).

3.4.2 UAV multispectral data collection for spectral reflectance

The DJI Phantom 4 Multispectral drone (<https://www.dji.com/global/p4-multispectral>) was used to capture images for spectral reflectance data (Figure 12). The DJI Phantom 4 Multispectral imaging system consists of a six-camera array of 1/2.9-inch CMOS sensors: an RGB camera as well as five multispectral cameras. The multispectral camera covers specific bands: Blue (B) at $450 \text{ nm} \pm 16 \text{ nm}$, Green (G) at $560 \text{ nm} \pm 16 \text{ nm}$, Red (R) at $650 \text{ nm} \pm 16 \text{ nm}$, Red edge (RE) at $730 \text{ nm} \pm 16 \text{ nm}$, and Near-infrared (NIR) at 840 nm

± 26 nm. Additionally, the drone is equipped with the DJI Onboard D-RTK system, which ensures high-precision positioning at the centimetre level when used in conjunction with the DJI D-RTK2 unit. The multispectral survey flights were planned to achieve a side and front overlap of 80%, ensuring sufficient image coverage undertaken during midday hours, typically between 1100 and 1300, to minimise the presence of shadows and optimise the data quality. Images were also captured with a spatial grain of ca. 5 mm.

Table 3. [Multispectral survey flight parameters](#)

Menu	Parameter	Setting
Basic	Drone:	Phantom 4 Multispectral
	Shooting angle:	Parallel to Main Path
	Capture model:	Capture at Equal Time Intervals
	Flight course mode:	Scan Mode
	Altitude:	20 m (1.1 cm spatial grain)
Advanced	Front Overlap ratio:	80 %
	Side Overlap Ratio:	80 %
	Course Angle:	
	Margin:	10 m
	End Mission Action:	Return home

a)



b)



Figure 12. Equipment used for multispectral survey. a) DJI Phantom 4 Multispectral drone. b) DJI D-RTK 2 high precision GNSS mobile station (Zutshwa, 26/03/2024).

3.5 Field sampling

After the aerial surveys, 30 circular harvest plots were selected with an area of ca. 0.342 m² at each AOI to facilitate the calibration of the allometric relationships between canopy height or vegetation indices and aboveground biomass. The plots were stratified across the range of canopy heights and herbaceous plant species. Each plot was assigned a unique ID code for identification (with the format “SXPXX”, where S is the site number, and P is the plot number), and then geolocated by holding the RTK-enabled multispectral drone 1 m above the centre, with the DJI-RTK2 as a base and the aircraft as a rover to obtain accurate relative positions (Figure 13).



Figure 13. 0.342m² circular quadrat and centre pin flag with plot ID. The herbaceous species shown is *Schmidtia kalahariensis* (Zutshwa, 26/03/24).

3.6 Biomass harvest

The ca. 0.342 m² plots were harvested down to the top litter layer using clippers. The biomass obtained from the harvest was partitioned in the field among various species, and all the material was packed in labelled bags.

3.6.1 Oven drying of samples

Samples for each component were oven-dried at 60°C for ≥ 48 h to a constant weight (after McIntire et al., 2022) (defined as $< 1\%$ change in mass in 24 h). The oven-dried samples were weighed to determine the biomass yield for each vegetation component and in total per unit area.

3.6.2 Plant palatability classification

Herbaceous plant species were classified into three foraging importance categories: high, average, and low grazing value. This classification was based on species' known palatability and preference by herbivores (after Van Oudtshoorn, 2012). Extending on the classification by (Van Oudtshoorn, 2012), *Tribulus terrestris*, a non-palatable forb was classified under the low grazing value category.

Table 4. Classification of herbaceous species by grazing value

Grazing value	Scientific name	Common name	Remarks
Low	<i>Schmidtia kalahariensis</i>	Kalahari Sour Grass (English)	An annual tufted grass that grows in dense clusters, covered in fine hairs and secreting an acidic substance during flowering. It has a sour smell, is sticky to the touch, and can cause skin irritation. It flowers year-round depending on rainfall, thrives in drought-stricken and overgrazed areas, and grows rapidly to protect open sand. Not preferred for grazing and should not be grazed heavily where it dominates (Van Oudtshoorn, 2012).
Low	<i>Tribulus terrestris</i>	Devil's thorn	Prostrate annual herb, entirely covered in long, whitish hairs. It features yellow petals and produces a hard, triangular drupe with sharp spines (Flora of Botswana, n.d.). It is unpalatable to livestock and grows in disturbed areas, effectively protecting soil from erosion.
Low	<i>Eragrostis pallens</i>	Broom Love Grass	This is a tall, hard, robust and dense perennial grass that is seldomly grazed. It is commonly used as a thatching grass and for brooms.
Average	<i>Stipagrostis uniplumis</i>	Silky bushman grass (English), Tshikitshane (SeTswana)	A tufted perennial grass with a shrub-like growth form. Its leaves are typically rolled and tough, with long white hairs on the upper part of the leaf sheath. It flowers from December to May. While not ideal for grazing, it is relatively well grazed in very dry and disturbed areas where it can become dominant (Van Oudtshoorn, 2012).
High	<i>Schmidtia pappophoroides</i>	Sand Quick (English), Molalaphage (SeTswana)	A perennial tufted grass that grows in a shrub-like form, often developing stolons or roots at the lower nodes. Its leaves are blue-green to grey-green and frequently covered in dense hairs. It typically flowers from October to June. Known as Sand quick, this grass is palatable and valued for its grazing quality. It offers an average leaf yield, is drought-resistant, and can withstand reasonably heavy grazing (Van Oudtshoorn, 2012).
High	<i>Stipagrostis ciliata</i>	Tall bushmen grass (English)	An erect perennial tufted grass. Leaves are mostly concentrated around the base. Dry leaves are curled. It is a palatable and very valuable grass in the dry western parts of Southern Africa. It produces good leaf yield and has a high nutritional value, even when the grass is dry. It is regarded as an indicator of good rangeland conditions, and effectively protects exposed soil against soil erosion (Van Oudtshoorn, 2012).

3.7 Image-based modelling

3.7.1 Photogrammetric data processing point cloud generation

RGB images from each of the three AOIs were processed using Structure from Motion (SfM) photogrammetry. The processing was performed using a high-performance computing system (full specifications provided in Appendix E).

Images and GCP coordinates were imported into Agisoft Metashape Professional edition (v2.1.1.17821) and converted to the same coordinate reference system (WGS84 UTM 34 S; EPSG:32734). The quality of the images was assessed using Metashape's image quality tool, retaining those with a sharpness rating of ≥ 0.75 for analysis (Cunliffe et al., 2020). To optimise camera locations, images were aligned with "highest" accuracy setting and a key point limit of 40,000 and tie point limit of 4000. The output was a sparse point cloud containing a paired set of multidimensional points from all images linked together by identical features. The sparse point cloud and estimated camera positions were evaluated for accuracy, and any clearly erroneous tie points, such as those far below ground or reconstructed high above ground, were manually removed. Additionally, the sparse point cloud was filtered to exclude points with a reprojection error greater than 0.55 pixels (Cunliffe et al., 2022). The sparse point cloud was then georeferenced by manually placing the marker for each of the 13 GCPs on photos corresponding to the GCPs. The software then estimated the positions of the GCP markers for the other images automatically, and markers were adjusted manually when necessary.

To ensure robustness and accuracy of the geo-referencing process, 15 projections were targeted for each GCP (Cunliffe et al., 2022). To spatially constrain the photogrammetric reconstructions, ten of the GCPs were used, while the remaining three, intended for accuracy assessment were deselected before optimising the camera parameters (Ribeiro-Gomes et al., 2016; Tian et al., 2021). During camera optimisation, we calculated the lens parameters including the focal length (f), principal point coordinates (c_x , c_y), radial distortion coefficients (k_1 , k_2), tangential distortion coefficients (p_1 , p_2), aspect

ratio, and skew coefficients (b_1 , b_2) (Cunliffe et al., 2022). Next, the sparse point cloud was converted into a dense point cloud, and depth filtering was set to "mild" to remove outlier points caused by noise or inaccurate focusing (Cunliffe et al., 2016; Lussem et al., 2019). 'Ultra-high' quality settings were used to preserve spatial detail. These steps resulted in a single, more detailed 3-D true colour point cloud.

We performed a two-step ground classification process using the Agisoft Metashape ground classification tool to distinguish ground points from other features in the point cloud data, which was crucial for generating accurate DTMs. Specific parameters were defined to guide the ground classification process, including a grid size of 0.05, maximum angle, maximum distance, and cell size. The automatic classification procedure consists of two steps. In the first step, the point cloud is divided into cells of a specified size, and the lowest point in each cell is detected. These points are then triangulated to form an initial approximation of the terrain model. Additionally, Metashape filters out some noise points to be classified as Low Points. In the second step, new points are added to the ground class if they meet two conditions: they lie within a certain distance from the terrain model, and the angle between the terrain model and the line connecting the new point with a ground point is less than a specified angle (Agisoft, 2024). This iterative process continues until all points have been evaluated and classified accordingly. Other studies have employed this filtering algorithm (Cunliffe et al., 2016; Tian et al., 2021). Finally, the point cloud was exported in a .laz format for subsequent analysis.

3.7.2 Canopy Height Modelling

Further analysis was conducted using R (R Core Team, 2023), and we utilised the lidR package (Roussel et al., 2020) for processing point cloud data. During the data import process, we included the 'c' attribute, representing the classification, in the point cloud dataset. We filtered out the ground points class from the point cloud and generated a DTM using an inverse distance weighting (IDW) algorithm. The heights above ground (HAG) of the point cloud were normalised using the DTM as a reference, ensuring that all points were adjusted to their relative heights above the ground surface. For the Canopy Height Model (CHM), we used the DSM triangulation algorithm, which triangulates the

remaining points. Post-processing steps included filling gaps and smoothing the CHM using the terra package (Hijmans, 2020) (Figure 13). Although these steps aimed to improve data quality, Slade et al., (2024) noted that canopy height retrieval is generally insensitive to spatial gaps in point cloud reconstructions, suggesting that the gap-filling process may have a limited impact on height estimation accuracy. Figure 15 illustrates the workflow for deriving the canopy height model and vegetation indices. The mean canopy height values from each plot (Figure 15) were extracted using the R package "exactextractr" (Bason, 2019).

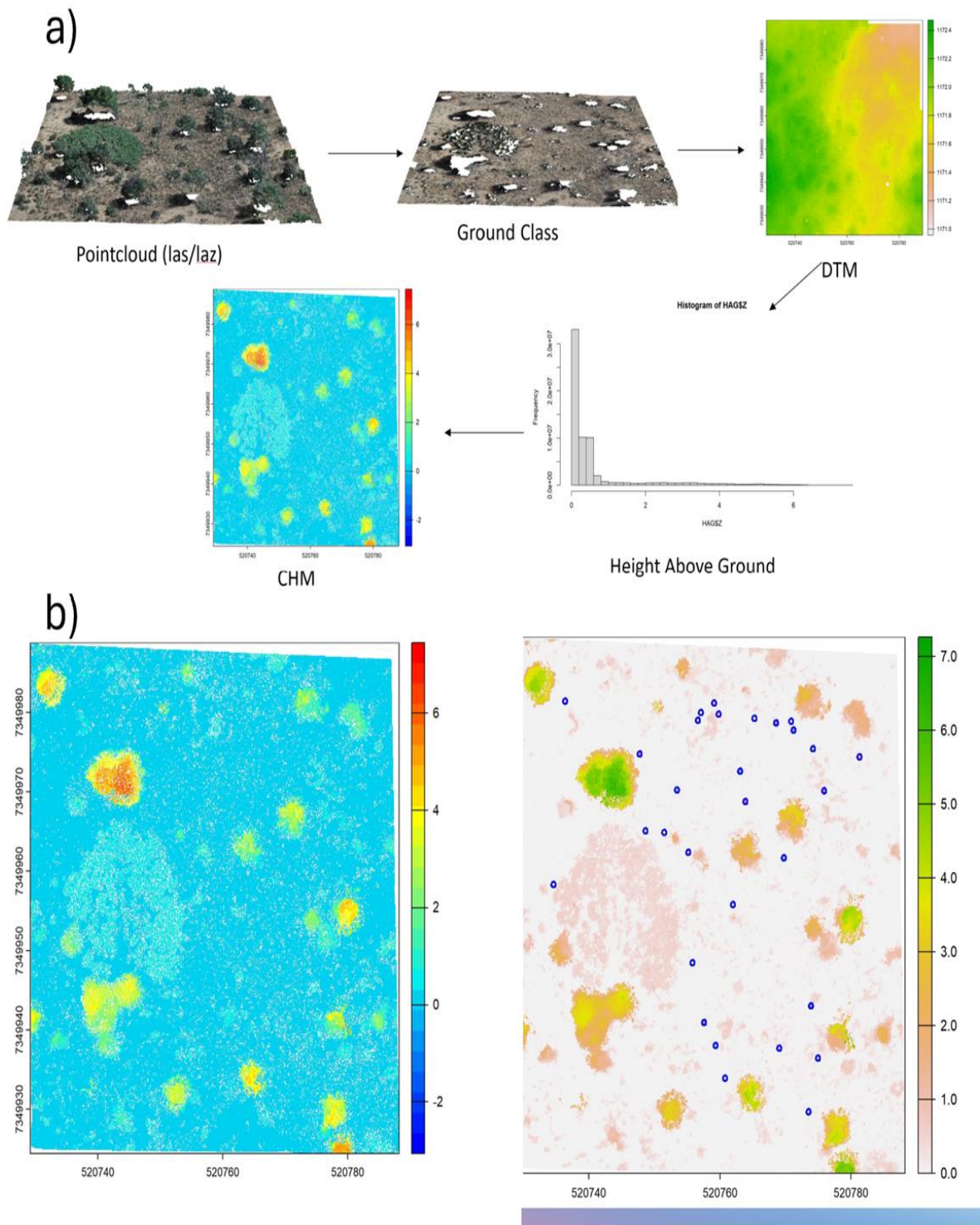


Figure 14. Accurate canopy height modelling and smoothing techniques in R (a) Workflow using the *lidR* package (Roussel et al., 2020), showing steps from data import, ground point filtering, DTM generation with IDW, height normalisation, to CHM creation using DSM triangulation. (b) Smoothing of the CHM using the *terra* package (Hijmans, 2020), illustrating the process of filling spatial gaps. Blue circles represent biomass harvest plots.

3.8 Processing vegetation indices

We used Agisoft Metashape Professional edition (v2.1.1.17821) software to process the multispectral images collected for this study. The software allowed us to align the images, generate depth maps, DSMs, and create Orthomosaics for each AOI. From these multispectral Orthomosaics, we derived vegetation indices in R using the terra package (Hijmans, 2020). During preliminary analysis, the NDVI and the OSAVI vegetation indices exhibited high correlation (Pearson's $r = 1$). To avoid multicollinearity issues and ensure stable regression results, only one index was selected. NDVI was chosen due to its widespread use, simplicity, and high sensitivity to vegetation changes (Bazzo et al., 2023). The mean NDVI values in each plot (Figure 15) were also extracted using the R package "exactextractr" (Bason, 2019).

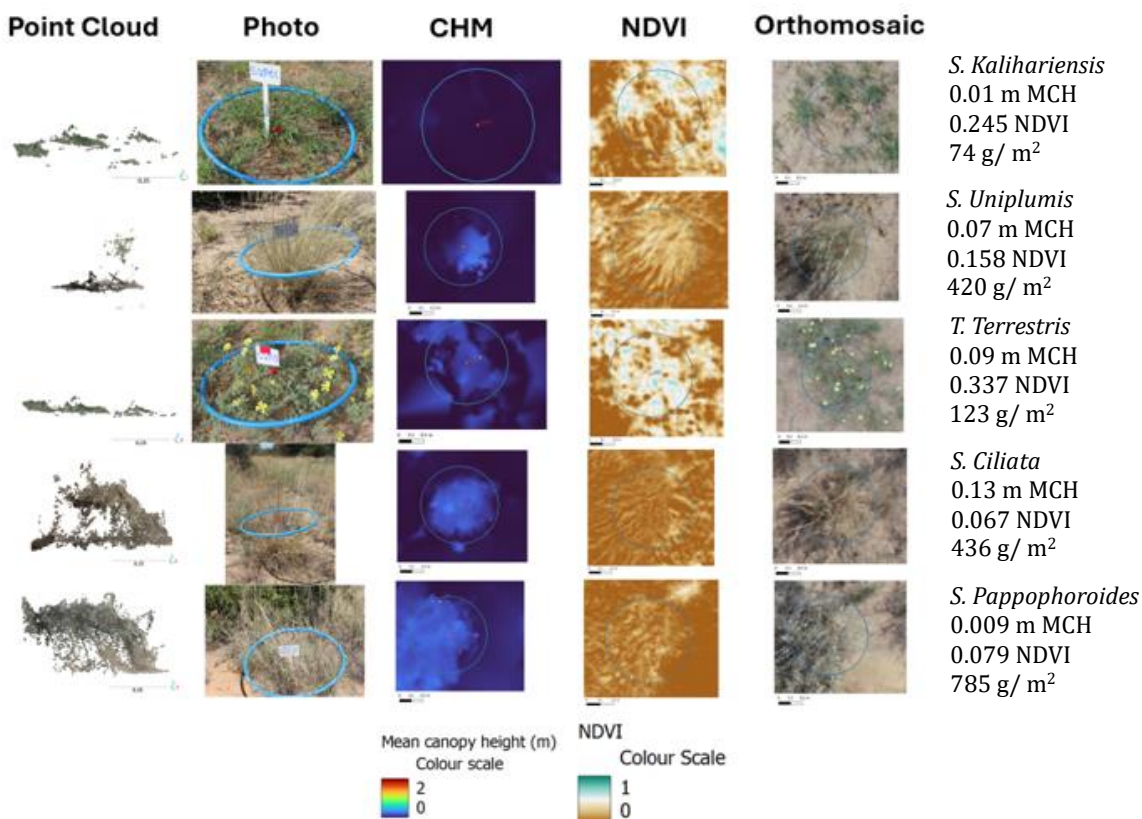


Figure 15. Visualisations of reconstructed point clouds and plant scale canopy heights of individual plants. Accompanying photographs of each plant individual were taken from slightly different viewpoints to the point cloud renderings. The columns displays: (i) point clouds, (ii) accompanying photographs, (iii) canopy height models (CHM), (iv) NDVI, and (v) orthomosaic photographs. The blue circles indicate the harvest plot buffers, MCH means Mean Canopy Height.

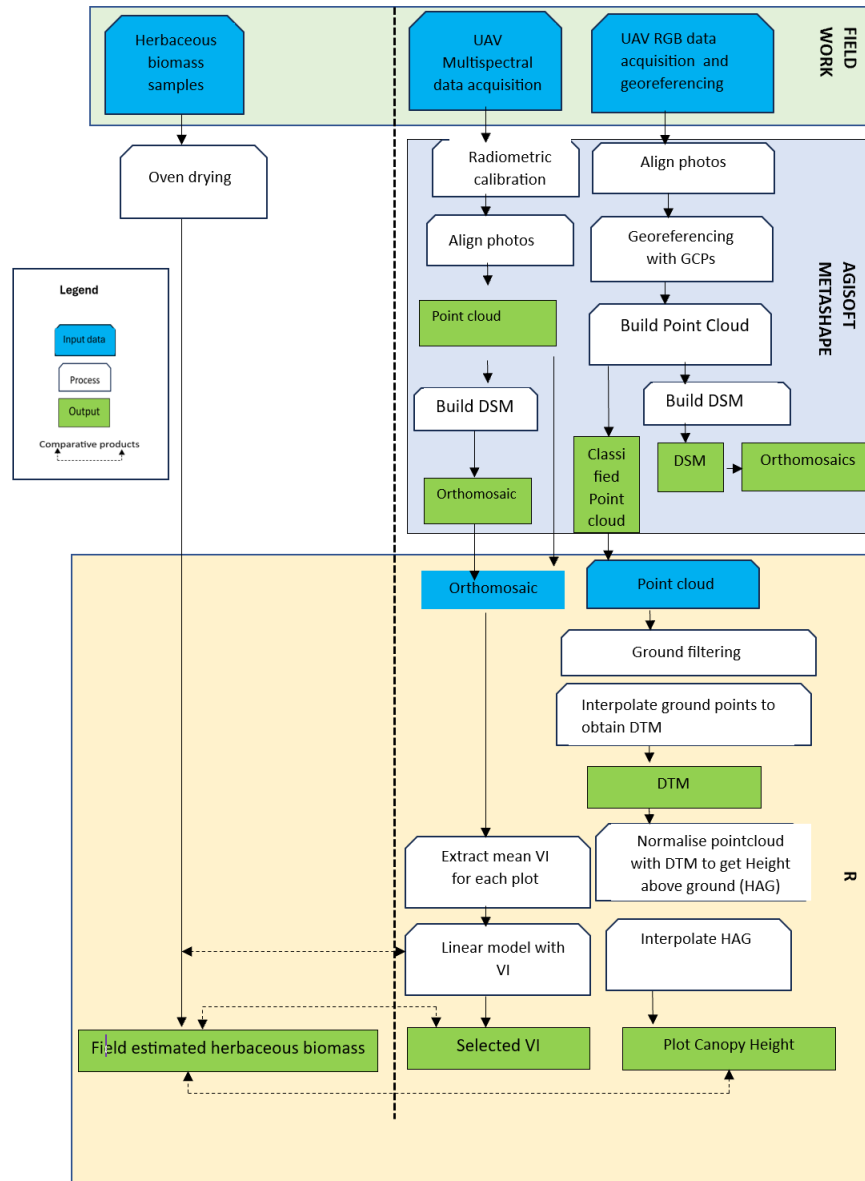


Figure 16. The general workflow of the UAV observations of canopy height and spectral reflectance used to characterise AGB (right side). The field observations (right side) were used for calibrating allometric relationships between height or spectral reflectance.

3.9 Statistical analysis

Statistical analyses were conducted using R (v4.4.2, R Core Team, 2023). Initial exploration revealed that outliers contributed to a left-hand skew in the distribution, violating the assumptions of homoscedasticity and normality of residuals (Appendix B). To address this, robust regression was applied using the 'lmrob' function from the 'robustbase' package (Maechler et al., 2024) to evaluate the relationship between AGB and UAV-derived metrics of canopy height and spectral reflectance (NDVI).

Robust regression was used to fit linear models predicting AGB observations from mean canopy height and NDVI for each grazing value category. *Schmidtia kalahariensis*, *Eragrostis pallens*, and *Tribulus terrestris* were classified as low grazing value species, *Stipagrostis uniplumis* was classified as average grazing value, while *Stipagrostis ciliata* and *Schmidtia pappophoroides* were classified as high grazing value herbaceous species. Model performance for each grazing value category was validated using leave-one-out cross validation (LOOCV) to compute the mean out-of-sample prediction error, which was divided by the model slope to obtain relative errors for each model (Cunliffe et al., 2022).

To evaluate the accuracy and transferability of AGB prediction models, AGB landscape models were applied to each AOI categorised by grazing intensity. These models, initially trained using robust regression techniques on the entire dataset, were tested within the low, average, and high grazing intensity levels to evaluate their performance and transferability in these conditions. We evaluated the relationship between predicted and observed herbaceous biomass within each grazing intensity category. Performance metrics such as R^2 , root mean square error (RMSE) and mean absolute error (MAE) were derived to quantify the accuracy of the predictions. Residual analysis was performed to identify patterns and biases in model predictions, providing insights into the robustness of the models under varying grazing conditions. Additionally, regression plots were created to visually compare the predicted biomass against the observed biomass.

4 Results

4.1 How well can aboveground biomass in Kalahari savanna ecosystems be predicted by fine-scale UAV observations of canopy height and spectral reflectance?

UAV-derived canopy height was a strong predictor of AGB at the landscape level. The regression equation showed a strong positive relationship between AGB and Mean Canopy Height (Table 5). The intercept was estimated at 58.40 (SE = 11.44, $t = 5.105$, $p < 0.001$), and the coefficient for Mean Canopy Height was 2384.82 (SE = 142.06, $t = 16.787$, $p < 0.001$), indicating that for each 1 m increase in canopy height, AGB increased by approximately 2385 g/m².

The model explained 72 % of the variation in AGB (Multiple $R^2 = 0.718$), with an adjusted R^2 of 0.715. The residual standard error was 73.97, suggesting a relatively good fit of the model to the data. Convergence was achieved after 12 Iteratively Reweighted Least Squares (IRWLS) iterations. Outliers were identified in the dataset, with six observations had robustness weights close to zero ($|weight| < 0.0011$), indicating they were influential points. Seven observations had weights near 1, while the remaining 77 observations had weights ranging from 0.07279 to 0.99880, with a median weight of 0.96010.

The final regression equation for predicting AGB from Mean Canopy Height is:

$$\text{AGB (g/m}^2\text{)} = 58.40 + 2384.82 \times \text{Mean Canopy Height (m)}$$

In contrast, the robust regression model for vegetation greenness as measured by NDVI indicated that it was not a significant predictor of AGB. The model yielded a coefficient for NDVI of -0.1491 (SE = 244.6106, $t = -0.001$, $p = 1.000$), indicating a very weak and

statistically non-significant relationship between AGB and NDVI (Table 4). The intercept estimate was 136.9707 (SE = 70.1471, $t = 1.953$, $p = 0.054$), which is marginally significant at the 0.05 level.

The model's fit was poor, with an R-squared of 1.187×10^{-8} and an adjusted R-squared of -0.011, suggesting that NDVI does not explain the variation in AGB effectively. The robust residual standard error was 95.43, indicating a substantial amount of unexplained variation in the residuals. Convergence was reached after 19 Iteratively Reweighted Least Squares (IRWLS) iterations. However, when the data was stratified by species, a positive relationship between NDVI and AGB emerged within some species, revealing Simpson's paradox (Figure 17), where the overall trend at the landscape level reversed within individual species.

Table 5. Model summaries for aboveground biomass as predicted from Mean Canopy Height.

Predictors		Estimates	CI	P
(Intercept)		58.40	35.67- 81.14	<0.001
Mean Canopy Height (m)		2384.82	2102.49- 2667.14	<0.001
Observations		90		
R ² /R ² adjusted		0.72 / 0.72		

Table 6. Model summaries for aboveground biomass as predicted from NDVI.

Predictors		Estimates	CI	P
(Intercept)		136.97	-2.41- 276.37	0.054
NDVI		-0.15	486.26- 485.96	1.000
Observations		90		
R ² /R ² adjusted		0.00 / -0.011		

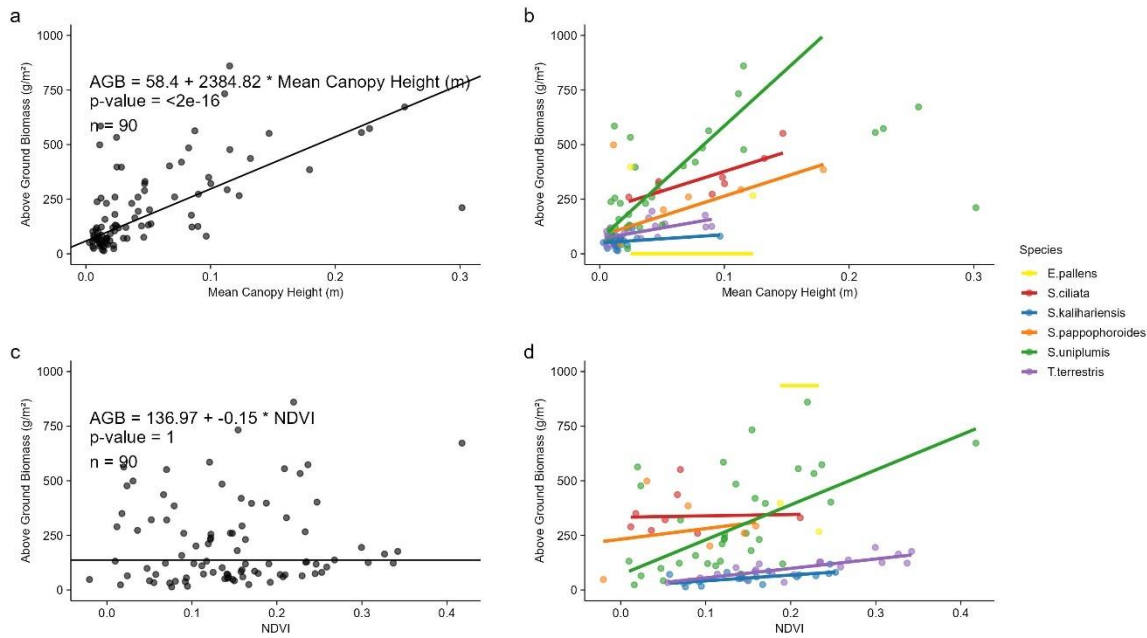


Figure 17. Canopy height strongly predicted aboveground biomass, while NDVI reveals more variable species-specific relationships. The linear models were fitted using robust regression. (a) AGB was strongly predicted by Mean Canopy Height at the landscape level. (b) when stratified by species, the relationship between AGB and Canopy Height was consistent across species. (c) NDVI showed a statistically non-significant relationship with AGB at the landscape level, indicating limited predictive power. (d) When stratified by species, the relationship between AGB and NDVI revealed Simpson's paradox, where the overall trend at the landscape level reversed within individual species.

4.2 How well can herbaceous biomass of foraging importance be predicted by fine-scale UAV observations of canopy height and spectral reflectance?

Mean canopy height was a stronger predictor of AGB compared to NDVI across all forage classes, with robust regression models providing good approximations of the relationships between mean canopy height and AGB (Figure 18). For the low grazing value forages, the robust regression model with canopy height yielded a slope of 1317.57 g m² ($p = 0.004$), with an adjusted R^2 of 0.48, indicating a moderate but statistically significant relationship between canopy height and AGB (Table 6). When NDVI was used as the predictor in this category, the model fit was stronger (slope = 424.18 g m², adjusted $R^2 = 0.58$, $p < 0.001$), but it showed a higher relative error of 8.67%.

In the average grazing value forages, the relationship between canopy height and AGB was stronger, with a slope of 5197.27 g m², adjusted R^2 of 0.68, and a relative error of 24.6 %. NDVI in this category had a weaker relationship (slope = 1599.17 g m², adjusted $R^2 = 0.39$), with a higher relative error of 24.96%, although both predictors were highly significant ($p < 0.001$).

In the high grazing value category, the predictive ability of canopy height was stronger, with a slope of 1592.55 g m², adjusted R^2 of 0.39, and a relative error of 10.12%. The p -value for the canopy height model approached statistical significance ($p = 0.054$). NDVI in this category performed poorly, showing a negative slope of -34.41 g m² and a negative R^2 of -0.083, with an exceptionally large relative error of -279471 %, indicating that NDVI was not a useful predictor for AGB in high grazing intensity areas.

Table 7. Model performance metrics for predicting Aboveground Biomass (AGB) Using UAV-Derived Canopy Height and NDVI across different grazing value categories

Grazing value	Predictor	Species	N	Slope (g m ⁻²)	R ² _adjusted	Relative Error	p
Low	CH	3	43	1317.57	0.48	2.98	0.004
Low	NDVI	3		424.18	0.58	8.67	<0.001
Average	CH	1	33	5197.27	0.68	24.6	<0.001
Average	NDVI	1		1599.17	0.39	24.96	<0.001
High	CH	2	14	1592.55	0.39	10.12	0.054
High	NDVI	2		-34.41	-0.083	-279471	0.952

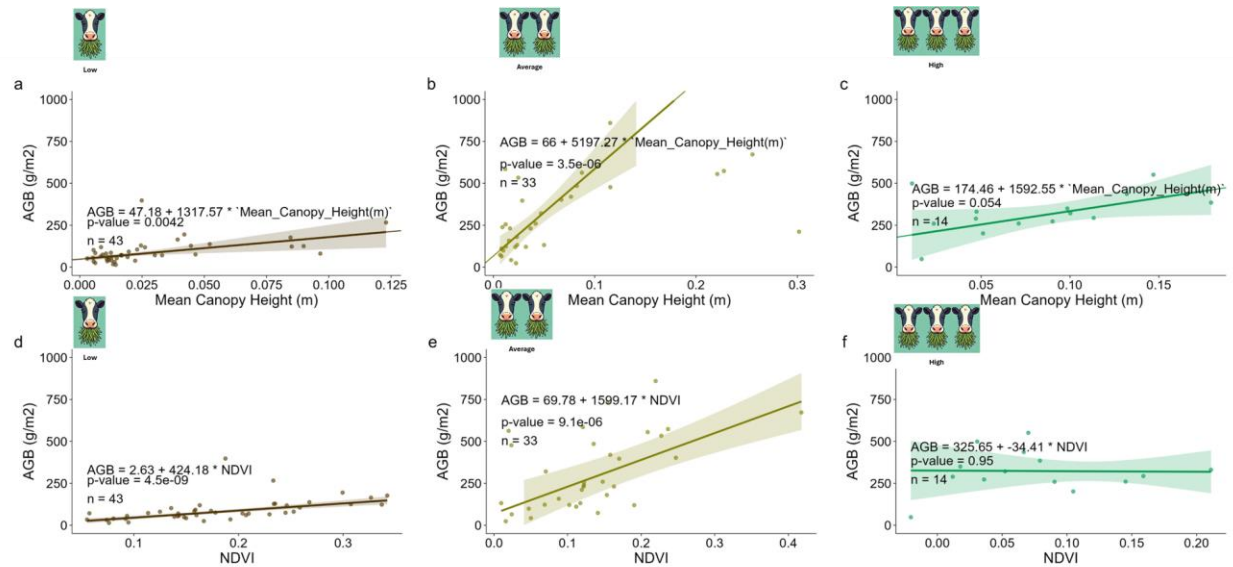


Figure 18. Canopy height is a strong predictor of aboveground biomass across all grazing value categories, while NDVI shows inconsistent predictive power. Canopy height is a strong predictor of AGB all grazing value forage categories, while NDVI shows inconsistent predictive power. Panels (a), (b), and (c) illustrate the regression models for mean canopy height and aboveground biomass for Low, Medium, and High grazing value forage categories, respectively. Panels (d), (e), and (f) depict the regression models for NDVI and AGB for the same grazing value categories.

4.3 Do these relationships between biomass components and remotely sensed attributes differ across different levels of grazing intensity?

At AOI1, characterised by heavy grazing, the landscape CHM exhibited a RMSE of 118.08 g/m² and a MAE of 70.09 g/m². The model explained approximately 40.5% of the variability in observed AGB, indicated by an R^2 value of 0.405. Additionally, the mean residuals were 8.16 g/m², suggesting a relatively small average deviation from the observed values.

Conversely, at AOI2, which was the moderately grazed site, the CHM achieved an RMSE of 164.23 g/m² and an MAE of 97.86 g/m². The model explained 50.9% of the variability in observed AGB ($R^2 = 0.509$), representing the highest predictive power among the three AOIs. However, the mean residuals in this area were 51.72 g/m², indicating a relatively higher level of average deviation of predicted from field measured observed AGB compared to other sites.

At AOI3, characterised by low grazing intensity, the CHM achieved a RMSE of 172.75 g/m² and an MAE of 115.76 g/m², indicating a decline in prediction accuracy. The model only explained 29.7% of the variability in observed AGB ($R^2 = 0.297$), which was the lowest among the AOIs. The mean residuals were 31.98 g/m². These results are summarised in Table 7 and illustrated in Figure 19, which display the corresponding regression plots for each AOI.

Table 8. Summary of model performance metrics for predicting AGB using Canopy Height Model across varying levels of grazing intensity

Model	Site grazing intensity	RMSE (g/m ²)	MAE (g/m ²)	R ²	Mean Residual (g/m ²)
Landscape level Canopy Height Model	Low	118.08	70.09	0.41	8.16
	Moderate	164.23	97.86	0.51	51.72
	High	172.75	115.76	0.30	31.98

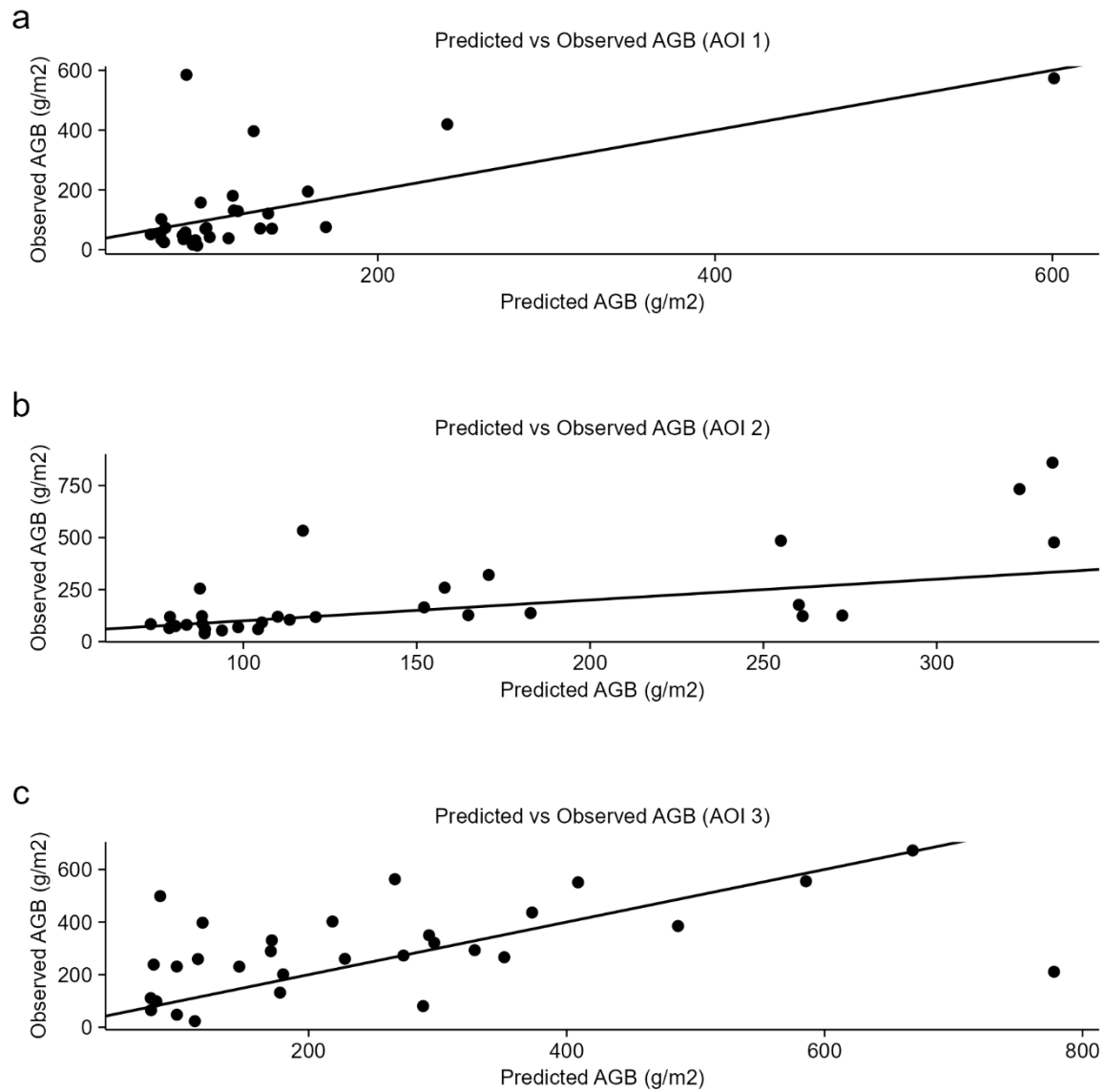


Figure 19. The canopy height model is reproducible and predicts AGB across all grazing intensities. Relationship between field-observed AGB and predicted AGB using the Canopy Height AGB landscape model transfer across grazing gradients. a) Area of Interest (AOI1) representing heavily grazed landscapes, b) AOI2 represented moderately grazed landscapes, c) AOI3 represented low grazing intensity landscapes.

5 Discussion

5.1 How well can aboveground biomass in Kalahari savanna ecosystems be predicted by fine-scale UAV observations of canopy height and spectral reflectance?

The study demonstrated that canopy height derived from UAV-SfM is a strong predictor of AGB, explaining approximately 72% of the variability in AGB. This strong relationship suggests that at landscape level, canopy height is a reliable predictor of biomass in semi-arid ecosystems like the Kalahari savanna. Similar results have been reported for pooled grass species in temperate grasslands, where canopy height was used to predict dry matter yield across various legume-grass mixtures, including red clover (*Trifolium pratense* L.) and Italian ryegrass (*Lolium multiflorum* Lam.), with an R^2 of 0.73 (Grüner et al., 2019). Other studies utilising SfM derived canopy height as a predictor of AGB have also reported strong relationships (Alonzo et al., 2018; Ballesteros et al., 2018; Bendig et al., 2015; Cunliffe et al., 2020, 2022; Grüner et al., 2019; Guerra-Hernández et al., 2017; Jayathunga et al., 2019; J. Lin et al., 2018; Moeckel et al., 2017; Zahawi et al., 2015). The mean canopy height of non-woody plant functional types, such as ferns ($R^2 = 0.99$), forbs ($R^2 = 0.47$), graminoids ($R^2 = 0.75$), and succulents ($R^2 = 0.75$), has been reported to show extremely strong relationships (Cunliffe et al., 2020, 2022).

Additionally, while the accuracy of individual species models varied ($R^2 = 0.62$ – 0.81), the mean canopy height and ground-level AGB data exhibited a good correlation ($R^2 = 0.73$) for pooled grass species (Grüner et al., 2019). The strong relationship between canopy height derived from UAV-SfM and AGB in this study aligns well with previous research, demonstrating that canopy height can be an excellent predictor of biomass. The slope of the canopy height model in this study was like those derived from disk pasture meter measurements in earlier studies (Zambatis et al., 2006), where similar slope was reported (2384 g/m^2). This consistency across different measurement techniques further reinforces the value of canopy height as a reliable metric for estimating AGB in semi-arid ecosystems, such as the Kalahari savanna.

However, at landscape level, vegetation greenness as measured by NDVI was not a significant predictor of AGB. The results of the NDVI model showed that it is not a reliable predictor of AGB at landscape level. It had a large residual standard error (88.95 g/m²), a negligible adjusted R² (-0.01), and a statistically non-significant p-value (1.000). The effectiveness of NDVI as a predictor of AGB could have been affected by factors such as spatially variable soil backgrounds and the presence of senescent vegetation. Previous studies, (Fern et al., 2018b), have documented similar challenges when using NDVI for biomass estimation, noting that environmental factors such as soil moisture and nutrient availability can significantly influence NDVI values.

Additionally, Fajji et al., (2017) conducted their study in semi-arid Kalahari savanna environments and found that vegetation indices, particularly NDVI and SAVI, were less effective in predicting AGB in areas with high grazing intensity compared to those with low grazing intensity. This reduced effectiveness was attributed to the presence of senescent or dry vegetation and a higher proportion of bare soil in heavily grazed sites. In these areas, the accumulation of standing dead material and litter increases, resulting in more exposed ground. As such, since non-photosynthetic vegetation reflects more visible light, indices relying on the contrast between visible and near-infrared reflectance are likely to struggle to accurately estimate AGB (Fern et al., 2018b; Tian et al., 2021). Moreover, the increased reflectance from dry vegetation further restricts the response of spectral indices to biomass variations, particularly as the contrast between green biomass and dry soil diminishes when vegetation dries out. NDVI had a positive relationship with AGB but explained only a small proportion of the variance (R² between 0.14 and 0.23), with the presence of moss cover significantly influencing the NDVI-phytomass relationship. This suggests limitations in using NDVI to estimate biomass in complex Arctic ecosystems (Cunliffe et al., 2020).

In the Kalahari savanna context, similar challenges may be observed because of the heterogeneous vegetation. Stress-related indices, which respond to both near and middle infrared wavelengths, have shown promise in other regions in the Kalahari plateau by accurately predicting vegetation cover (Amputu et al., 2023, 2024b). However, this study

demonstrates that the widely accepted assumption that plant greenness directly correlates with high biomass is not universally accurate. The relationship between vegetation indices and AGB is often highly species and location specific (Li et al., 2016). Species-specific analyses in this study revealed that NDVI could predict AGB within certain species, demonstrating Simpson's paradox (Figure 17). This phenomenon, where trends observed in aggregated data differ from those seen in stratified data, indicates that NDVI's predictive power is context-dependent (Anuar et al., 2023). For some species, NDVI captured variations in biomass effectively, while for others, it did not. This disparity may result from differences in species' reflectance properties and how they respond to environmental stressors. Previous studies, such as (Pettorelli et al., 2014), have documented similar challenges when using NDVI for biomass estimation, noting that environmental factors such as soil moisture and nutrient availability can significantly influence NDVI values. Additionally, the work of Zhang et al., (2014) emphasised the importance of species-specific calibration when applying NDVI for biomass prediction, as different species exhibit varying reflectance characteristics that can skew results.

5.2 How well can herbaceous biomass of foraging importance be predicted by fine-scale UAV observations of canopy height and spectral reflectance?

Across all herbaceous plant foraging importance categories (low, average, high), the relationship between biomass and canopy height was linear (R^2 between 0.22 and 0.66). For every 1 m increase in canopy height, AGB increased by 984.02 g/m², 5170.51 g/m², and 1570.51 g/m² for herbaceous plants of low, average, and high grazing importance respectively. However, the relationship between biomass and NDVI varied for NDVI between forage plant grazing importance categories (R^2 between -0.07 and 0.56). It was only for low grazing value plants that NDVI showed promising predictive ability. The strong predictive ability of NDVI for low grazing value species, indicated by an adjusted R^2 of 0.58 and a relative error of 8.67 %, suggests its high effectiveness in estimating biomass in intensively grazed areas. This effectiveness can be attributed to the homogeneity and the dominance by non-palatable herbaceous species such as *T.*

terrestris and *S. kalahariensis*, which appeared lush and green and consequently are captured by NDVI. Similar to our results, other studies (Fajji et al., 2017) have shown that NDVI is effective in homogenous, green and lush vegetation of low foraging importance (as found in low grazing areas) but less so in heterogeneous or degraded landscapes (as seen in high grazing areas). Despite the promise of NDVI, canopy height demonstrated a lower relative error (2.98%) and a higher adjusted R^2 value (0.48), indicating its superior predictive power for biomass estimation in these environments. This finding contrasts with previous studies that have suggested structural metrics, like canopy height, are less effective for low-growing herbaceous plants that accumulate biomass by spreading out horizontally, rather than growing tall and narrow (Cunliffe et al., 2022; Fajji et al., 2017; Jayathunga et al., 2019). While canopy height's predictive power was moderate for low-growing species, it still outperformed NDVI, which is commonly considered less effective for biomass estimation in overgrazed or degraded landscapes (Fern et al., 2018b). This study underscores the need for considering structural metrics like canopy height, even for species with different growth habits, challenging the conventional belief that low-growing plants with a spreading growth form are poorly predicted by structural attributes.

For average grazing value species, canopy height emerged as the superior predictor, with an adjusted R^2 of 0.68, explaining a substantial portion of the variance in AGB. The strong relationship between canopy height and biomass in these moderately grazed areas can be attributed to the structural complexity and increased biomass levels, where canopy height serves as a more direct indicator (Alonzo et al., 2018; Balestra et al., 2024; Bendig et al., 2015; Cunliffe et al., 2022; Grüner et al., 2019; Guerra-Hernández et al., 2017; Jayathunga et al., 2019; Moeckel et al., 2017; Zahawi et al., 2015). Although NDVI was still a predictor, it was less effective in this category, with an adjusted R^2 of 0.39 and a relative error of 24.96%. *Stipagrostis uniplumis*, the only herbaceous species classified in the average grazing value category, was observed in either slightly greener or browner phenological conditions. This variability in phenological states may have led to inconsistent NDVI readings, as NDVI is sensitive to changes in vegetation greenness. If *S. uniplumis* was predominantly browner, it may have resulted in lower NDVI values, potentially skewing the predictive relationship between NDVI and AGB. A phenological

spectral variation within the *S. uniplumis* grass species was also observed (Bantelmann et al., 2024).

In the case of high grazing value species, canopy height maintained a good allometric relationship with AGB, with an adjusted R^2 of 0.39 and a relative error of 10.12 %. However, NDVI did not reliably predict AGB in these areas, as evidenced by its negative adjusted ($R^2 = -0.08$) and a negative relative error (-279471 %). This bias means that NDVI could underestimate herbaceous biomass of foraging importance. The weak relationship between NDVI and AGB of foraging importance was due to reduced greenness and the predominant brownish, senescent phenological state of *S. pappophoroides* and *S. ciliata*. Our findings underscore the need for caution when deriving AGB maps based on spectral reflectance in heterogeneous Kalahari savanna ecosystems.

While the study established that canopy height is a strong predictor of AGB across all grazing value categories, a limitation of this research is that spectral information was not used to classify the herbaceous species. Future studies could utilise spectral data to try to isolate specific plant species (Wu et al., 2024). This approach could refine canopy height models and improve the accuracy of AGB estimations in broader scales.

5.3 Do these relationships between biomass components and remotely sensed attributes differ across different levels of grazing intensity?

The study indicated that the canopy height model developed from SfM is transferable across different spatial contexts within this dryland savannah. Specifically, it successfully predicted AGB across varying levels of grazing intensity. This model's ability to predict AGB across grazing intensity gradients suggests that it is robust and adaptable, which is crucial for scaling biomass estimation efforts in similar ecosystems. This transferability allows for the application of the model in other dryland regions, potentially offering a reliable tool for vegetation monitoring and management. However, the transferability of the NDVI model was limited due to the phenological variability of the herbaceous plants

and the limited predictive power of vegetation greenness as measured by NDVI. Previous studies (Amputu et al., 2024b; Chen et al., 2023) have demonstrated the transferability of models utilising spectral reflectance for biomass estimation. These studies have shown that spectral reflectance metrics can reliably predict vegetation biomass across different spatial and temporal contexts. It is worth noting however that these studies were for agriculture and forest ecosystems where the model transferability could be less affected due to the characteristic homogeneous setup of these systems.

Spectral reflectance models were successfully applied to various spatial contexts in Kalahari savanna ecosystems (Amputu et al., 2024b). However, they recommend testing these models in different seasons. Although the Canopy Height model demonstrated high transferability, further research is required to investigate its applicability across different times of the year and in other savannas with varying climatic conditions and species composition. Additionally, it is important to consider integrating canopy height and spectral reflectance data (Lu et al., 2021; Wang et al., 2022).

6 Conclusion

This study demonstrated that UAV-derived canopy height, obtained through Structure from Motion (SfM) photogrammetry, is a robust predictor of aboveground biomass (AGB) in the Kalahari savanna ecosystem, with a strong correlation ($R^2 = 0.72$). This finding underscores the potential of fine-scale UAV observations for accurately estimating biomass, which is crucial for effective rangeland management. However, the Normalised Difference Vegetation Index (NDVI), commonly used to measure vegetation greenness, proved to be a poor predictor of AGB, highlighting the need for more sophisticated and nuanced approaches when using spectral data for biomass estimation in ecosystems with variable phenology and plant composition.

The study also found that the relationship between AGB and UAV-derived canopy height was similar across different categories of herbaceous plant foraging importance (low, average, high) and varying levels of grazing intensity. This consistency suggests that linear allometric functions based on canopy height can be effectively applied at the ecosystem level, offering a reliable method for biomass estimation across different grazing pressures. Moreover, the canopy height model developed from SfM showed high transferability across different spatial contexts within the dryland savannah, successfully predicting AGB across varying levels of grazing intensity. This model's robustness and adaptability are crucial for scaling biomass estimation efforts in similar ecosystems.

Future studies should aim to integrate UAV-derived structural data, such as canopy height, with spectral data to enhance the accuracy of biomass estimations. This integration could refine canopy height models and improve their predictive capacity, particularly in distinguishing between different plant species. Additionally, further research is required to test the applicability of the canopy height model across different times of the year and in other savannas with varying climatic conditions and species composition. Seasonal and temporal testing will help determine the model's robustness and reliability in diverse ecological settings.

Given the limitations of traditional and satellite-based remote sensing methods in capturing fine-scale variations, UAV-based monitoring should be prioritised for detailed rangeland assessments. This approach will provide high-resolution data that can inform more precise and effective rangeland management strategies.

To optimise the utility of UAV technology in rangeland monitoring, it is essential to build capacity and provide training for researchers and practitioners. This will enhance their ability to effectively utilise fine-scale remote sensing tools and develop new approaches tailored to the challenges of African rangelands. Finally, the insights gained from this study should be integrated into rangeland management policies and practices. Land managers and policymakers should leverage UAV-derived data to make informed decisions that promote sustainable rangeland use and address the challenges posed by grazing-induced degradation and climate variability.

7 Open Research

The code for this analysis is available at

[https://github.com/TESS-Laboratory/Nare et al rangeland condition with UAS.git](https://github.com/TESS-Laboratory/Nare_et_al_rangeland_condition_with_UAS.git).

8 References

- Adler, P., Raff, D., & Lauenroth, W. (2001). The effect of grazing on the spatial heterogeneity of vegetation. *Oecologia*, 128(4), 465–479. <https://doi.org/10.1007/s004420100737>
- Agisoft. (2024). *Agisoft Metashape User Manual Professional Edition, Version 2.1*. Copyright © 2024 Agisoft LLC. https://www.agisoft.com/pdf/metashape-pro_2_1_en.pdf
- Agüera-Vega, F., Ferrer-González, E., Carvajal-Ramírez, F., Martínez-Carricondo, P., Rossi, P., & Mancini, F. (2022). Influence of AGL flight and off-nadir images on UAV-SfM accuracy in complex morphology terrains. *Geocarto International*, 37(26), 12892–12912. <https://doi.org/10.1080/10106049.2022.2074147>
- Ahirwal, J., Nath, A., Brahma, B., Deb, S., Sahoo, U. K., & Nath, A. J. (2021). Patterns and driving factors of biomass carbon and soil organic carbon stock in the Indian Himalayan region. *Science of The Total Environment*, 770, 145292. <https://doi.org/10.1016/j.scitotenv.2021.145292>
- Akanyang, L. (2019). *Pastoralists, Free-Ranging Livestock and Wildlife Interactions: Adaptation to Land Use Change and Grazing Resources Variability in Kalahari North, Botswana* [Doctor of Philosophy]. The University of Leeds, School of Geography.
- Al-bukhari, A., Hallett, S., & Brewer, T. (2018). A review of potential methods for monitoring rangeland degradation in Libya. *Pastoralism*, 8(1), 13. <https://doi.org/10.1186/s13570-018-0118-4>
- Alonzo, M., Andersen, H.-E., Morton, D., & Cook, B. (2018). Quantifying Boreal Forest Structure and Composition Using UAV Structure from Motion. *Forests*, 9(3), 119. <https://doi.org/10.3390/f9030119>
- Amjad, M. (2014). Seasonal and Altitudinal Variation of Herbaceous Biomass of Nikyal Range Land, District Kotli Azad Jammu and Kashmir. *Annual Research & Review in Biology*, 4(6), 936–944. <https://doi.org/10.9734/ARRB/2014/5990>

- Amputu, V., Knox, N., Braun, A., Heshmati, S., Retzlaff, R., Röder, A., & Tielbörger, K. (2023). Unmanned aerial systems accurately map rangeland condition indicators in a dryland savannah. *Ecological Informatics*, 75, 102007.
<https://doi.org/10.1016/j.ecoinf.2023.102007>
- Amputu, V., Männer, F., Tielbörger, K., & Knox, N. (2024a). Spatio-Temporal Transferability of Drone-Based Models to Predict Forage Supply in Drier Rangelands. *Remote Sensing*, 16(11), 1842. <https://doi.org/10.3390/rs16111842>
- Amputu, V., Männer, F., Tielbörger, K., & Knox, N. (2024b). Spatio-Temporal Transferability of Drone-Based Models to Predict Forage Supply in Drier Rangelands. *Remote Sensing*, 16(11), 1842. <https://doi.org/10.3390/rs16111842>
- Anderson, K., & Gaston, K. J. (2013). Lightweight unmanned aerial vehicles will revolutionize spatial ecology. *Frontiers in Ecology and the Environment*, 11(3), 138–146.
<https://doi.org/10.1890/120150>
- Anuar, N. I., Khalid, N., Tahar, K. N., & Othman, A. N. (2023). Analyze the Relationship Between Aboveground Biomass and NDVI Values Derived from UAV Multispectral Imagery. *IOP Conference Series: Earth and Environmental Science*, 1240(1), 012015.
<https://doi.org/10.1088/1755-1315/1240/1/012015>
- Aplin, P., Awuah, K. T., Marston, C. G., Powell, I., & Smit, I. P. J. (2021). Machine Learning Classification of Plant Functional Types in Southern African Savannas Using Worldview-3 Imagery. *2021 IEEE International Geoscience and Remote Sensing Symposium IGARSS*, 1604–1607. <https://doi.org/10.1109/IGARSS47720.2021.9554715>
- Archibald, S., Roy, D. P., Van Wilgen, B. W., & Scholes, R. J. (2009). What limits fire? An examination of drivers of burnt area in Southern Africa. *Global Change Biology*, 15(3), 613–630. <https://doi.org/10.1111/j.1365-2486.2008.01754.x>
- Arroyo-Mora, J. P., Kalacska, M., Løke, T., Schläpfer, D., Coops, N. C., Lucanus, O., & Leblanc, G. (2021). Assessing the impact of illumination on UAV pushbroom hyperspectral

- imagery collected under various cloud cover conditions. *Remote Sensing of Environment*, 258, 112396. <https://doi.org/10.1016/j.rse.2021.112396>
- Assmann, J. J., Kerby, J. T., Cunliffe, A. M., & Myers-Smith, I. H. (2019). Vegetation monitoring using multispectral sensors—Best practices and lessons learned from high latitudes. *Journal of Unmanned Vehicle Systems*, 7(1), 54–75. <https://doi.org/10.1139/juvs-2018-0018>
- Awasthi, B., Karki, S., Regmi, P., Dhimi, D. S., Thapa, S., & Panday, U. S. (2020). Analyzing the Effect of Distribution Pattern and Number of GCPs on Overall Accuracy of UAV Photogrammetric Results. In K. Jain, K. Khoshelham, X. Zhu, & A. Tiwari (Eds.), *Proceedings of UASG 2019* (Vol. 51, pp. 339–354). Springer International Publishing. https://doi.org/10.1007/978-3-030-37393-1_29
- Baghi, Gholami, Naghmeh, & Oldeland, J. (2019). Do soil-adjusted or standard vegetation indices better predict above ground biomass of semi-arid, saline rangelands in North-East Iran? *International Journal of Remote Sensing*, 40(22), 8223–8235. <https://doi.org/10.1080/01431161.2019.1606958>
- Balestra, M., Choudhury, M. A. M., Pierdicca, R., Chiappini, S., & Marcheggiani, E. (2024). UAV-Spherical Data Fusion Approach to Estimate Individual Tree Carbon Stock for Urban Green Planning and Management. *Remote Sensing*, 16(12), 2110. <https://doi.org/10.3390/rs16122110>
- Ballesteros, R., Ortega, J. F., Hernandez, D., & Moreno, M. A. (2018). Onion biomass monitoring using UAV-based RGB imaging. *Precision Agriculture*, 19(5), 840–857. <https://doi.org/10.1007/s11119-018-9560-y>
- Bantelmann, P., Wyss, D., Pius, E. T., & Kappas, M. (2024). Spectral imaging of grass species in arid ecosystems of Namibia. *Frontiers in Remote Sensing*, 5, 1368551. <https://doi.org/10.3389/frsen.2024.1368551>

- Bareth, G., & Schellberg, J. (2018). Replacing Manual Rising Plate Meter Measurements with Low-cost UAV-Derived Sward Height Data in Grasslands for Spatial Monitoring. *PFG – Journal of Photogrammetry, Remote Sensing and Geoinformation Science*, 86(3–4), 157–168. <https://doi.org/10.1007/s41064-018-0055-2>
- Baskaran, B., Radhakrishnan, K., Muthukrishnan, G., Prasath, R. N., Balaji, K. P., & Pandian, S. R. (2017). An autonomous UAV-UGV system for eradication of invasive weed prosopis juliflora. *2017 Conference on Information and Communication Technology (CICT)*, 1–6. <https://doi.org/10.1109/INFOCOMTECH.2017.8340590>
- Bason, D. (2019). *Exactextractr* [Computer software]. (ISciences, LLC).
- Bastin, G., Cowley, R., Friedel, M., & Materne, C. (2024). Applying two remotely-sensed methods for monitoring grazing impacts in the Australian arid zone. *The Rangeland Journal*, 45(4), 141–159. <https://doi.org/10.1071/RJ23030>
- Basupi, L. V., Quinn, C. H., & Dougill, A. J. (2019). Adaptation strategies to environmental and policy change in semi-arid pastoral landscapes: Evidence from Ngamiland, Botswana. *Journal of Arid Environments*, 166, 17–27. <https://doi.org/10.1016/j.jaridenv.2019.01.011>
- Bazzo, C. O. G., Kamali, B., Hütt, C., Bareth, G., & Gaiser, T. (2023). A Review of Estimation Methods for Aboveground Biomass in Grasslands Using UAV. *Remote Sensing*, 15(3), 639. <https://doi.org/10.3390/rs15030639>
- Bendig, J., Yu, K., Aasen, H., Bolten, A., Bennertz, S., Broscheit, J., Gnyp, M. L., & Bareth, G. (2015). Combining UAV-based plant height from crop surface models, visible, and near infrared vegetation indices for biomass monitoring in barley. *International Journal of Applied Earth Observation and Geoinformation*, 39, 79–87. <https://doi.org/10.1016/j.jag.2015.02.012>
- Bennett, J. E. (2013). Institutions and governance of communal rangelands in South Africa. *African Journal of Range & Forage Science*, 30(1–2), 77–83. <https://doi.org/10.2989/10220119.2013.776634>

- Bjorkman, A. D., Myers-Smith, I. H., Elmendorf, S. C., Normand, S., Rüger, N., Beck, P. S. A., Blach-Overgaard, A., Blok, D., Cornelissen, J. H. C., Forbes, B. C., Georges, D., Goetz, S. J., Guay, K. C., Henry, G. H. R., HilleRisLambers, J., Hollister, R. D., Karger, D. N., Kattge, J., Manning, P., ... Weiher, E. (2018). Plant functional trait change across a warming tundra biome. *Nature*, 562(7725), 57–62. <https://doi.org/10.1038/s41586-018-0563-7>
- Bond, W. J. (2008). What Limits Trees in C₄ Grasslands and Savannas? *Annual Review of Ecology, Evolution, and Systematics*, 39(1), 641–659. <https://doi.org/10.1146/annurev.ecolsys.39.110707.173411>
- Borra-Serrano, I., De Swaef, T., Muylle, H., Nuyttens, D., Vangeyte, J., Mertens, K., Saeys, W., Somers, B., Roldán-Ruiz, I., & Lootens, P. (2019). Canopy height measurements and non-destructive biomass estimation of *Lolium perenne* swards using UAV imagery. *Grass and Forage Science*, 74(3), 356–369. <https://doi.org/10.1111/gfs.12439>
- Breshears, D. D. (2006). The grassland–forest continuum: Trends in ecosystem properties for woody plant mosaics? *Frontiers in Ecology and the Environment*, 4(2), 96–104. [https://doi.org/10.1890/1540-9295\(2006\)004\[0096:TGCTIE\]2.0.CO;2](https://doi.org/10.1890/1540-9295(2006)004[0096:TGCTIE]2.0.CO;2)
- Campbell, J. B., & Wynne, R. H. (2011). *Introduction to remote sensing* (5th ed). Guilford Press.
- Capolupo, A., Kooistra, L., Berendonk, C., Boccia, L., & Suomalainen, J. (2015). Estimating Plant Traits of Grasslands from UAV-Acquired Hyperspectral Images: A Comparison of Statistical Approaches. *ISPRS International Journal of Geo-Information*, 4(4), 2792–2820. <https://doi.org/10.3390/ijgi4042792>
- Catchpole, W. R., & Wheeler, C. J. (1992). Estimating plant biomass: A review of techniques. *Australian Journal of Ecology*, 17(2), 121–131. <https://doi.org/10.1111/j.1442-9993.1992.tb00790.x>
- Caughlan, L. (2001). Cost considerations for long-term ecological monitoring. *Ecological Indicators*, 1(2), 123–134. [https://doi.org/10.1016/S1470-160X\(01\)00015-2](https://doi.org/10.1016/S1470-160X(01)00015-2)

- Cen, H., Wan, L., Zhu, J., Li, Y., Li, X., Zhu, Y., Weng, H., Wu, W., Yin, W., Xu, C., Bao, Y., Feng, L., Shou, J., & He, Y. (2019). Dynamic monitoring of biomass of rice under different nitrogen treatments using a lightweight UAV with dual image-frame snapshot cameras. *Plant Methods*, 15(1), 32. <https://doi.org/10.1186/s13007-019-0418-8>
- Chaves, M., Picoli, M., & Sanches, I. (2020). Recent Applications of Landsat 8/OLI and Sentinel-2/MSI for Land Use and Land Cover Mapping: A Systematic Review. *Remote Sensing*, 12(18), 3062. <https://doi.org/10.3390/rs12183062>
- Chen, R., He, B., Quan, X., Lai, X., & Fan, C. (2023). Improving Wildfire Probability Modeling by Integrating Dynamic-Step Weather Variables over Northwestern Sichuan, China. *International Journal of Disaster Risk Science*, 14(2), 313–325. <https://doi.org/10.1007/s13753-023-00476-z>
- Collado, A. (2002). Satellite remote sensing analysis to monitor desertification processes in the crop-rangeland boundary of Argentina. *Journal of Arid Environments*, 52(1), 121–133. [https://doi.org/10.1016/S0140-1963\(01\)90980-2](https://doi.org/10.1016/S0140-1963(01)90980-2)
- Colomina, I., & Molina, P. (2014). Unmanned aerial systems for photogrammetry and remote sensing: A review. *ISPRS Journal of Photogrammetry and Remote Sensing*, 92, 79–97. <https://doi.org/10.1016/j.isprsjprs.2014.02.013>
- Craine, J. M., Nippert, J. B., Elmore, A. J., Skibbe, A. M., Hutchinson, S. L., & Brunsell, N. A. (2012). Timing of climate variability and grassland productivity. *Proceedings of the National Academy of Sciences*, 109(9), 3401–3405. <https://doi.org/10.1073/pnas.1118438109>
- Crutsinger, G. M., Short, J., & Sollenberger, R. (2016). The future of UAVs in ecology: An insider perspective from the Silicon Valley drone industry. *Journal of Unmanned Vehicle Systems*, 4(3), 161–168. <https://doi.org/10.1139/juvs-2016-0008>

- Cunliffe, A., Cunliffe, A., & Anderson, K. (2019). Measuring Above-ground Biomass with Drone Photogrammetry: Data Collection Protocol. *Protocol Exchange*.
<https://doi.org/10.1038/protex.2018.134>
- Cunliffe, A. M., & Anderson, K. (2019). Measuring Above-ground Biomass with Drone Photogrammetry: Data Collection Protocol. *Protocol Exchange*.
<https://doi.org/10.1038/protex.2018.134>
- Cunliffe, A. M., Anderson, K., Boschetti, F., Brazier, R. E., Graham, H. A., Myers-Smith, I. H., Astor, T., Boer, M. M., Calvo, L. G., Clark, P. E., Cramer, M. D., Encinas-Lara, M. S., Escarzaga, S. M., Fernández-Guisuraga, J. M., Fisher, A. G., Gdulová, K., Gillespie, B. M., Griebel, A., Hanan, N. P., ... Wojcikiewicz, R. (2022). Global application of an unoccupied aerial vehicle photogrammetry protocol for predicting aboveground biomass in non-forest ecosystems. *Remote Sensing in Ecology and Conservation*, 8(1), 57–71.
<https://doi.org/10.1002/rse2.228>
- Cunliffe, A. M., Brazier, R. E., & Anderson, K. (2016). Ultra-fine grain landscape-scale quantification of dryland vegetation structure with drone-acquired structure-from-motion photogrammetry. *Remote Sensing of Environment*, 183, 129–143.
<https://doi.org/10.1016/j.rse.2016.05.019>
- Cunliffe, A. M., J Assmann, J., N Daskalova, G., Kerby, J. T., & Myers-Smith, I. H. (2020). Aboveground biomass corresponds strongly with drone-derived canopy height but weakly with greenness (NDVI) in a shrub tundra landscape. *Environmental Research Letters*, 15(12), 125004. <https://doi.org/10.1088/1748-9326/aba470>
- Davi, H., Soudani, K., Deckx, T., Dufrene, E., Le Dantec, V., & François, C. (2006). Estimation of forest leaf area index from SPOT imagery using NDVI distribution over forest stands. *International Journal of Remote Sensing*, 27(5), 885–902.
<https://doi.org/10.1080/01431160500227896>

- Dikgang, J., & Muchapondwa, E. (2017). Local communities' valuation of environmental amenities around the Kgalagadi Transfrontier Park in Southern Africa. *Journal of Environmental Economics and Policy*, 6(2), 168–182.
<https://doi.org/10.1080/21606544.2016.1240631>
- DJI Enterprise. (2024, March 29). Ground Sample Distance. *Learn Everything You Need to Know about GSD and Why It's Important for Drone Surveying*. <https://enterprise-insights.dji.com/blog/ground-sample-distance>
- Domingo, D., Ørka, H. O., Næsset, E., Kachamba, D., & Gobakken, T. (2019). Effects of UAV Image Resolution, Camera Type, and Image Overlap on Accuracy of Biomass Predictions in a Tropical Woodland. *Remote Sensing*, 11(8), 948.
<https://doi.org/10.3390/rs11080948>
- Doughty, C., & Cavanaugh, K. (2019). Mapping Coastal Wetland Biomass from High Resolution Unmanned Aerial Vehicle (UAV) Imagery. *Remote Sensing*, 11(5), 540.
<https://doi.org/10.3390/rs11050540>
- Dougill, A. J., Akanyang, L., Perkins, J. S., Eckardt, F. D., Stringer, L. C., Favretto, N., Atlhopheng, J., & Mulale, K. (2016). Land use, rangeland degradation and ecological changes in the southern Kalahari, Botswana. *African Journal of Ecology*, 54(1), 59–67.
<https://doi.org/10.1111/aje.12265>
- Dougill, A. J., & Thomas, A. D. (2004). Kalahari sand soils: Spatial heterogeneity, biological soil crusts and land degradation. *Land Degradation & Development*, 15(3), 233–242.
<https://doi.org/10.1002/ldr.611>
- Duarte, L., Silva, P., & Teodoro, A. (2018). Development of a QGIS Plugin to Obtain Parameters and Elements of Plantation Trees and Vineyards with Aerial Photographs. *ISPRS International Journal of Geo-Information*, 7(3), 109. <https://doi.org/10.3390/ijgi7030109>
- E. Mbaiwa, J., & T. Thakadu, O. (2022). Postcolonialism, protected areas and Basarwa of Central Kalahari Game Reserve. In M. Ramutsindela, F. Matose, & T. Mushonga (Eds.),

The Violence of Conservation in Africa. Edward Elgar Publishing.

<https://doi.org/10.4337/9781800885615.00019>

El-Ashmawy, K. L. A. (2014). A comparison between analytical aerial photogrammetry, laser scanning, total station and global positioning system surveys for generation of digital terrain model. *Geocarto International*, 1–9.

<https://doi.org/10.1080/10106049.2014.883438>

Eskandari, R., Mahdianpari, M., Mohammadimanesh, F., Salehi, B., Brisco, B., & Homayouni, S. (2020). Meta-analysis of Unmanned Aerial Vehicle (UAV) Imagery for Agro-environmental Monitoring Using Machine Learning and Statistical Models. *Remote Sensing*, 12(21), 3511. <https://doi.org/10.3390/rs12213511>

ESRI. (2024). GIS Dictionary. In *GIS Dictionary*. ESRI. <https://support.esri.com/en-us/gis-dictionary>

Fajji, N. G., Palamuleni, L. G., & Mlambo, V. (2017). Evaluating derived vegetation indices and cover fraction to estimate rangeland aboveground biomass in semi-arid environments. *South African Journal of Geomatics*, 6(3), 333. <https://doi.org/10.4314/sajg.v6i3.5>

Fang, F., McNeil, B. E., Warner, T. A., Maxwell, A. E., Dahle, G. A., Eutsler, E., & Li, J. (2020). Discriminating tree species at different taxonomic levels using multi-temporal WorldView-3 imagery in Washington D.C., USA. *Remote Sensing of Environment*, 246, 111811. <https://doi.org/10.1016/j.rse.2020.111811>

Fern, R. R., Foxley, E. A., Bruno, A., & Morrison, M. L. (2018a). Suitability of NDVI and OSAVI as estimators of green biomass and coverage in a semi-arid rangeland. *Ecological Indicators*, 94, 16–21. <https://doi.org/10.1016/j.ecolind.2018.06.029>

Fern, R. R., Foxley, E. A., Bruno, A., & Morrison, M. L. (2018b). Suitability of NDVI and OSAVI as estimators of green biomass and coverage in a semi-arid rangeland. *Ecological Indicators*, 94, 16–21. <https://doi.org/10.1016/j.ecolind.2018.06.029>

Flora of Botswana. (n.d.). *Tribulus terrestris* L.

Fonstad, M. A., Dietrich, J. T., Courville, B. C., Jensen, J. L., & Carbonneau, P. E. (2013).

Topographic structure from motion: A new development in photogrammetric measurement. *Earth Surface Processes and Landforms*, 38(4), 421–430.

<https://doi.org/10.1002/esp.3366>

Franceschini, M., Becker, R., Wichern, F., & Kooistra, L. (2022). Quantification of Grassland

Biomass and Nitrogen Content through UAV Hyperspectral Imagery—Active Sample

Selection for Model Transfer. *Drones*, 6(3), 73. <https://doi.org/10.3390/drones6030073>

Fraser, B. T., & Congalton, R. G. (2018). Issues in Unmanned Aerial Systems (UAS) Data

Collection of Complex Forest Environments. *Remote Sensing*, 10(6), 908.

<https://doi.org/10.3390/rs10060908>

Fuhlendorf, S. D., Fynn, R. W. S., McGranahan, D. A., & Twidwell, D. (2017). Heterogeneity as

the Basis for Rangeland Management. In D. D. Briske (Ed.), *Rangeland Systems* (pp.

169–196). Springer International Publishing. https://doi.org/10.1007/978-3-319-46709-2_5

Gallacher, D. (2019). Drone-Based Vegetation Assessment in Arid Ecosystems. In B. Gul, B.

Böer, M. A. Khan, M. Clüsener-Godt, & A. Hameed (Eds.), *Sabkha Ecosystems* (Vol. 49,

pp. 91–98). Springer International Publishing. https://doi.org/10.1007/978-3-030-04417-6_7

Gašparović, M., Seletković, A., Berta, A., Balenović, I., University of Zagreb, Faculty of

Geodesy, Chair of Photogrammetry and Remote Sensing, Kačićeva 26, HR-10000

Zagreb, Croatia, University of Zagreb, Faculty of Forestry, Department of Forest

Inventory and Management, Svetošimunska 25, HR-10000 Zagreb, Croatia, Oikon Ltd.

Institute of Applied Ecology, Department of Natural Resources Management, Trg

Senjskih Uskoka 1-2, HR-10000 Zagreb, Croatia, & Croatian Forest Research Institute,

Division for Forest Management and Forestry Economics, Trnjanska cesta 35, HR-

10000 Zagreb, Croatia. (2017). The Evaluation of Photogrammetry-Based DSM from

- Low-Cost UAV by LiDAR-Based DSM. *South-East European Forestry*, 8(2).
<https://doi.org/10.15177/seefor.17-16>
- Geißler, K., Blaum, N., Von Maltitz, G. P., Smith, T., Bookhagen, B., Wanke, H., Hipondoka, M., Hamunyelae, E., Lohmann, D., Lüdtke, D. U., Mbidzo, M., Rauchecker, M., Hering, R., Irob, K., Tietjen, B., Marquart, A., Skhosana, F. V., Herkenrath, T., & Uugulu, S. (2024). Biodiversity and Ecosystem Functions in Southern African Savanna Rangelands: Threats, Impacts and Solutions. In G. P. Von Maltitz, G. F. Midgley, J. Veitch, C. Brümmer, R. P. Rötter, F. A. Viehberg, & M. Veste (Eds.), *Sustainability of Southern African Ecosystems under Global Change* (Vol. 248, pp. 407–438). Springer International Publishing. https://doi.org/10.1007/978-3-031-10948-5_15
- Gillan, J. K., Karl, J. W., & Van Leeuwen, W. J. D. (2020). Integrating drone imagery with existing rangeland monitoring programs. *Environmental Monitoring and Assessment*, 192(5), 269. <https://doi.org/10.1007/s10661-020-8216-3>
- Gindraux, S., Boesch, R., & Farinotti, D. (2017). Accuracy Assessment of Digital Surface Models from Unmanned Aerial Vehicles' Imagery on Glaciers. *Remote Sensing*, 9(2), 186. <https://doi.org/10.3390/rs9020186>
- Gomes Pessoa, G., Caceres Carrilho, A., Takahashi Miyoshi, G., Amorim, A., & Galo, M. (2021). Assessment of UAV-based digital surface model and the effects of quantity and distribution of ground control points. *International Journal of Remote Sensing*, 42(1), 65–83. <https://doi.org/10.1080/01431161.2020.1800122>
- González-Jorge, H., Martínez-Sánchez, J., Bueno, M., & Arias, A. P. (2017). Unmanned Aerial Systems for Civil Applications: A Review. *Drones*, 1(1), 2.
<https://doi.org/10.3390/drones1010002>
- Government of Botswana. (2000). *Botswana National Atlas*. The Department of Surveys and Mapping, Botswana.

- Grüner, E., Astor, T., & Wachendorf, M. (2019). Biomass Prediction of Heterogeneous Temperate Grasslands Using an SfM Approach Based on UAV Imaging. *Agronomy*, 9(2), 54. <https://doi.org/10.3390/agronomy9020054>
- Guerra-Hernández, J., González-Ferreiro, E., Monleón, V., Faías, S., Tomé, M., & Díaz-Varela, R. (2017). Use of Multi-Temporal UAV-Derived Imagery for Estimating Individual Tree Growth in Pinus pinea Stands. *Forests*, 8(8), 300. <https://doi.org/10.3390/f8080300>
- Guimarães, N., Pádua, L., Marques, P., Silva, N., Peres, E., & Sousa, J. J. (2020). Forestry Remote Sensing from Unmanned Aerial Vehicles: A Review Focusing on the Data, Processing and Potentialities. *Remote Sensing*, 12(6), 1046. <https://doi.org/10.3390/rs12061046>
- Gülci, S., Akay, A. E., Aricak, B., & Sariyildiz, T. (2022). Recent Advances in UAV-Based Structure-from-Motion Photogrammetry for Aboveground Biomass and Carbon Storage Estimations in Forestry. In M. N. Suratman (Ed.), *Concepts and Applications of Remote Sensing in Forestry* (pp. 395–409). Springer Nature Singapore. https://doi.org/10.1007/978-981-19-4200-6_20
- Gupta, S. G., Ghonge, M., & Jawandhiya, P. M. (2013). Review of Unmanned Aircraft System (UAS). *SSRN Electronic Journal*. <https://doi.org/10.2139/ssrn.3451039>
- Harmse, C. J., Dreber, N., & Trollope, W. S. (2019). Disc pasture meter calibration to estimate grass biomass production in the arid dunefield of the south-western Kalahari. *African Journal of Range & Forage Science*, 36(3), 161–164. <https://doi.org/10.2989/10220119.2019.1610905>
- Hartmann, W. L., Fishlock, V., & Leslie, A. (2021). First guidelines and suggested best protocol for surveying African elephants (*Loxodonta africana*) using a drone. *KOEDOE - African Protected Area Conservation and Science*, 63(1). <https://doi.org/10.4102/koedoe.v63i1.1687>

- Haydock, K., & Shaw, N. (1975). The comparative yield method for estimating dry matter yield of pasture. *Australian Journal of Experimental Agriculture*, 15(76), 663.
<https://doi.org/10.1071/EA9750663>
- Heermans, B., Van Rooyen, J., Fynn, R., Biggs, D., Lewis, M., & McNutt, J. (2021). Husbandry and Herding: A Community-Based Approach to Addressing Illegal Wildlife Trade in Northern Botswana. *Frontiers in Conservation Science*, 2, 675493.
<https://doi.org/10.3389/fcosc.2021.675493>
- Hijmans, R. J. (2020). *terra: Spatial Data Analysis* (p. 1.7-78) [Dataset].
<https://doi.org/10.32614/CRAN.package.terra>
- Hobbs, R. J., & Norton, D. A. (1996). Towards a Conceptual Framework for Restoration Ecology. *Restoration Ecology*, 4(2), 93–110. <https://doi.org/10.1111/j.1526-100X.1996.tb00112.x>
- Höfle, B., & Rutzinger, M. (2011). Topographic airborne LiDAR in geomorphology: A technological perspective. *Zeitschrift Für Geomorphologie, Supplementary Issues*, 55(2), 1–29. <https://doi.org/10.1127/0372-8854/2011/0055S2-0043>
- Hoppe, F., Zhusui Kyzy, T., Usupbaev, A., & Schickhoff, U. (2016). Rangeland degradation assessment in Kyrgyzstan: Vegetation and soils as indicators of grazing pressure in Naryn Oblast. *Journal of Mountain Science*, 13(9), 1567–1583.
<https://doi.org/10.1007/s11629-016-3915-5>
- Hughes, A. R., Inouye, B. D., Johnson, M. T. J., Underwood, N., & Vellend, M. (2008). Ecological consequences of genetic diversity. *Ecology Letters*, 11(6), 609–623.
<https://doi.org/10.1111/j.1461-0248.2008.01179.x>
- Jahn, N. (2016). *europemc: R Interface to the Europe PubMed Central RESTful Web Service* (p. 0.4.3) [Dataset]. <https://doi.org/10.32614/CRAN.package.europemc>

- James, J. J., Sheley, R. L., Erickson, T., Rollins, K. S., Taylor, M. H., & Dixon, K. W. (2013). A systems approach to restoring degraded drylands. *Journal of Applied Ecology*, 50(3), 730–739. <https://doi.org/10.1111/1365-2664.12090>
- Jamsranjav, C., Reid, R. S., Fernández-Giménez, M. E., Tsevelee, A., Yadamsuren, B., & Heiner, M. (2018). Applying a dryland degradation framework for rangelands: The case of Mongolia. *Ecological Applications*, 28(3), 622–642. <https://doi.org/10.1002/eap.1684>
- Jansen, V., Traynor, A. C. E., Karl, J. W., Lepak, N., & Sprinkle, J. (2022). Monitoring grazing use: Strategies for leveraging technology and adapting to variability. *Rangelands*, 44(1), 64–77. <https://doi.org/10.1016/j.rala.2021.07.005>
- Jayathunga, S., Owari, T., & Tsuyuki, S. (2019). Digital Aerial Photogrammetry for Uneven-Aged Forest Management: Assessing the Potential to Reconstruct Canopy Structure and Estimate Living Biomass. *Remote Sensing*, 11(3), 338. <https://doi.org/10.3390/rs11030338>
- Jhariya, M. K., & Singh, L. (2021). Herbaceous diversity and biomass under different fire regimes in a seasonally dry forest ecosystem. *Environment, Development and Sustainability*, 23(5), 6800–6818. <https://doi.org/10.1007/s10668-020-00892-x>
- Jiang, Q., Fang, S., Peng, Y., Gong, Y., Zhu, R., Wu, X., Ma, Y., Duan, B., & Liu, J. (2019). UAV-Based Biomass Estimation for Rice-Combining Spectral, TIN-Based Structural and Meteorological Features. *Remote Sensing*, 11(7), 890. <https://doi.org/10.3390/rs11070890>
- Jing, R., Gong, Z., Zhao, W., Pu, R., & Deng, L. (2017). Above-bottom biomass retrieval of aquatic plants with regression models and SfM data acquired by a UAV platform – A case study in Wild Duck Lake Wetland, Beijing, China. *ISPRS Journal of Photogrammetry and Remote Sensing*, 134, 122–134. <https://doi.org/10.1016/j.isprsjprs.2017.11.002>

- Joetzjer, E., Pillet, M., Ciais, P., Barbier, N., Chave, J., Schlund, M., Maignan, F., Barichivich, J., Luyssaert, S., Hérault, B., Von Poncet, F., & Poulter, B. (2017). Assimilating satellite-based canopy height within an ecosystem model to estimate aboveground forest biomass. *Geophysical Research Letters*, *44*(13), 6823–6832.
<https://doi.org/10.1002/2017GL074150>
- Kachamba, D., Ørka, H., Gobakken, T., Eid, T., & Mwase, W. (2016). Biomass Estimation Using 3D Data from Unmanned Aerial Vehicle Imagery in a Tropical Woodland. *Remote Sensing*, *8*(11), 968. <https://doi.org/10.3390/rs8110968>
- Kalahari Research & Conservation. (2018). *Community Engagements with Kalahari Research and Conservation*. <https://www.krcbots.org/>
- Karl, J. W., Herrick, J. E., & Pyke, D. A. (2017). Monitoring Protocols: Options, Approaches, Implementation, Benefits. In D. D. Briske (Ed.), *Rangeland Systems* (pp. 527–567). Springer International Publishing. https://doi.org/10.1007/978-3-319-46709-2_16
- Karunaratne, S., Thomson, A., Morse-McNabb, E., Wijesingha, J., Stayches, D., Copland, A., & Jacobs, J. (2020). The Fusion of Spectral and Structural Datasets Derived from an Airborne Multispectral Sensor for Estimation of Pasture Dry Matter Yield at Paddock Scale with Time. *Remote Sensing*, *12*(12), 2017. <https://doi.org/10.3390/rs12122017>
- Kashe, K., Heath, R., Heath, A., Teketay, D., & Thupe, B. O. (2020). Potential Impact of Alien Invasive Plant Species on Ecosystem Services in Botswana: A Review on *Prosopis juliflora* and *Salvinia molesta*. In S. O. Keitumetse, L. Hens, & D. Norris (Eds.), *Sustainability in Developing Countries* (pp. 11–31). Springer International Publishing. https://doi.org/10.1007/978-3-030-48351-7_2
- Keeping, D., Burger, J. H., Keitsile, A. O., Gielen, M.-C., Mudongo, E., Wallgren, M., Skarpe, C., & Foote, A. L. (2018). Can trackers count free-ranging wildlife as effectively and efficiently as conventional aerial survey and distance sampling? Implications for citizen

- science in the Kalahari, Botswana. *Biological Conservation*, 223, 156–169.
<https://doi.org/10.1016/j.biocon.2018.04.027>
- Kendie, G., Addisu, S., & Abiyu, A. (2021). Biomass and soil carbon stocks in different forest types, Northwestern Ethiopia. *International Journal of River Basin Management*, 19(1), 123–129. <https://doi.org/10.1080/15715124.2019.1593183>
- Kgosikoma, O., E. (2012). Bush encroachment in relation to rangeland management systems and environmental conditions in Kalahari ecosystem of Botswana. *AFRICAN JOURNAL OF AGRICULTURAL RESEARCH*, 7(15). <https://doi.org/10.5897/AJAR11.2374>
- Kitagawa, E., Muraki, H., Yoshinaga, K., Yamagishi, J., & Tsumura, Y. (2018). RESEARCH ON SHAPE CHARACTERISTIC OF 3D MODELING SOFTWARE (SfM/MVS) IN UAV AERIAL IMAGES. *Journal of Japan Society of Civil Engineers, Ser. F3 (Civil Engineering Informatics)*, 74(2), II_143-II_148. https://doi.org/10.2208/jscejcei.74.II_143
- Klodt, M., Herzog, K., Töpfer, R., & Cremers, D. (2015). Field phenotyping of grapevine growth using dense stereo reconstruction. *BMC Bioinformatics*, 16(1), 143.
<https://doi.org/10.1186/s12859-015-0560-x>
- Knapp, A. K., Beier, C., Briske, D. D., Classen, A. T., Luo, Y., Reichstein, M., Smith, M. D., Smith, S. D., Bell, J. E., Fay, P. A., Heisler, J. L., Leavitt, S. W., Sherry, R., Smith, B., & Weng, E. (2008). Consequences of More Extreme Precipitation Regimes for Terrestrial Ecosystems. *BioScience*, 58(9), 811–821. <https://doi.org/10.1641/B580908>
- Knox, N. M., Skidmore, A. K., Van Der Werff, H. M. A., Groen, T. A., De Boer, W. F., Prins, H. H. T., Kohi, E., & Peel, M. (2013). Differentiation of plant age in grasses using remote sensing. *International Journal of Applied Earth Observation and Geoinformation*, 24, 54–62. <https://doi.org/10.1016/j.jag.2013.02.004>
- Kumar, L., & Mutanga, O. (2017). Remote Sensing of Above-Ground Biomass. *Remote Sensing*, 9(9), 935. <https://doi.org/10.3390/rs9090935>

- Laca, E. A. (2009). New Approaches and Tools for Grazing Management. *Rangeland Ecology & Management*, 62(5), 407–417. <https://doi.org/10.2111/08-104.1>
- Lancaster, I. N. (1978). The Pans of the Southern Kalahari, Botswana. *The Geographical Journal*, 144(1), 81. <https://doi.org/10.2307/634651>
- Lee, K., Lee, Y.-E., Park, C.-W., Hong, S.-Y., & Na, S. (2016). Study on Reflectance and NDVI of Aerial Images using a Fixed-Wing UAV “Ebee.” *Korean Journal of Soil Science and Fertilizer*, 49(6), 731–742. <https://doi.org/10.7745/KJSSF.2016.49.6.731>
- Lehnert, L. W., Meyer, H., Meyer, N., Reudenbach, C., & Bendix, J. (2014). A hyperspectral indicator system for rangeland degradation on the Tibetan Plateau: A case study towards spaceborne monitoring. *Ecological Indicators*, 39, 54–64. <https://doi.org/10.1016/j.ecolind.2013.12.005>
- Leistner, O., A. (1967). *The Plant Ecology of The Southern Kalahari*. The Government Printer, Pretoria.
- Lewis, A. D. (1936). Sand Dunes of the Kalahari Within the Borders of the Union. *South African Geographical Journal*, 19(1), 22–32. <https://doi.org/10.1080/03736245.1936.10559174>
- Li, W., Niu, Z., Chen, H., Li, D., Wu, M., & Zhao, W. (2016). Remote estimation of canopy height and aboveground biomass of maize using high-resolution stereo images from a low-cost unmanned aerial vehicle system. *Ecological Indicators*, 67, 637–648. <https://doi.org/10.1016/j.ecolind.2016.03.036>
- Liang, S. (2003). *Quantitative Remote Sensing of Land Surfaces* (1st ed.). Wiley. <https://doi.org/10.1002/047172372X>
- Lillesand, T. M., Kiefer, R. W., & Chipman, J. W. (2015). *Remote sensing and image interpretation* (Seventh edition). Wiley.
- Lin, J., Wang, M., Ma, M., & Lin, Y. (2018). Aboveground Tree Biomass Estimation of Sparse Subalpine Coniferous Forest with UAV Oblique Photography. *Remote Sensing*, 10(11), 1849. <https://doi.org/10.3390/rs10111849>

- Lin, X., Chen, J., Lou, P., Yi, S., Qin, Y., You, H., & Han, X. (2021). Improving the estimation of alpine grassland fractional vegetation cover using optimized algorithms and multi-dimensional features. *Plant Methods*, 17(1), 96. <https://doi.org/10.1186/s13007-021-00796-5>
- Lindenmayer, D. B., & Likens, G. E. (2018). *Effective ecological monitoring* (Second edition). Csiro Publishing.
- Liniger, H., P., & Studer, R., M. (2019). *Sustainable rangeland management in sub-Saharan Africa—Guidelines to good practice*.
- Lomax, G. A., Powell, T. W. R., Lenton, T. M., Economou, T., & Cunliffe, A. M. (2024). Untangling the environmental drivers of gross primary productivity in African rangelands. *Communications Earth & Environment*, 5(1), 500. <https://doi.org/10.1038/s43247-024-01664-5>
- Lu, D. (2006). The potential and challenge of remote sensing-based biomass estimation. *International Journal of Remote Sensing*, 27(7), 1297–1328. <https://doi.org/10.1080/01431160500486732>
- Lu, J., Cheng, D., Geng, C., Zhang, Z., Xiang, Y., & Hu, T. (2021). Combining plant height, canopy coverage and vegetation index from UAV-based RGB images to estimate leaf nitrogen concentration of summer maize. *Biosystems Engineering*, 202, 42–54. <https://doi.org/10.1016/j.biosystemseng.2020.11.010>
- Lu, N., Zhou, J., Han, Z., Li, D., Cao, Q., Yao, X., Tian, Y., Zhu, Y., Cao, W., & Cheng, T. (2019). Improved estimation of aboveground biomass in wheat from RGB imagery and point cloud data acquired with a low-cost unmanned aerial vehicle system. *Plant Methods*, 15(1), 17. <https://doi.org/10.1186/s13007-019-0402-3>
- Lussem, U., Bolten, A., Gnyp, M. L., Jasper, J., & Bareth, G. (2018). EVALUATION OF RGB-BASED VEGETATION INDICES FROM UAV IMAGERY TO ESTIMATE FORAGE YIELD IN GRASSLAND. *The International Archives of the Photogrammetry, Remote*

Sensing and Spatial Information Sciences, XLII–3, 1215–1219.

<https://doi.org/10.5194/isprs-archives-xlii-3-1215-2018>

- Lussem, U., Bolten, A., Menne, J., Gnyp, M. L., Schellberg, J., & Bareth, G. (2019). Estimating biomass in temperate grassland with high resolution canopy surface models from UAV-based RGB images and vegetation indices. *Journal of Applied Remote Sensing*, 13(03), 1. <https://doi.org/10.1117/1.JRS.13.034525>
- Maechler, M., Todorov, V., Ruckstuhl, A., Salibian-Barrera, M., Koller, M., & Conceicao, E. L. T. (2024). *robustbase: Basic Robust Statistics* (p. 0.99-3) [Dataset]. <https://doi.org/10.32614/CRAN.package.robustbase>
- Maesano, M., Santopuoli, G., Moresi, F., Matteucci, G., Lasserre, B., & Scarascia Mugnozza, G. (2022). Above ground biomass estimation from UAV high resolution RGB images and LiDAR data in a pine forest in Southern Italy. *iForest - Biogeosciences and Forestry*, 15(6), 451–457. <https://doi.org/10.3832/ifer3781-015>
- Maimaitijiang, M., Sagan, V., Sidike, P., Maimaitiyiming, M., Hartling, S., Peterson, K. T., Maw, M. J. W., Shakoor, N., Mockler, T., & Fritsch, F. B. (2019). Vegetation Index Weighted Canopy Volume Model (CVMVI) for soybean biomass estimation from Unmanned Aerial System-based RGB imagery. *ISPRS Journal of Photogrammetry and Remote Sensing*, 151, 27–41. <https://doi.org/10.1016/j.isprsjprs.2019.03.003>
- Manfreda, S., McCabe, M., Miller, P., Lucas, R., Pajuelo Madrigal, V., Mallinis, G., Ben Dor, E., Helman, D., Estes, L., Ciraolo, G., Müllerová, J., Tauro, F., De Lima, M., De Lima, J., Maltese, A., Frances, F., Caylor, K., Kohv, M., Perks, M., ... Toth, B. (2018). On the Use of Unmanned Aerial Systems for Environmental Monitoring. *Remote Sensing*, 10(4), 641. <https://doi.org/10.3390/rs10040641>
- Mangewa, L. J., Ndakidemi, P. A., & Munishi, L. K. (2019). Integrating UAV Technology in an Ecological Monitoring System for Community Wildlife Management Areas in Tanzania. *Sustainability*, 11(21), 6116. <https://doi.org/10.3390/su11216116>

- Marcial-Pablo, M. D. J., Gonzalez-Sanchez, A., Jimenez-Jimenez, S. I., Ontiveros-Capurata, R. E., & Ojeda-Bustamante, W. (2019). Estimation of vegetation fraction using RGB and multispectral images from UAV. *International Journal of Remote Sensing*, 40(2), 420–438. <https://doi.org/10.1080/01431161.2018.1528017>
- Marsett, R. C., Qi, J., Heilman, P., Biedenbender, S. H., Carolyn Watson, M., Amer, S., Weltz, M., Goodrich, D., & Marsett, R. (2006). Remote Sensing for Grassland Management in the Arid Southwest. *Rangeland Ecology & Management*, 59(5), 530–540. <https://doi.org/10.2111/05-201R.1>
- Maruatona, P. B., & Moses, O. (2022). Assessment of the onset, cessation, and duration of rainfall season over Botswana. *Modeling Earth Systems and Environment*, 8(2), 1657–1668. <https://doi.org/10.1007/s40808-021-01178-5>
- Mbaiwa, J. E. (2005). Enclave tourism and its socio-economic impacts in the Okavango Delta, Botswana. *Tourism Management*, 26(2), 157–172. <https://doi.org/10.1016/j.tourman.2003.11.005>
- Mbokodo, I. L., Bopape, M.-J. M., Ndarana, T., Mbatha, S. M. S., Muofhe, T. P., Singo, M. V., Xulu, N. G., Mohomi, T., Ayisi, K. K., & Chikoore, H. (2023). Heatwave Variability and Structure in South Africa during Summer Drought. *Climate*, 11(2), 38. <https://doi.org/10.3390/cli11020038>
- McGranahan, D. A. (2008). Managing private, commercial rangelands for agricultural production and wildlife diversity in Namibia and Zambia. *Biodiversity and Conservation*, 17(8), 1965–1977. <https://doi.org/10.1007/s10531-008-9339-y>
- McIntire, C., D., Cunliffe, A., M., Boschetti, F., & Litvak, M., E. (2022). Allometric Relationships for Predicting Aboveground Biomass, Sapwood, and Leaf Area of Two-Needle Piñon Pine (*Pinus edulis*) Amid Open-Grown Conditions in Central New Mexico. *Forest Science*, 68(2), 152–161. <https://doi.org/10.1093/forsci/fxac001>

- Mesas-Carrascosa, F.-J., Torres-Sánchez, J., Clavero-Rumbao, I., García-Ferrer, A., Peña, J.-M., Borra-Serrano, I., & López-Granados, F. (2015). Assessing Optimal Flight Parameters for Generating Accurate Multispectral Orthomosaics by UAV to Support Site-Specific Crop Management. *Remote Sensing*, 7(10), 12793–12814.
<https://doi.org/10.3390/rs71012793>
- Meshesha, D. T., Ahmed, M. M., Abdi, D. Y., & Haregeweyn, N. (2020). Prediction of grass biomass from satellite imagery in Somali regional state, eastern Ethiopia. *Heliyon*, 6(10), e05272. <https://doi.org/10.1016/j.heliyon.2020.e05272>
- Meyer, T., Holloway, P., Christiansen, T. B., Miller, J. A., D’Odorico, P., & Okin, G. S. (2019). An Assessment of Multiple Drivers Determining Woody Species Composition and Structure: A Case Study from the Kalahari, Botswana. *Land*, 8(8), 122.
<https://doi.org/10.3390/land8080122>
- Michez, A., Bauwens, S., Brostaux, Y., Hiel, M.-P., Garré, S., Lejeune, P., & Dumont, B. (2018). How Far Can Consumer-Grade UAV RGB Imagery Describe Crop Production? A 3D and Multitemporal Modeling Approach Applied to *Zea mays*. *Remote Sensing*, 10(11), 1798. <https://doi.org/10.3390/rs10111798>
- Midgley, G. F., & Bond, W. J. (2015). Future of African terrestrial biodiversity and ecosystems under anthropogenic climate change. *Nature Climate Change*, 5(9), 823–829.
<https://doi.org/10.1038/nclimate2753>
- Miller, J. R., Hare, E. W., & Wu, J. (1990). Quantitative characterization of the vegetation red edge reflectance 1. An inverted-Gaussian reflectance model. *International Journal of Remote Sensing*, 11(10), 1755–1773. <https://doi.org/10.1080/01431169008955128>
- Millington, A. C., & Townshend, J. (2009). *Biomass assessment*. Earthscan.
- Moeckel, T., Safari, H., Reddersen, B., Fricke, T., & Wachendorf, M. (2017). Fusion of Ultrasonic and Spectral Sensor Data for Improving the Estimation of Biomass in

- Grasslands with Heterogeneous Sward Structure. *Remote Sensing*, 9(1), 98.
<https://doi.org/10.3390/rs9010098>
- Moleele, N. M., & Perkins, J. S. (1998a). Encroaching woody plant species and boreholes: Is cattle density the main driving factor in the Olifants Drift communal grazing lands, south-eastern Botswana? *Journal of Arid Environments*, 40(3), 245–253.
<https://doi.org/10.1006/jare.1998.0451>
- Moleele, N. M., & Perkins, J. S. (1998b). Encroaching woody plant species and boreholes: Is cattle density the main driving factor in the Olifants Drift communal grazing lands, south-eastern Botswana? *Journal of Arid Environments*, 40(3), 245–253.
<https://doi.org/10.1006/jare.1998.0451>
- Morais, T. G., Teixeira, R. F. M., Figueiredo, M., & Domingos, T. (2021). The use of machine learning methods to estimate aboveground biomass of grasslands: A review. *Ecological Indicators*, 130, 108081. <https://doi.org/10.1016/j.ecolind.2021.108081>
- Mori, A. S., Furukawa, T., & Sasaki, T. (2013). Response diversity determines the resilience of ecosystems to environmental change. *Biological Reviews*, 88(2), 349–364.
<https://doi.org/10.1111/brv.12004>
- Myers-Smith, I. H., Kerby, J. T., Phoenix, G. K., Bjerke, J. W., Epstein, H. E., Assmann, J. J., John, C., Andreu-Hayles, L., Angers-Blondin, S., Beck, P. S. A., Berner, L. T., Bhatt, U. S., Bjorkman, A. D., Blok, D., Bryn, A., Christiansen, C. T., Cornelissen, J. H. C., Cunliffe, A. M., Elmendorf, S. C., ... Wipf, S. (2020a). Complexity revealed in the greening of the Arctic. *Nature Climate Change*, 10(2), 106–117.
<https://doi.org/10.1038/s41558-019-0688-1>
- Myers-Smith, I. H., Kerby, J. T., Phoenix, G. K., Bjerke, J. W., Epstein, H. E., Assmann, J. J., John, C., Andreu-Hayles, L., Angers-Blondin, S., Beck, P. S. A., Berner, L. T., Bhatt, U. S., Bjorkman, A. D., Blok, D., Bryn, A., Christiansen, C. T., Cornelissen, J. H. C., Cunliffe, A. M., Elmendorf, S. C., ... Wipf, S. (2020b). Complexity revealed in the

- greening of the Arctic. *Nature Climate Change*, 10(2), 106–117.
<https://doi.org/10.1038/s41558-019-0688-1>
- Naeem, S., & Li, S. (1997). Biodiversity enhances ecosystem reliability. *Nature*, 390(6659), 507–509. <https://doi.org/10.1038/37348>
- Nagendran, S. K., Tung, W. Y., & Mohamad Ismail, M. A. (2018). Accuracy assessment on low altitude UAV-borne photogrammetry outputs influenced by ground control point at different altitude. *IOP Conference Series: Earth and Environmental Science*, 169, 012031. <https://doi.org/10.1088/1755-1315/169/1/012031>
- Newcome, L. R. (2004). *Unmanned aviation: A brief history of unmanned aerial vehicles*. American institute of aeronautics and astronautics.
- Niamir-Fuller, M., & Huber-Sannwald, E. (2020). Pastoralism and Achievement of the 2030 Agenda for Sustainable Development: A Missing Piece of the Global Puzzle. In S. Lucatello, E. Huber-Sannwald, I. Espejel, & N. Martínez-Tagüeña (Eds.), *Stewardship of Future Drylands and Climate Change in the Global South* (pp. 41–55). Springer International Publishing. https://doi.org/10.1007/978-3-030-22464-6_3
- Niu, Y., Zhang, L., Zhang, H., Han, W., & Peng, X. (2019). Estimating Above-Ground Biomass of Maize Using Features Derived from UAV-Based RGB Imagery. *Remote Sensing*, 11(11), 1261. <https://doi.org/10.3390/rs11111261>
- O'Connor, T. G., Puttick, J. R., & Hoffman, M. T. (2014). Bush encroachment in southern Africa: Changes and causes. *African Journal of Range & Forage Science*, 31(2), 67–88.
<https://doi.org/10.2989/10220119.2014.939996>
- Oduor, C. O., Karanja, N. K., Onwonga, R. N., Mureithi, S. M., Pelster, D., & Nyberg, G. (2018). Enhancing soil organic carbon, particulate organic carbon and microbial biomass in semi-arid rangeland using pasture enclosures. *BMC Ecology*, 18(1), 45.
<https://doi.org/10.1186/s12898-018-0202-z>

- Ota, T., Ahmed, O. S., Minn, S. T., Khai, T. C., Mizoue, N., & Yoshida, S. (2019). Estimating selective logging impacts on aboveground biomass in tropical forests using digital aerial photography obtained before and after a logging event from an unmanned aerial vehicle. *Forest Ecology and Management*, 433, 162–169.
<https://doi.org/10.1016/j.foreco.2018.10.058>
- Palik, M., & Nagy, M. (2019). Brief history of UAV development. *Repüléstudományi Közlemények*, 31(1), 155–166. <https://doi.org/10.32560/rk.2019.1.13>
- Parent, J. R., Witharana, C., & Bradley, M. (2022). Classifying and Georeferencing Indoor Point Clouds With ArcGIS. *Photogrammetric Engineering & Remote Sensing*, 88(6), 383–390.
<https://doi.org/10.14358/PERS.21-00048R2>
- Perkins, J. S. (2018). Southern Kalahari piospheres: Looking beyond the sacrifice zone. *Land Degradation & Development*, 29(9), 2778–2784. <https://doi.org/10.1002/ldr.2968>
- Perkins, J. S. (2019). ‘Only connect’: Restoring resilience in the Kalahari ecosystem. *Journal of Environmental Management*, 249, 109420.
<https://doi.org/10.1016/j.jenvman.2019.109420>
- Pettorelli, N., Laurance, W. F., O’Brien, T. G., Wegmann, M., Nagendra, H., & Turner, W. (2014). Satellite remote sensing for applied ecologists: Opportunities and challenges. *Journal of Applied Ecology*, 51(4), 839–848. <https://doi.org/10.1111/1365-2664.12261>
- Pickup, G., & Chewings, V. H. (1994). A grazing gradient approach to land degradation assessment in arid areas from remotely-sensed data. *International Journal of Remote Sensing*, 15(3), 597–617. <https://doi.org/10.1080/01431169408954099>
- Piipponen, J., Jalava, M., De Leeuw, J., Rizayeva, A., Godde, C., Cramer, G., Herrero, M., & Kummu, M. (2022). Global trends in grassland carrying capacity and relative stocking density of livestock. *Global Change Biology*, 28(12), 3902–3919.
<https://doi.org/10.1111/gcb.16174>

- Poley, L. G., & McDermid, G. J. (2020). A Systematic Review of the Factors Influencing the Estimation of Vegetation Aboveground Biomass Using Unmanned Aerial Systems. *Remote Sensing*, 12(7), 1052. <https://doi.org/10.3390/rs12071052>
- Porporato, A., Laio, F., Ridolfi, L., Caylor, K. K., & Rodriguez-Iturbe, I. (2003). Soil moisture and plant stress dynamics along the Kalahari precipitation gradient. *Journal of Geophysical Research: Atmospheres*, 108(D3), 2002JD002448. <https://doi.org/10.1029/2002JD002448>
- Possoch, M., Bieker, S., Hoffmeister, D., Bolten, A., Schellberg, J., & Bareth, G. (2016). MULTI-TEMPORAL CROP SURFACE MODELS COMBINED WITH THE RGB VEGETATION INDEX FROM UAV-BASED IMAGES FOR FORAGE MONITORING IN GRASSLAND. *ISPRS - International Archives of the Photogrammetry, Remote Sensing and Spatial Information Sciences*, XLI-B1, 991–998. <https://doi.org/10.5194/isprsarchives-XLI-B1-991-2016>
- Prabhakara, K., Hively, W. D., & McCarty, G. W. (2015). Evaluating the relationship between biomass, percent groundcover and remote sensing indices across six winter cover crop fields in Maryland, United States. *International Journal of Applied Earth Observation and Geoinformation*, 39, 88–102. <https://doi.org/10.1016/j.jag.2015.03.002>
- Psomas, A., Kneubühler, M., Huber, S., Itten, K., & Zimmermann, N. E. (2011). Hyperspectral remote sensing for estimating aboveground biomass and for exploring species richness patterns of grassland habitats. *International Journal of Remote Sensing*, 32(24), 9007–9031. <https://doi.org/10.1080/01431161.2010.532172>
- R Core Team. (2023). *R: A language and environment for statistical computing* (Version 4.3.0) [Computer software]. (Vienna, Austria: R Foundation for Statistical Computing).
- Retallack, A., Finlayson, G., Ostendorf, B., Clarke, K., & Lewis, M. (2023). Remote sensing for monitoring rangeland condition: Current status and development of methods.

- Environmental and Sustainability Indicators*, 19, 100285.
<https://doi.org/10.1016/j.indic.2023.100285>
- Revermann, R., Krewenka, K., M., Schmiedel, U., Olwoch, J., M., Helmschrot, J., & Jürgens, N. (Eds.). (2018). *Climate change and adaptive land management in southern Africa: Assessments, changes, challenges, and solutions*. Klaus Hess Publishers.
- Ribeiro-Gomes, K., Hernandez-Lopez, D., Ballesteros, R., & Moreno, M. A. (2016). Approximate georeferencing and automatic blurred image detection to reduce the costs of UAV use in environmental and agricultural applications. *Biosystems Engineering*, 151.
<https://doi.org/10.1016/j.biosystemseng.2016.09.014>
- Roodt, V. (2015). *Grasses & Grazers of Botswana and the surrounding savanna*. Penguin Random House South Africa (Pty) Ltd.
- Roth, L., & Streit, B. (2018). Predicting cover crop biomass by lightweight UAS-based RGB and NIR photography: An applied photogrammetric approach. *Precision Agriculture*, 19(1), 93–114. <https://doi.org/10.1007/s11119-017-9501-1>
- Roussel, J.-R., Auty, D., Coops, N. C., Tompalski, P., Goodbody, T. R. H., Meador, A. S., Bourdon, J.-F., De Boissieu, F., & Achim, A. (2020). lidR: An R package for analysis of Airborne Laser Scanning (ALS) data. *Remote Sensing of Environment*, 251, 112061.
<https://doi.org/10.1016/j.rse.2020.112061>
- Sankey, T. Ts., Leonard, J. M., & Moore, M. M. (2019). Unmanned Aerial Vehicle – Based Rangeland Monitoring: Examining a Century of Vegetation Changes. *Rangeland Ecology & Management*, 72(5), 858–863. <https://doi.org/10.1016/j.rama.2019.04.002>
- Santi, E., Tarantino, C., Amici, V., Bacaro, G., Blonda, Borselli, L., Rossi, M., Tozzi, S., & Torri, D. (2014). Fine-scale spatial distribution of biomass using satellite images. *Journal of Ecology and The Natural Environment*, 6(2), 75–86.
<https://doi.org/10.5897/JENE2013.0416>

- Sanz-Ablanedo, E., Chandler, J. H., Rodríguez-Pérez, J. R., & Ordóñez, C. (2018). Accuracy of Unmanned Aerial Vehicle (UAV) and SfM Photogrammetry Survey as a Function of the Number and Location of Ground Control Points Used. *Remote Sensing*, 10(10), 1606. <https://doi.org/10.3390/rs10101606>
- Schmiedel, U., Jacke, V., Hachfeld, B., & Oldeland, J. (2021). Response of Kalahari vegetation to seasonal climate and herbivory: Results of 15 years of vegetation monitoring. *Journal of Vegetation Science*, 32(1), e12927. <https://doi.org/10.1111/jvs.12927>
- Schroeder, R., McDonald, K., Chapman, B., Jensen, K., Podest, E., Tessler, Z., Bohn, T., & Zimmermann, R. (2015). Development and Evaluation of a Multi-Year Fractional Surface Water Data Set Derived from Active/Passive Microwave Remote Sensing Data. *Remote Sensing*, 7(12), 16688–16732. <https://doi.org/10.3390/rs71215843>
- Shahbazi, M., Sohn, G., Théau, J., & Menard, P. (2015). Development and Evaluation of a UAV-Photogrammetry System for Precise 3D Environmental Modeling. *Sensors*, 15(11), 27493–27524. <https://doi.org/10.3390/s151127493>
- Skarpe, C. (1986). Plant community structure in relation to grazing and environmental changes along a north-south transect in the western Kalahari. *Vegetatio*, 68(1), 3–18. <https://doi.org/10.1007/BF00031575>
- Slade, G., Anderson, K., Graham, H. A., & Cunliffe, A. M. (2024). Repeated drone photogrammetry surveys demonstrate that reconstructed canopy heights are sensitive to wind speed but relatively insensitive to illumination conditions. *International Journal of Remote Sensing*, 1–18. <https://doi.org/10.1080/01431161.2024.2377832>
- Slade, G., Fawcett, D., Cunliffe, A. M., Brazier, R. E., Nyaupane, K., Mauritz, M., Vargas, S., & Anderson, K. (2023). Optical reflectance across spatial scales—An intercomparison of transect-based hyperspectral, drone, and satellite reflectance data for dry season rangeland. *Drone Systems and Applications*, 11, 1–20. <https://doi.org/10.1139/dsa-2023-0003>

- Tehrany, M. S., Kumar, L., & Drielsma, M. J. (2017). Review of native vegetation condition assessment concepts, methods and future trends. *Journal for Nature Conservation*, 40, 12–23. <https://doi.org/10.1016/j.jnc.2017.08.004>
- Théau, J., Lauzier-Hudon, É., Aubé, L., & Devillers, N. (2021). Estimation of forage biomass and vegetation cover in grasslands using UAV imagery. *PLOS ONE*, 16(1), e0245784. <https://doi.org/10.1371/journal.pone.0245784>
- Thenkabail, P. S., Lyon, J. G., & Huete, A. (Eds.). (2019). *Hyperspectral remote sensing of vegetation* (Second edition). CRC Press, Taylor & Francis Group.
- Thenkabail, Ph. D. (Ed.). (2015). *Remotely Sensed Data Characterization, Classification, and Accuracies* (0 ed.). CRC Press. <https://doi.org/10.1201/b19294>
- Thomas, D. S. G., & Wiggs, G. F. S. (2022). Dunes of the Southern Kalahari. In F. D. Eckardt (Ed.), *Landscapes and Landforms of Botswana* (pp. 131–154). Springer International Publishing. https://doi.org/10.1007/978-3-030-86102-5_8
- Tian, Y., Bian, Z., Lei, S., Ji, C., Zhao, Y., Zhang, S., Duan, L., & Sedlak, V. (2021). A Process-Oriented Method for Rapid Acquisition of Canopy Height Model From RGB Point Cloud in Semiarid Region. *IEEE Journal of Selected Topics in Applied Earth Observations and Remote Sensing*, 14, 12187–12198. <https://doi.org/10.1109/JSTARS.2021.3129472>
- Tilman, D., Reich, P. B., & Knops, J. M. H. (2006). Biodiversity and ecosystem stability in a decade-long grassland experiment. *Nature*, 441(7093), 629–632. <https://doi.org/10.1038/nature04742>
- Tmušić, G., Manfreda, S., Aasen, H., James, M. R., Gonçalves, G., Ben-Dor, E., Brook, A., Polinova, M., Arranz, J. J., Mészáros, J., Zhuang, R., Johansen, K., Malbeteau, Y., De Lima, I. P., Davids, C., Herban, S., & McCabe, M. F. (2020). Current Practices in UAS-based Environmental Monitoring. *Remote Sensing*, 12(6), 1001. <https://doi.org/10.3390/rs12061001>

- Todd, S. W., Hoffer, R. M., & Milchunas, D. G. (1998). Biomass estimation on grazed and ungrazed rangelands using spectral indices. *International Journal of Remote Sensing*, 19(3), 427–438. <https://doi.org/10.1080/014311698216071>
- Tokozwayo, S., Mopipi, K., & Timpong-Jones, E. C. (2021). Influence of Tree Density on Vegetation Composition and Soil Chemical Properties in Savanna Rangeland of Eastern Cape, South Africa. *Agricultural Sciences*, 12(10), 991–1002. <https://doi.org/10.4236/as.2021.1210064>
- Turner, M. G. (2005). Landscape Ecology: What Is the State of the Science? *Annual Review of Ecology, Evolution, and Systematics*, 36(1), 319–344. <https://doi.org/10.1146/annurev.ecolsys.36.102003.152614>
- Vahidi, M., Shafian, S., Thomas, S., & Maguire, R. (2023). Pasture Biomass Estimation Using Ultra-High-Resolution RGB UAVs Images and Deep Learning. *Remote Sensing*, 15(24), 5714. <https://doi.org/10.3390/rs15245714>
- Van Oudtshoorn, F. (2012). *Guide to grasses of Southern Africa* (3rd. rev. ed). Briza Publications.
- Vellend, M. (2006). THE CONSEQUENCES OF GENETIC DIVERSITY IN COMPETITIVE COMMUNITIES. *Ecology*, 87(2), 304–311. <https://doi.org/10.1890/05-0173>
- Viljanen, N., Honkavaara, E., Näsi, R., Hakala, T., Niemeläinen, O., & Kaivosoja, J. (2018). A Novel Machine Learning Method for Estimating Biomass of Grass Swards Using a Photogrammetric Canopy Height Model, Images and Vegetation Indices Captured by a Drone. *Agriculture*, 8(5), 70. <https://doi.org/10.3390/agriculture8050070>
- Villanueva, J. K. S., & Blanco, A. C. (2019). OPTIMIZATION OF GROUND CONTROL POINT (GCP) CONFIGURATION FOR UNMANNED AERIAL VEHICLE (UAV) SURVEY USING STRUCTURE FROM MOTION (SFM). *The International Archives of the Photogrammetry, Remote Sensing and Spatial Information Sciences*, XLII-4/W12, 167–174. <https://doi.org/10.5194/isprs-archives-XLII-4-W12-167-2019>

- Villoslada, M., Bergamo, T. F., Ward, R. D., Burnside, N. G., Joyce, C. B., Bunce, R. G. H., & Sepp, K. (2020). Fine scale plant community assessment in coastal meadows using UAV based multispectral data. *Ecological Indicators*, 111, 105979.
<https://doi.org/10.1016/j.ecolind.2019.105979>
- Vossen, P. (1990). Rainfall and Agricultural Production in Botswana. *Afrika Focus*, 6(2).
<https://doi.org/10.21825/af.v6i2.18102>
- Wang, L., D'Odorico, P., Ringrose, S., Coetzee, S., & Macko, S. A. (2007). Biogeochemistry of Kalahari sands. *Journal of Arid Environments*, 71(3), 259–279.
<https://doi.org/10.1016/j.jaridenv.2007.03.016>
- Wang, Z., Ma, Y., Chen, P., Yang, Y., Fu, H., Yang, F., Raza, M. A., Guo, C., Shu, C., Sun, Y., Yang, Z., Chen, Z., & Ma, J. (2022). Estimation of Rice Aboveground Biomass by Combining Canopy Spectral Reflectance and Unmanned Aerial Vehicle-Based Red Green Blue Imagery Data. *Frontiers in Plant Science*, 13, 903643.
<https://doi.org/10.3389/fpls.2022.903643>
- Webb, N. P., Okin, G. S., Bhattachan, A., D'Odorico, P., Dintwe, K., & Tatlhego, M. (2020). Ecosystem dynamics and aeolian sediment transport in the southern Kalahari. *African Journal of Ecology*, 58(2), 337–344. <https://doi.org/10.1111/aje.12700>
- Westhuizen, H. C. V. D., Preez, C. C. D., & Snyman, H. A. (2022). Rangeland Degradation Impacts on Vegetation Cover, Soil Properties and Ecosystem Functioning in an Arid and Semi-Arid Climate, South Africa. *Journal of Geoscience and Environment Protection*, 10(02), 10–32. <https://doi.org/10.4236/gep.2022.102002>
- Westoby, M. J., Brasington, J., Glasser, N. F., Hambrey, M. J., & Reynolds, J. M. (2012). 'Structure-from-Motion' photogrammetry: A low-cost, effective tool for geoscience applications. *Geomorphology*, 179, 300–314.
<https://doi.org/10.1016/j.geomorph.2012.08.021>

- Wiens, J. A., & Milne, B. T. (1989). Scaling of ?landscapes? In landscape ecology, or, landscape ecology from a beetle's perspective. *Landscape Ecology*, 3(2), 87–96.
<https://doi.org/10.1007/BF00131172>
- Wijesingha, J., Moeckel, T., Hensgen, F., & Wachendorf, M. (2019). Evaluation of 3D point cloud-based models for the prediction of grassland biomass. *International Journal of Applied Earth Observation and Geoinformation*, 78, 352–359.
<https://doi.org/10.1016/j.jag.2018.10.006>
- Winter, S. L., Fuhlendorf, S. D., Goad, C. L., Davis, C. A., Hickman, K. R., & Leslie Jr, D. M. (2012). Restoration of the fire–grazing interaction in *Artemisia filifolia* shrubland. *Journal of Applied Ecology*, 49(1), 242–250. <https://doi.org/10.1111/j.1365-2664.2011.02067.x>
- Wu, J., Huang, K., Luo, Y., Long, X., Yu, C., Xiong, H., & Du, J. (2024). Identification of Dominant Species and Their Distributions on an Uninhabited Island Based on Unmanned Aerial Vehicles (UAVs) and Machine Learning Models. *Remote Sensing*, 16(10), 1652. <https://doi.org/10.3390/rs16101652>
- Wylie, B. K., Meyer, D. J., Tieszen, L. L., & Mannel, S. (2002). Satellite mapping of surface biophysical parameters at the biome scale over the North American grasslands. *Remote Sensing of Environment*, 79(2–3), 266–278. [https://doi.org/10.1016/S0034-4257\(01\)00278-4](https://doi.org/10.1016/S0034-4257(01)00278-4)
- Xue, J., & Su, B. (2017). Significant Remote Sensing Vegetation Indices: A Review of Developments and Applications. *Journal of Sensors*, 2017, 1–17.
<https://doi.org/10.1155/2017/1353691>
- Yu, J. J., Kim, D. W., Lee, E. J., & Son, S. W. (2020). Determining the Optimal Number of Ground Control Points for Varying Study Sites through Accuracy Evaluation of Unmanned Aerial System-Based 3D Point Clouds and Digital Surface Models. *Drones*, 4(3), 49. <https://doi.org/10.3390/drones4030049>

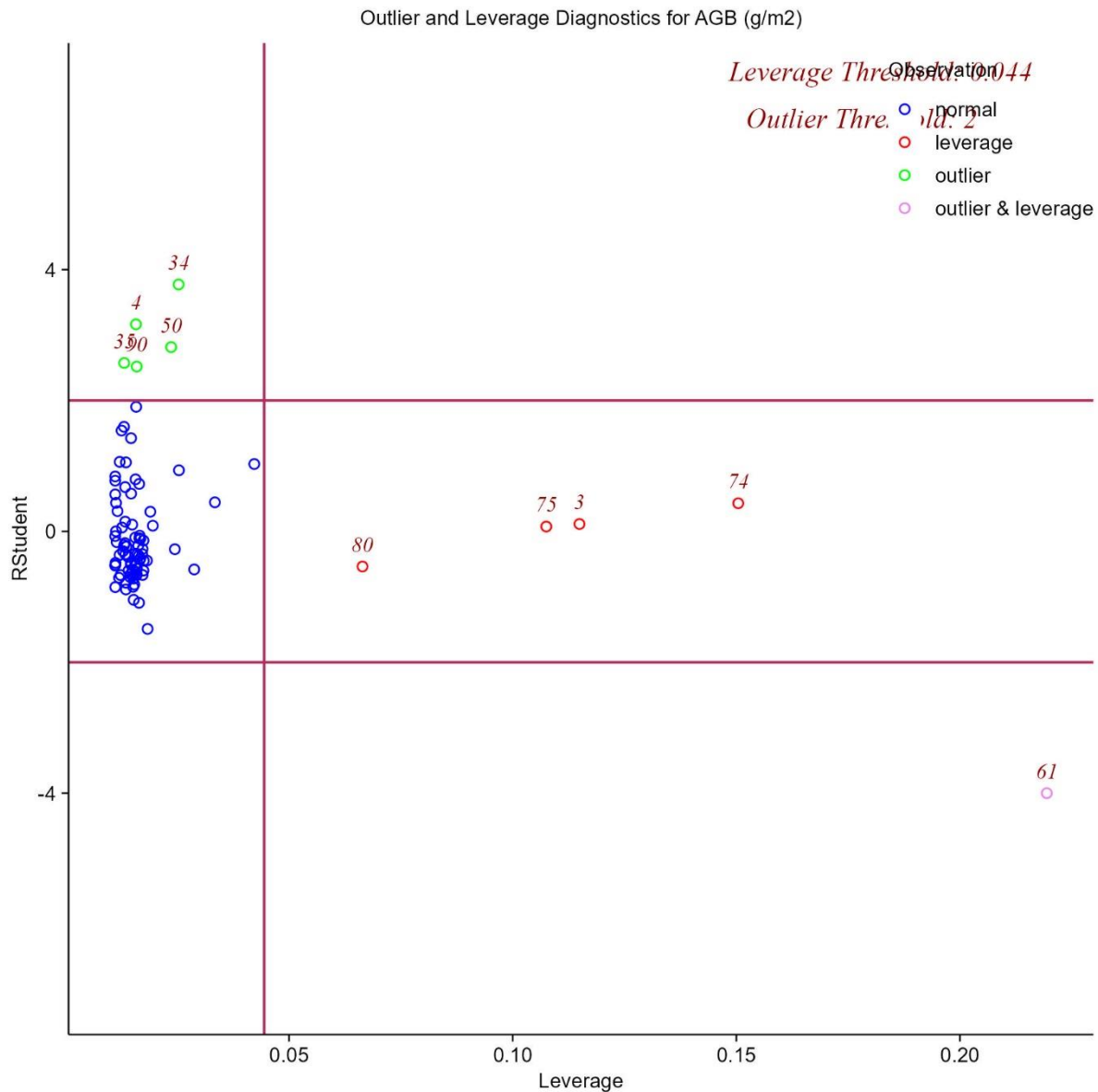
- Zahawi, R. A., Dandois, J. P., Holl, K. D., Nadwodny, D., Reid, J. L., & Ellis, E. C. (2015). Using lightweight unmanned aerial vehicles to monitor tropical forest recovery. *Biological Conservation*, 186, 287–295. <https://doi.org/10.1016/j.biocon.2015.03.031>
- Zambatis, N., Zacharias, P., Morris, C., & Derry, J. (2006). Re-evaluation of the disc pasture meter calibration for the Kruger National Park, South Africa. *African Journal of Range & Forage Science*, 23(2), 85–97. <https://doi.org/10.2989/10220110609485891>
- Zhang, G., Ganguly, S., Nemani, R. R., White, M. A., Milesi, C., Hashimoto, H., Wang, W., Saatchi, S., Yu, Y., & Myneni, R. B. (2014). Estimation of forest aboveground biomass in California using canopy height and leaf area index estimated from satellite data. *Remote Sensing of Environment*, 151, 44–56. <https://doi.org/10.1016/j.rse.2014.01.025>
- Zhang, X., Bao, Y., Wang, D., Xin, X., Ding, L., Xu, D., Hou, L., & Shen, J. (2021). Using UAV LiDAR to Extract Vegetation Parameters of Inner Mongolian Grassland. *Remote Sensing*, 13(4), 656. <https://doi.org/10.3390/rs13040656>
- Zimmer, K., Amputu, V., Schwarz, L.-M., Linstädter, A., & Sandhage-Hofmann, A. (2024). Soil characteristics within vegetation patches are sensitive indicators of savanna rangeland degradation in central Namibia. *Geoderma Regional*, 36, e00771. <https://doi.org/10.1016/j.geodrs.2024.e00771>

9 Appendices

Appendix A. Number of samples per species and grazing value

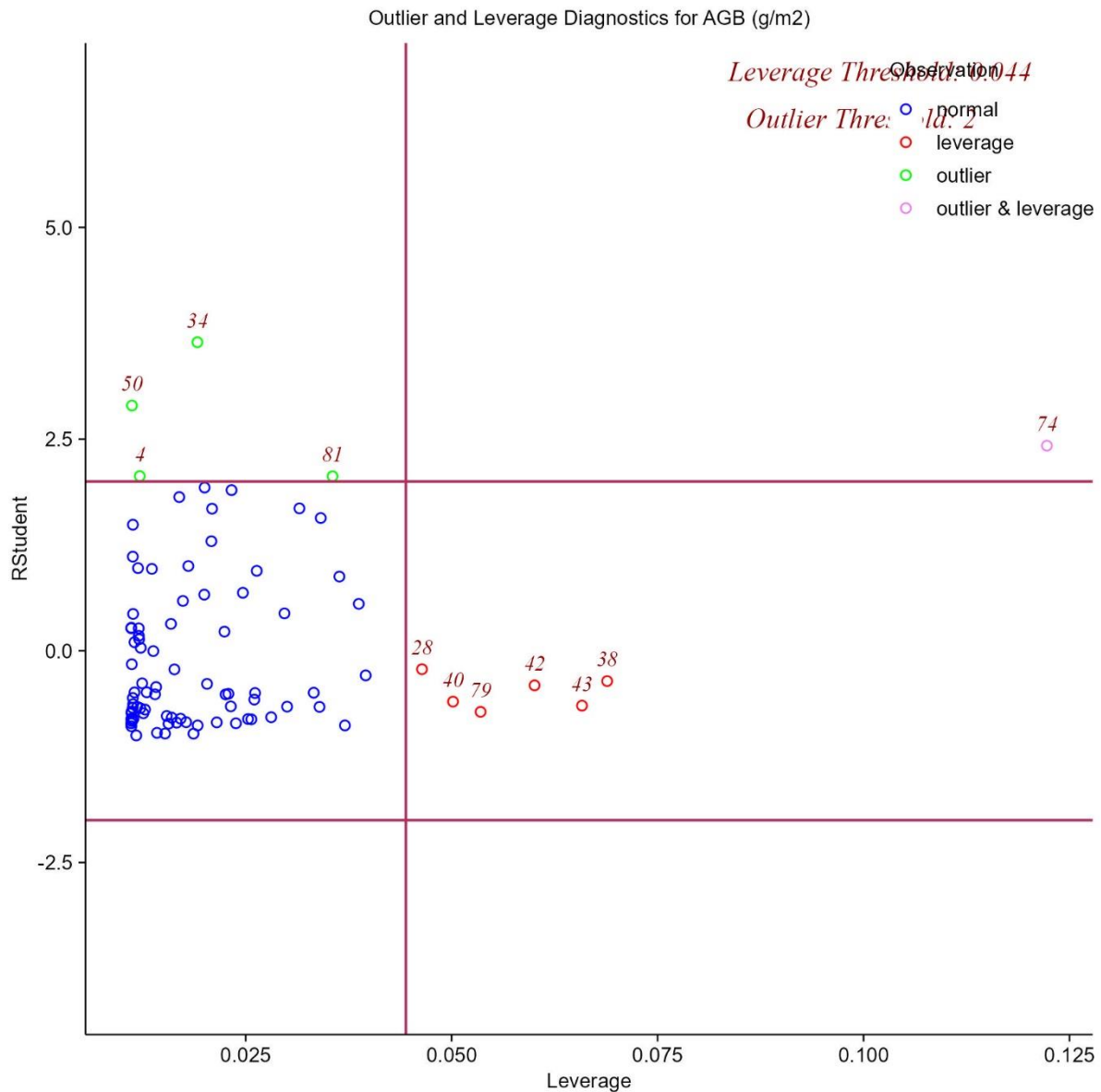
Species	Grazing value	Sample count
<i>Schmidtia kalihariensis</i>	Low	20
<i>Schmidtia pappophoroides</i>	High	6
<i>Stipagrostis ciliata</i>	High	8
<i>Stipagrostis uniplumis</i>	Average	33
<i>Tribulus terrestris</i>	Low	21
<i>Eragrostis pallens</i>	Low	2

Appendix B. Outlier and leverage diagnosis for Canopy Height.



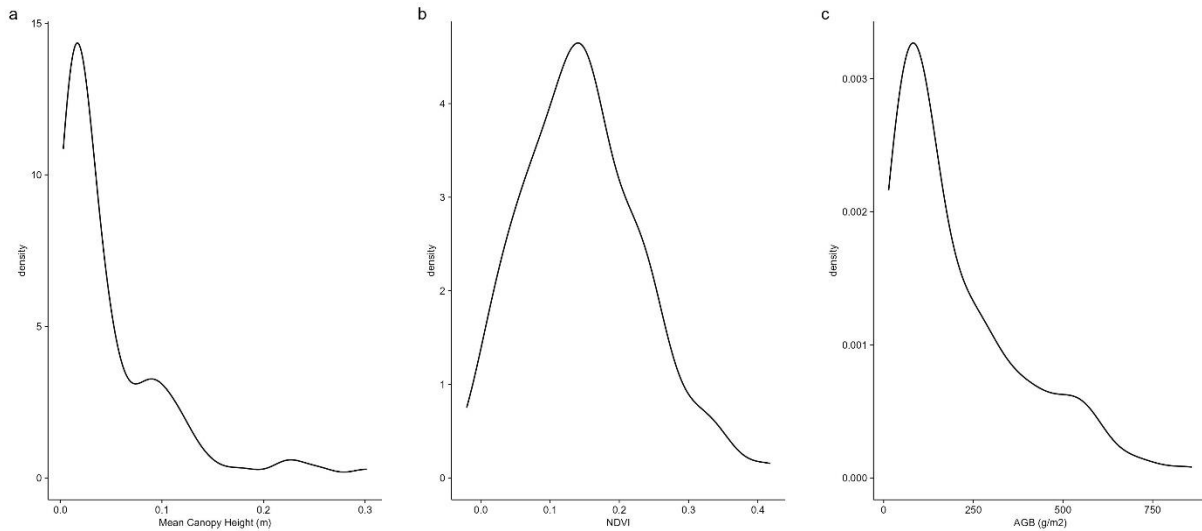
This plot reveals the influential observations in the robust regression model. The x-axis represents leverage values, highlighting observations with significant influence on the model. The y-axis displays studentized residuals, identifying potential outliers with values exceeding ± 2 . 6 observations c(4,34,35,50,61,90) were outliers with $|\text{weight}| = 0$ (< 0.0011); 7 weights are ≈ 1 .

Appendix C. Outlier and leverage diagnosis for NDVI.



This plot reveals the influential observations in the robust regression model. The x-axis represents leverage values, highlighting observations with significant influence on the model. The y-axis displays studentized residuals, identifying potential outliers with values exceeding ± 2 . 6 observations c(4,34,35,50,61,90) were outliers with $|weight| = 0$ (< 0.0011); 7 weights are ≈ 1 .

Appendix D. Density plot for distribution of Canopy Height, NDVI, and AGB.



Density plots show the distribution of (a) UAV derived Mean canopy height, (b) NDVI, and (c) aboveground biomass (AGB) data.

Appendix E. Computational hardware specifications.

Component	Specification
Processor	12th Gen Intel® Core™ i9-12900HK
Base Frequency	2.50 GHz
RAM	32 GB
Operation System	64-bit, x64-based architecture
Software Used	Agisoft Metashape Professional edition (v2.1.1.17821)